PNAS Proceedings of the National Academy of Sciences of the United States of America

Supplementary Information for

Global collision-risk hotspots of marine traffic and the world's largest fish, the whale shark

Freya C. Womersley, Nicolas E. Humphries, Nuno Queiroz, Marisa Vedor, Ivo da Costa, Miguel Furtado, John P. Tyminski, Katya Abrantes, Gonzalo Araujo, Steffen S. Bach, Adam Barnett, Michael L. Berumen, Sandra Bessudo Lion, Camrin D. Braun, Elizabeth Clingham, Jesse E. M. Cochran, Rafael de la Parra, Stella Diamant, Alistair D.M. Dove, Christine L. Dudgeon, Mark V. Erdmann, Eduardo Espinoza, Richard Fitzpatrick, Jaime González Cano, Jonathan R. Green, Hector M. Guzman, Royale Hardenstine, Abdi Hasan, Fábio H.V. Hazin, Alex R. Hearn, Robert E. Hueter, Mohammed Y. Jaidah, Jessica Labaja, Felipe Ladino, Bruno C.L. Macena, John J. Morris Jr., Bradley M. Norman, Cesar Peñaherrera-Palma, Simon J. Pierce, Lina M. Quintero, Dení Ramírez-Macías, Samantha D. Reynolds, Anthony J. Richardson, David P. Robinson, Christoph A. Rohner, David R.L. Rowat, Marcus Sheaves, Mahmood S. Shivji, Abraham B. Sianipar, Gregory B. Skomal, German Soler, Ismail Syakurachman, Simon R. Thorrold, Harry D. Webb, Bradley M. Wetherbee, Timothy D. White, Tyler Clavelle, David A. Kroodsma, Michele Thums, Luciana C. Ferreira, Mark G. Meekan, Lucy M. Arrowsmith, Emily K. Lester, Megan M. Meyers, Lauren R. Peel, Ana M.M. Sequeira, Victor M. Eguíluz, Carlos M. Duarte & David W. Sims

Freya C. Womersley & David W. Sims

Email: f.womersley@mba.ac.uk | dws@mba.ac.uk

This PDF file includes:

Contents

1. Supplementary Methods

1.1 Study regions

The global ocean was divided into seven distinct regions: north Atlantic (NA), south Atlantic (SA), northwest Indian Ocean (NIO), southwest Indian Ocean (SIO), east Indian Ocean (EIO), west Pacific (WP) and east Pacific (EP) (Fig. S2*A*). Region boundaries were defined based on a combination of whale shark distribution (1), geographical features, and the Food and Agriculture Organization major fishing area boundaries (http://www.fao.org). Individual whale sharks were assigned a region based on the geographical centroid of their estimated track positions. Mean monthly vessel overlap and collision risk index (CRI) were examined on three nested scales: (*i*) globally; (*ii*) within each of the seven major regions highlighted above; (*iii*) and within sub-regions where hotspots of high potential collision risk were identified in the main analysis, which included the Arabian Gulf (AG) (26°N 52°E), the Red Sea (RS) (22°N 38°E) and the Gulf of Mexico (GOM) (25°N 90°W).

1.2 Study animals and tagging procedures

A total of 348 whale sharks were tagged with satellite-linked transmitters between 2005 and 2019 at numerous sites within the Atlantic, Indian and Pacific Oceans. This included 39 individuals tagged in the north Atlantic, 14 in the south Atlantic, 44 in the northwest Indian Ocean, 26 in the southwest Indian Ocean, 74 in the east Indian Ocean, 62 in the west Pacific and 89 in the east Pacific (Table S2). Three types of satellite-transmitter tag, which provided location estimates at different spatio-temporal resolutions and accuracies, were provided by data owners and quality-checked before analyses. These included, Global Positioning System (FastLoc® GPS) transmitters, position-only advanced research and global observation satellite (ARGOS) transmitters and pop-off satellite archival transmitters (PSAT). Tags were attached anterior to the first dorsal fin region (usually with tethers) or mounted onto the fin of free-swimming animals or animals captured in bagan lift-net fisheries by trained personnel. All animal-handling procedures were approved by institutional ethical review committees and carried out in accordance with laws of the countries where they were undertaken (see section 8 *'Details of ethical compliance and approvals'*). A total of 106 females (mean total length (TL) 7.76 m ± s.d. 2.47) and 165 males (mean TL 6.20 m ± s.d. 1.51) plus 77 of unknown sex, ranging from 3 to 13.1 m TL were tagged and grouped into one of six size classes (3 m; 3-6 m; 6-9 m; 9-12 m; > 12 m; and unmeasured size, herein unknown size). Combined, tracks had a total duration of 52,246 tracking days and 15,508 transmitting days with a mean duration of 150.13 (± s.d. 157.57) days per individual (median 102.5 days, Table S2). The total distance covered by all tracked whale sharks was 684,279 km, with a mean distance moved of 1,966.3 km (median 1,310.8 km, n = 348 tracks) per track, and a mean daily movement distance of 19.5 km (median 14.3 km d^{-1}, n = 348 tracks) per individual (Table S2).

1.3 Track processing

Data received from PSAT tags (n = 92 tracks) were provided as either files with positions that had been previously reconstructed using proprietary geolocation software provided by the tag manufacturers, as decoded files with no prior geolocation, or as original track files (for example, Microwave Telemetry instrument data files). In the first case, positions were estimated prior to collation for this study using software algorithms (for example, Wildlife Computers GPE2) in which estimated day-length was used to determine latitude, and daily maximal rate-of-change in light intensity was used to estimate local time of midnight or midday for determining longitude (2). In the latter cases, tag manufacturer software was used to generate geolocated tracks from decoded data with no prior geolocation, and original track files were decoded using tag manufacturer software (for example, Wildlife Computers DAP) prior to running geolocation. Track files were processed following previously published methodology (3), where geolocated positions were corrected using the UKFSST state-space model (SSM) (4) (UKFSST R package) and a bathymetric correction applied to the initial Kalman positions (analyzepsat R add-on) to estimate the most probable track (MPT) of the animal. UKFSST corrected geolocations were parameterised with standard deviation (s.d.) constants, which produces the smallest mean deviation from concurrent ARGOS positions (5). Although this procedure does not make corrected tracks from a light-based PSAT tag as accurate as those from an ARGOS device, it does provide a consistent characterisation of the positional accuracy across different tag types, allowing the uncertainty in position to propagate into analysis methods. A continuous-time correlated random walk (CTCRW) Kalman filter SSM (6) (R package crawl) was applied to the MPT, which produced a single position estimate per day using model parameters implemented in the SSM.

Data received from ARGOS transmitters (n = 254 tracks) were provided as files containing raw ARGOS (Doppler frequency shift) position estimates with an associated positional accuracy class (location class: 3, 2, 1, 0, A, B and Z). Position estimates with location class Z, assigned for a failed attempt at obtaining a position, were discarded prior to processing. A speed filter of 3 m s^{-1} was applied to the remaining raw position estimates, which were analysed point to point to remove outlier locations (3). A daily time-series of locations of each ARGOS track was estimated using the CTCRW SSM (6). Data received from FastLoc® GPS transmitters (n = 2 tracks) were provided as files with raw GPS positions exported from tag manufacturer software. Raw GPS locations were assigned as location class 3 and run through the speed filter and CTCRW SSM (6) to generate daily positions. For days where multiple raw GPS positions were sampled, the centroid of positions was taken and used as the daily position estimate. For the overlap and collision risk analyses, FastLoc® GPS corrected tracks were treated equally to ARGOS tracks, while for the fine-scale movement tracking analysis, the high-resolution FastLoc® GPS files with multiple positions per day, were used.

1.4 Global vessel traffic

Automatic Identification Systems (AIS) are on-board vessel navigation systems used to provide collision detection capabilities for all vessels >300 gross tons as required by the International Maritime Organisation (IMO). AIS data collected by coastal stations and satellites can be used to provide information on the position and characteristics (e.g., identity, speed, heading and activity) of broadcasting vessels. Due to its global coverage of many thousands of large vessel locations, AIS data has expanded beyond its original safety system remit and has enabled analysis of the distribution of vessel movements in space and time (7, 8). For our global analysis, gridded products were purchased from Exact Earth (http://www.exactearth.com) for the years of 2011 to 2014 at 0.25 × 0.25° cell resolution. AIS coverage for these years matched the majority of whale shark tracking data and spanned the mid-point of years when tags were deployed (2005 to 2019) with 69% of tag deployments occurring up to 2015 (Table S17).

Within each 0.25 × 0.25° grid cell, the total number of unique vessels present per month was provided for vessels classified as cargo, fishing, passenger, tanker and 'other'. The 'other' category includes research vessels, law vessels, vessels conducting surveys and logistic services for industry, and any other vessel not covered by the preceding explicit categories (8). For the main analysis, all vessel classes were aggregated into 12-monthly global vessel density maps under the assumption that any interaction with an underway vessel >300 gross tons poses a serious risk to whale sharks. Although they also likely pose a threat to whale sharks, smaller vessels were excluded here because at present there is no means to explore collision risk fully from vessels <300 gross tons globally, as AIS is not a requirement on vessels below this size. Furthermore, in this study we focus on the potential for lethal collisions which are more likely to result from impacts with larger vessels and that have the potential to influence population sizes directly. Analyses were then performed for each vessel category.

For each month, global vessel movements were classified as 'traffic density' where number of unique vessels per 0.25 × 0.25° cell were averaged across all available years to give a mean monthly density per relative year (Table S1). Monthly global distributions of traffic density were mapped and overlaid with whale shark monthly spatial density of locations, for all individuals, to determine spatial overlap intensity and collision risk index (CRI) (see sections 1.8 *'Spatial overlap'* and 1.10 *'Collision risk index'*). Between 2011 and 2014, AIS data coverage increased as more vessels were fitted with AIS receivers and more satellites were launched. Although the global geographic distribution of vessel activity was broadly similar across years, the increase in coverage was reflected in the annual maximum number of vessels within a grid cell (1,573.58 in 2011; 10,851.80 in 2014). Therefore, the overlap and risk analyses were also performed for each year separately between 2011 and 2014. To check that the main AIS dataset we used was representative of the general vessel movement patterns monitored with AIS by different data providers, we also analysed data for 2014 and 2017-2019 provided by Global

Fishing Watch (https://globalfishingwatch.org) (Table S1). For this analysis, a 0.25 × 0.25° gridded product for the year 2014 was directly compared to the Exact Earth data used in the main analysis for the cargo vessel type (Fig. S15, S16). Following this, data for the years 2017 to 2019 were compared with the cargo outputs from the main analysis. It was not possible to completely merge the full datasets from different vessel monitoring providers as we were unable to control for potential differences in satellite coverage, levels of interpolation between vessel locations, or vessel categorisation. Nevertheless, spatial patterns of overlap and collision risk remained very similar between datasets indicating our results were consistent irrespective of the source of AIS data used (Table S14, Table S18 and Fig. S16, S17).

1.5 Fine scale simultaneous shark-vessel interactions

The Gulf of Mexico was selected to explore fine-scale shark-vessel interactions because (*i*) the dataset contained two FastLoc® GPS tracks from the region with an accuracy ranging from <170 m (five satellites) to <30 m (eight satellites) (9-11), (*ii*) individuals in the region were exposed to high relative collision risk, and (*iii*) fine-scale vessel movement data were available online from National Oceanic and Atmospheric Administration (2020) (https://coast.noaa.gov). AIS data from the region were monitored using ground-based antennas, which can have limited message reception performance across long distances, and this analysis was therefore considered a conservative estimate as coverage may not always reach the central Gulf. Shark tracks were analysed at the highest resolution with multiple positions per day and a total tracking duration of 181 days (Table S4*A*). Vessel tracks were downloaded for the time periods corresponding to the whale shark tracks and filtered to include only those within the maximum geographical extent of the shark tracks. To simplify processing, vessel tracks were interpolated to one position every hour and further filtered to highlight close passes with whale shark positions. For each shark position, the closest point-of-approach (CPA) time and distance was calculated for every vessel track in the dataset. The CPA was defined by identifying the closest point in time between each shark position and vessel AIS position and calculating the horizontal distance between the shark and vessel based on these positions (12). Vessel tracks were further filtered to include only those with CPA times within a maximum of 20 minutes and CPA distances within 20 km, which were considered passes to be used in further filtering to quantify close spatial interactions. Most CPA locations were well within the assigned cut off indicating the frequency of close interactions was high. This process was repeated using the high-resolution vessel tracks (no prior temporal interpolation) from the filtered selection to ensure calculations were based on known locations of both sharks and vessels.

1.6 Whale shark collision zone use

To incorporate the use of the sea surface by whale sharks into the collision risk analysis, the concept of collision zone use (13) was applied (Table S1). Here, PSAT depth sensor tags were used to determine the proportion of total tracked time spent in the top 20-25 m of the water column within each of the

study regions for which there were appropriate data. A collision risk zone of ≤20 m was selected based on similar studies on cetaceans (13), where comparable depth limits have been applied to quantify collision risk, taking into account the radius of hydrodynamic draw that can pull an animal towards a vessel hull as it passes over (14). A collision risk zone of ≤25 m was applied to whale sharks occupying the east Pacific region, as predefined depth bins needed to summarise data prior to satellite relay did not allow for a ≤20 m assessment in this region.

Depth data were stored in time-at-depth histogram files from 97 tags (total of 28,847 tracking days and 15,185 transmitting days). Time at depth was sampled at varying intervals (from 3 to 60 s), with tags programmed to store data in user-determined bins (of either 3, 4, 6, 8, 9, 12, 24 h) of varying depth ranges (m, binned into 12 or 14 intervals). Data from all tags were pooled and bins of varied depth limits were sorted into a database. The cumulative proportion of time spent in the defined collision risk zone was extracted from each time interval window and summarised to generate a median proportion of total tracked time. The median was selected, as although whale sharks exhibited a broad vertical extent, depth use was skewed toward surface layers. A total of 39,143 depth records were analysed, 17,510 of which had an associated geographical location (Table S3). To calculate the overall proportion of collision zone use per region, all records were used to generate a regional median. Only records with a corresponding geographical position available were used to explore differences between collision zone use when whale sharks were transitioning waters on the shelf (≤200 m depth) or off the shelf (>200 m depth) (hereafter termed coastal and oceanic, respectively). In these cases, bathymetric depth was extracted for each position from gridded bathymetry data aggregated to 1 × 1° resolution (which is similar to the broad geographical error field associated with PSAT tags (3, 15, 16) (GEBCO 30' 2020, General Bathymetric Chart of Oceans, https://www.gebco.net/). Depth records where the associated location was in waters with a depth ≤200 m were assigned as coastal and those in waters >200 m depth were assigned as oceanic. Regional medians for each depth class were obtained from these subsets and converted into a fraction for use in the collision risk analysis.

To explore differences in collision zone use between sexes, a subset region with the largest data sample (north Atlantic, n = 24 depth histograms) was selected in which depth records were summarised by individual for the duration of the track before median collision zone use was calculated for each sex (Table S19). To explore monthly variations in collision zone use, a subset region with the largest data sample (west Pacific, n = 38 depth histograms) was selected, where collision zone use was calculated as a summary of depth records within each month (Table S20). Values derived from control comparisons between sexes and over monthly timescales were incorporated into the risk metrics on a regional scale in the north Atlantic for sex and in the west Pacific for month. To explore differences in collision zone use between individuals of different sexes and between coastal or oceanic associated depth records within each region, two-sample Kolmogorov-Smirnov tests were performed using the

statistics package for R (17). For coastal locations in the east Pacific region, where no dive data were available, the ratio of collision zone use from the west Pacific region was applied to generate a coastal median (55.6%) for incorporating into the potential collision exposure calculations (see section 1.9 *'Potential collision exposure index'*), and for the south Atlantic, medians from the north Atlantic were applied (Table S3).

1.7 Spatial density analysis

To reduce potential bias of the measure of whale shark spatial density within the collision risk metrics, any gaps between consecutive locations within each raw track file were interpolated into a daily time series of one position per day over a maximum gap of three days. The maximum number of days over which to interpolate between estimated positions was selected based on the median gap frequency of reconstructed tracks (3 days, Table S21). As is often the case with water-breathing fish that do not need to surface to breathe, longer temporal gaps in satellite-based tracking data occur compared to air-breathing marine animals that surface regularly. This difference can potentially result in whale sharks having long temporal gaps in location data and hence extensive interpolated movements driven by the underlying CTCRW SSM (6) rather than actual movement patterns (18). Consequently, gaps that exceeded three days were not interpolated, thus avoiding the inclusion of unrepresentative interpolated location estimates. Each location was assigned a weight that accounts for biases in whale shark spatial location density associated with shorter tracks near the tagging location and variable track lengths (3, 19). Each daily location estimate of an individual was weighted by the inverse of the number of all individuals with location estimates for the same relative day of their track:

$$W_{it} = \frac{1}{n_t}, \text{ for } i \in I,$$

where W_{it} is the weight for the t^{th} location estimate of the track of the i^{th} individual, n_t is the total number of individuals with a location estimate on the t^{th} relative day, and I is the set of all individuals. Location weights after a threshold day of the relative track were fixed equal to the weight on the day corresponding to the 85$^{\text{th}}$ percentile of track lengths. To account for variation in number of individuals with a day gap on a given relative day, every relative day of an individual track was included in the weighting procedure irrespective of whether a position was recorded on that day. Weights for all individuals (W_{it}) were normalised so that they summed to unity to ensure all individuals contributed equally to global whale shark relative-spatial-density estimates (3):

$$D_{it} = \sum_{i \epsilon I} \sum_{t=1}^{T_i} W_{it},$$

where D_{it} is the relative density contribution for the t^{th} location estimate for the i^{th} individual, and T_i is the total number of location estimates for the i^{th} individual. The relative density contributions for all location estimates for each individual (D_{it}) were summed within each 0.25 × 0.25° resolution cell of the study area for each month of a relative year, which gave 12 relative spatial density maps per individual to compare with the corresponding monthly vessel density maps. Density maps of all individuals were summed within a month and the mean annual D_{it} per grid cell for a relative year was calculated from the 12 monthly relative densities per grid cell to provide the global relative density of tracked whale sharks used to generate Figure 2*A*. At this stage, density was assigned to grid cells with 0.25 × 0.25° resolution irrespective of the geolocation error associated with different tag types as a preliminary step prior to the overlap and CRI calculations (where spatial averaging was applied within each cell; see sections 1.8 *'Spatial overlap'* and 1.10 *'Collision risk index'*). For PSAT tags (n = 92 tracks) which have a larger spatial error associated with geolocated positions than ARGOS tags (n = 256 tracks) (3, 15, 16), density values assigned to one 0.25 x 0.25° resolution cell may include locations that in reality were in adjacent cells and, as such, may not provide an accurate summation of density within a specific cell. To reduce potential effects on estimates of spatial density based on PSAT geolocation error fields, a radius of 2.5° (>10 times the upper 95% confidence intervals of the mean daily movement distances of whale sharks, C.I. = 21.57 km) was applied to each weighted cell location when mapping the density hotspots in Figure 2*A* and Figure S3*A*. The radius parameter determines the circular area around each density location where the point will have an influence and was chosen to be greater than the error field associated with PSAT tags (3, 15, 16). In this procedure, PSAT locations associated with a specific 0.25 × 0.25° resolution cell can contribute to surrounding density calculations up to a distance of 2.5°. This allows for the possibility that the actual position falls somewhere other than the assigned point within this field thus accounting for potential location errors. Density grids were also re-calculated at lower resolutions in the control analyses (see section 1.8 *'Spatial overlap'*). Maps were created using QGIS (20). The spatial coverage of 1 × 1° grid cells occupied by whale sharks per ocean region was between 13.6% (east Indian Ocean) and 3.4% (south Atlantic) of total grid cells within the defined boundaries (Table S22).

1.8 Spatial overlap

In this study, spatial overlap serves as a measure of co-occurrence between a tracked whale shark and global large vessel movements. Spatial overlap was calculated as the number of 0.25 × 0.25° grid cells where both whale sharks and vessels were located, as a function of all whale shark grid cells occupied in a mean month. This can be summarised as:

$$\text{Spatial overlap } (\%) = 100\frac{n_c}{n_o},$$

Where n_c is the number of grid cells occupied by an individual tracked whale shark that overlap with vessel occupied cells (i.e., cells where the two groups co-occur) and n_o is the total number of grid cells occupied by an individual tracked whale shark. The mean monthly spatial overlap per whale shark was determined from the 12 monthly spatial overlap values. Due to the lower spatial accuracy for PSAT tags (n = 92; 26.4% of total tracks), vessel traffic density was averaged for 1.25° latitude by 0.75° longitude (5 × 3-cell grid) around each shark position (similar to the broad geographical error field associated with PSAT tags (3, 15, 16)). This procedure allows for monthly PSAT geolocated shark locations to fall within one of six potential 0.25 × 0.25° resolution cells surrounding the estimated position (7 in total, for 1.25° latitude by 0.75° longitude) where they may overlap with vessel presence. The overlap for each seven-cell grid was averaged over all grids in a month before summarising per individual. This accounts for some of the potential bias related to the different error fields associated with PSAT and ARGOS tags (3, 15, 16). Monthly gridded locations deemed too close to land to reflect overlap accurately were removed from the overlap grid analysis for both tag types (i.e. grid cells with associated bathymetric depth ≤0 m and no associated vessel data, n = 555 shark occurrence cells). The mean monthly averaged overlap was calculated per region, sex and size class.

For our analyses, a fixed 0.25 × 0.25° global geographical grid cell (in which 0.25° ≈ 27.65 km) was chosen as this was the finest resolution available for global vessel movements and because it exceeded the upper 95% confidence intervals of the mean daily movement distances of whale sharks (Table S2, mean = 19.53 km, C.I. = 21.57 km). In addition to the 0.25 × 0.25° resolution, the effect of grid cell size on estimates of spatial overlap was examined by calculating overlap with all whale sharks at 2 × 2°, 1 × 1°, 0.75 × 0.75° and 0.5 × 0.5° resolutions. For these analyses a similar cell-averaging method was used for the lower spatial accuracy PSAT tags at 0.75 × 0.75° resolution (vessel traffic density averaged for 1.5° latitude and 0.75° longitude using a 2 × 1 randomised cell grid) and 0.5 × 0.5° resolution (vessel traffic density averaged for 1.5° latitude and 0.5° longitude using a 3 × 1-cell grid). These analyses were also repeated using ARGOS and PSAT track data independently to check for consistency in spatial overlap patterns and magnitude of overlap values irrespective of tag type used (Table S11).

1.9 Potential collision exposure index

Whale shark collision zone use was incorporated into the collision risk analysis using the concept of potential collision exposure index (13). This was defined as the number of vessels that a whale shark may be exposed to in the same relative month and cell, and therefore may be vulnerable to collision with, given their collision zone use (proportion of total tracked time spent shallower than 20 m or 25 m for the east Pacific, Table S1, see section 1.6 '*Whale shark collision zone use'*) (13). Empirical collision zone use values derived from the PSAT dive analysis were converted into a fraction between 0 and 1 (n = 97 tags, 28,847 tracking days, Table S3) before being assigned to a cell.

Bathymetric depth was extracted for each cell occupied by a whale shark, which was then classed as either coastal or oceanic with an associated collision zone use value. Potential collision exposure was calculated within each cell occupied by a shark before being incorporated into collision risk index (CRI) calculations (see section 1.10 '*Collision risk index*' below). It was also summarised on an individual monthly basis, where traffic density was scaled by collision zone use within individual occupied cells:

$$E_i = \frac{\sum_{t=1}^{n} v_t z_t}{n},$$

where E_i is the potential collision exposure for the i^{th} individual shark per month, z_t is the collision zone use associated with grid cell t occupied by a whale shark within a month of its track, v_t is the vessel traffic density within grid cell t occupied by a whale shark within a month of its track, and n is the number of grid cells occupied by an individual whale shark within a month of its track. As before, for PSAT tags with lower spatial accuracy (n = 92 tracks, 26.4% of total tracks), traffic density data (v_t) was averaged for 1.25° latitude by 0.75° longitude (5 × 3-cell grid) around each shark position before scaling each cell by collision zone use (z_t). Given that spatial density values were summed within each cell per individual per month, this allows for the possibility that a PSAT location and associated density was positioned in one of six 0.25 × 0.25° resolution cells surrounding the original location (7 in total, for 1.25° latitude by 0.75° longitude). By calculating the mean of surrounding vessel activity, this method reduces some of the potential bias related to the different error fields associated with PSAT and ARGOS tags (3, 15, 16).

To examine the sensitivity of potential collision exposure (E_i) and CRI to different values of collision zone use (z_t), further sensitivity analyses were run using feasible hypothetical values. In generating feasible alternatives, one collision zone use value was permuted and the other held at 45% (0.45) in accordance with the overall median of all records (45.7%, n = 39,143 depth records) and all individuals (45.5%, n = 97 tracks) (13). Scenarios were explored by calculating E_i using overall regional medians of collision zone use (z_t) without considering bathymetric environment (Table S3) and a theoretical ratio of 1:1 (0.45:0.45) for coastal and oceanic locations. Potential collision exposure (E_i) was also calculated with coastal collision zone use (z_t) fixed at 0.45 for ratios of 1:1.25 (0.45:0.5625), 1:1.5 (0.45:0.675), 1:1.75 (0.45:0.7875) and 1:0.75 (0.45:0.3375) and repeated with oceanic z_t fixed at 0.45. These variations account for a variety of surface use scenarios, with values ranging from 33.75% to 78.75% of total tracked time spent in waters shallower than 20 m. A further control analysis was performed within subset regions, where potential collision exposure (E_i) was calculated using collision zone values (z_t) derived from averaging surface use for individuals of different sex in the north Atlantic and across different months in the west Pacific (Table S19 and S20).

1.10 Collision risk index

Collision risk index (CRI) was calculated as the product of shark spatial density (D_{it}) and potential collision exposure index (E_i) (which is a product of vessel traffic density (v_t) and collision zone use (z_t)) (Table S1, see section 1.9 '*1.9 Potential collision exposure* index') and pertains to an individual shark per month. CRI represents the relative risk posed to a whale shark by vessels it may be exposed to within each occupied grid cell and was calculated as:

$$CRI = \frac{\sum_{t=1}^{n} e_t d_t}{n},$$

where CRI is the collision risk index for an individual shark per month, e_t is the potential collision exposure in grid cell t occupied by a whale shark within a month of its track, d_t is the relative density contribution for all location estimates of an individual shark summed in grid cell t within a month of its track, and n is the number of grid cells occupied by an individual whale shark within a month of its track. To estimate typical risk for whale sharks, the mean CRI was calculated by averaging individual shark mean CRI (the average of monthly CRI values) values within each ocean region, sex and size class. Because in this study spatial density (d_t) is a relative measure without absolute units, CRI is also a relative index without units. CRI maps were created for each individual within a month of their track. CRI was averaged within each 0.25 × 0.25° grid cell across all monthly individual maps for the 12 months to generate a global map displaying the spatial variation of overlap and mean CRI that individuals potentially experience within the total space occupied by whale sharks (Fig. 4*A*).

To explore differences among regions and demographic groups, statistical analysis of the mean monthly CRI calculated for each individual whale shark was undertaken. Individual mean monthly CRI values were not normally distributed (Shapiro-Wilk normality test $p < 0.001$), so a Kruskal-Wallis test was selected (with Pairwise Wilcoxon rank-sum tests selected for post hoc comparisons and corrected for multiple comparisons). Due to the difference in the number of tagged individuals in each region (NA, n = 39 tracks; NIO, n = 44 tracks; SIO, n = 26 tracks; EIO, n = 74 tracks; WP, n = 62 tracks; EP, n = 89 tracks), groups of 25 individuals were randomly selected and the Kruskal-Wallis tests performed. The south Atlantic was removed from this analysis due to the lower sample size in the region (n = 14 tracks). This procedure was repeated 1000 times and the percentage of times that significance ($p < 0.05$) was observed was recorded. For comparison between the sexes, individuals of unknown sex were removed prior to running the tests (male, n = 165, female, n = 106, unknown, n = 77). For comparison among size classes, individuals of an unknown size were removed as were those classed as >12 m in total length due to small sample size (n = 4 tracks), and groups of 10 individuals were randomly selected and the Kruskal-Wallis tests performed (3 m, n = 10 tracks; 3-6 m, n = 126; 6-9 m, n = 124 tracks; 9-

12 m; n = 27 tracks). The same procedure was used for comparisons between the Gulf of Mexico, the Arabian Gulf and the Red Sea (GOM, n = 37 tracks; AG, n = 14 tracks; RS, n = 26 tracks).

1.11 Relationship of CRI with scar frequency and known mortality

To explore the relationship between estimated CRI and documented vessel interactions with small vessels (through measures of vessel-related whale shark scarring frequency), spatially gridded CRI values derived from the mapped global mean (Fig. 4*A*) were averaged around local regions where published records of vessel related scarring were also available (Table S9). Mean regional CRI was calculated for each region by summarising CRI cells within a 12 × 12-cell grid around each reported study site (fixed 3 × 3° buffer region in which 3° ≈ 333 km, >10 times the upper 95% confidence intervals of the mean daily movement distances of whale sharks, C.I. = 21.57 km). It is possible that the recorded vessel-related shark injuries occurred outside of this buffer area, given the propensity of whale sharks to make long distance movements (Table S2). However, scarring has been used as a preliminary metric of local small vessel threats to this species in the absence of other data and this justification was applied in our analysis (see references in Table S9). Formally reported vessel-related scars included in this analysis were limited to those that were explicitly stated as resulting from a collision, although origin of injuries were not standardised across all study sites (see section 4.7 *'Collision risk index and scar frequency analysis'*).

To investigate whether CRI values were potentially indicative of mortality risk and relevant in a real-world context of shark and large vessel overlap, we explored the relationship between estimated CRI and confirmed mortality cases reported throughout the study regions. For the first time, we compiled a comprehensive collision-related mortality database for whale sharks (Table S8*A*). Through literature and online searches and communications with experts in the field, we recorded every known whale shark direct mortality that resulted from a collision with a large vessel, dating back to the 1930s. Each mortality case was mapped based on the closest geographical position available. In some cases, an exact position where the collision occurred was provided. In others, cases related to ports where the collision became apparent on a vessel's arrival or were recorded as occurring in a general area rather than a specific point in space. For this reason, we assigned each mortality case to within one of the broad regions used in our study. As a first step, we compared the number of mortality cases per region to our mean monthly CRI estimates to explore the relationship between potential large vessel collision risk experienced by the individuals tracked in our study and incidence of actual large vessel induced mortality cases that occurred in the same region. Due to the sparse vessel mortality data available for whale sharks, we explored sensitivity of our correlation outcomes by removing regions in turn and re-performing the test (Table S8*B*).

1.12 Horizontal and vertical movements in relation to shipping routes

The tracking data were used to examine vessel densities occurring along individual shark tracks and at the final reported satellite locations of individual whale sharks. Several ARGOS tracked sharks from each region (where suitably long tracks were available) were selected to explore where individuals crossed vessel routes when moving to and away from seasonal aggregation areas (Table S15). For this analysis, mean total vessel density (2011-2014 annual mean) was extracted for each location along a track and plotted in space and time. Additionally, among all the PSAT tracked sharks we analysed, there were some cases where the last vertical descent exceeded the maximum depth limit of the tag and the automatic release was triggered that detached the tag from the shark, enabling the device to float to the surface where it relayed depth and other data to ARGOS satellites. For these individuals, depth profiles were examined to explore vertical space use and determine if the final vertical descent to the tag's depth limit at the end of the track was indicative of a slowly sinking dead whale shark, potentially due to ship strike mortality, as opposed to a normal deep dive recorded from a live whale shark. One tag was physically recovered such that the entire track's archival depth time-series at 1 min intervals was available for detailed analysis. For the remaining sharks, depths were extracted from satellite-transmitted profiles of depth and temperature (PDT) assigned to sampling bins. Depths extracted from PDT sampling bins were assigned appropriate timestamps based on the sampling interval and number of bins. This method ensures each recorded depth is assigned an equal proportion of sampling interval time and provides the most parsimonious estimate of time at depth without more detailed archival time-series depth data being available. Reconstructed depth profiles were visually examined and those where the last vertical movements of the tag involved a descent and tag release >1000 m depth were plotted in space and the mean vessel density within the 1 × 1° grid cell where the tag attachment ended was calculated.

The last known satellite-transmitted locations of marine megafauna are a potentially valuable tool to infer mortality events (21, 22). Satellite transmissions will cease to be received by satellites when the transmitter is not dry (in air above the sea surface), therefore whale shark ship strike leading to mortality is expected to lead to cessation of transmissions as a whale shark will sink when dead (see section 4.1.1 *'Using tracking data to infer mortality'*). Whilst transmitters can fail and cease transmitting for a number of reasons unrelated to mortality (22, 23), we reasoned based on previous analyses (22, 23) that normal technical failures would occur randomly along a shark's trajectory rather than being more frequently associated in areas with higher vessel activity. In contrast, if whale shark mortalities due to ship strike were occurring frequently enough to contribute to an observed decrease in population numbers, then one possible signature of mortality occurring – in the absence of reported direct observations in tracked locations – would be that a last location occurs within a busy shipping lane (greater vessel activity) more often than expected (hypothesis 1) compared with random failure or loss that should be unrelated to shipping routes (hypothesis 2). The expectation of hypothesis 1 was

higher vessel density in the last grid cell where a shark was located than would be expected due to random chance, whereas the expectation of hypothesis 2 was that vessel density in last-location grid cells should be no different to random. The hypotheses were tested in two independent, complementary analyses. Firstly, the final location of all tracks (n = 348 tracks) was plotted over the main vessel dataset (2011-2014 annual mean) at a 1 × 1° resolution scale using mapping software. The overlap coefficient (*OC*) (24, 25) was calculated:

$$OC = 2\sum_t(p_{at}p_{bt})/(\sum_t p_{at}^2 + \sum_t p_{bt}^2),$$

where p_{at} represents the vessel density in grid cell t and p_{bt} represents the density of shark locations in grid cell t. This calculation provides a measure of overlap ranging from 0 (no overlap) to 1 (complete overlap) and accounts for the proportions of vessels and sharks within the entirety of the grid. The mean vessel density encountered in the shark final locations was also calculated using this method. To determine whether either measure for the final locations was higher than expected by chance, 100 alternative location sets were generated by randomly selecting one location (other than the final location) from each of the shark tracks. These randomly selected locations represent actual locations visited by the sharks that could have been the final location where the track ended potentially due to normal transmission failures or losses of tags. Overlap measures for all randomised location sets were computed and were compared using a one sample *t*-test. To complement this method an independent analysis was undertaken on the final locations of ARGOS tracked sharks only (n = 256 tracks), as these tags have greater spatial accuracy than PSAT tag tracks that were included in the previous test in addition to ARGOS tag tracks. This test allowed for any potential bias of the greater spatial location error of PSAT tags to be removed from assessing the vessel density in last locations of tracked whale sharks. In this analysis, the mean monthly vessel density within a cell was extracted for each final location corresponding to the same month as the location from the main dataset (2011-2014). Locations with no associated vessel data (too close to land) and less than 10 tracking days were removed from the analysis. For the remaining final locations (n = 184 locations), 100 random locations were generated from within the minimum convex polygon of the corresponding track. This technique assumes that the track could have ended anywhere within the area utilised by a specific shark. Mean monthly vessel density was extracted for each of the random points from the same month as the real final location. For each run (n = 100), the sum of vessel density was calculated from a set of the randomised locations which were then compared to the summed vessel density of the actual shark final locations using a one sample *t*-test. This was performed for all locations and repeated for those in oceanic waters only (>200 m depth, n = 98 locations).

For ARGOS tag tracks where we received transmitted diagnostic information (n = 62 tracks), we searched for indicators of battery exhaustion and bio-fouling to determine if these factors led to tag failure and a resultant cessation of transmissions (Fig. S14) (22). To assess battery exhaustion, we

developed two indicators to filter tracks: (*i*) battery voltage dropped below 3.0 V at any point in the track, and (*ii*) battery voltage dropped consecutively in 2 or more of the last 5 tag status transmissions (22). Because whale sharks do not exhibit a regular surfacing pattern and vary their use of the uppermost layer where tags can break the surface, relay of diagnostic and status information was often sporadic. It was possible, therefore, for battery voltage to drop below 3.0 V during a transmission but relay above 3.0 V on subsequent transmissions after recharging at depth. For this reason, we classified tags as ending due to battery exhaustion only if both (*i*) and (*ii*) indicators were apparent in the status information (Fig. S14 *A* and *B*). To assess the extent of bio-fouling we reviewed the wet and dry states of the saltwater switch using two indicators: (*iii*) the maximum dry state (arbitrary) value dropped below 150 on the final transmission, and (*iv*) the maximum dry state values dropped by more than 25% of the overall maximum in the last 5 tag status transmissions (22). Due to the aforementioned irregular surfacing behaviour of whale sharks, and the positioning of tags in the first dorsal region where animal movement may influence drying or the extent of the device that breaks the surface, we found that the maximum dry status values fluctuated over time. We therefore classified tags as failing due to bio-fouling only if both (*iii*) and (*iv*) indicators were apparent in the status information (Fig. S14 *C* and *D*). We carefully visually inspected status plots for all cases where battery exhaustion or bio-fouling was indicated for the tracks where we had available diagnostic information (n = 62 tracks). Of these, 12.9% (n = 8 of 62 tracks) occurred on busy vessel routes (Fig. S14).

Finally, to explore opportunities for collision mitigation, whale shark movements were mapped by calculating the number of track lines (trajectories) transecting 1 × 1° grid cells. The cells with the highest number of trajectories were then mapped within a boundary polygon. Track trajectory polygons demonstrated important geographic areas for whale sharks passing into and away from seasonal aggregation sites that were used by multiple individuals. The number of individuals present within each polygon was calculated on monthly timescales to explore seasonal variability and highlight the potential of combined tracking datasets to provide temporally dependent mitigation opportunities for whale sharks and other megafauna species at risk of collision.

2. Supplementary Tables

Table S1 | Risk metrics and definitions of concepts used to quantify collision risk adapted from elasmobranch (3) and cetacean research (13).

Metric	Definition	Details	Source
Traffic density	Mean number of vessels within a given 0.25 × 0.25° grid cell in a relative month (main analysis = mean month from years 2011-2014).	Unit is mean monthly vessel count. See *Supplementary Methods* section 1.4 *'Global vessel traffic'*.	ExactEarth (www.exactearth.com) Global Fishing Watch (www.globalfishingwatch.org) NOAA (fine-scale) (www.coast.noaa.gov)
Whale shark spatial density	Weighted and normalised density per individual whale shark within a given 0.25 × 0.25° grid cell for each month in a track*.	Unit of this risk metric is relative. Spatial density is calculated on an individual, monthly basis. See *Supplementary Methods* sections 1.3 '*Track Processing'* and 1.7 '*Spatial density analysis'*.	Satellite telemetry analysis
Whale shark collision zone use	Proportion of total tracked time spent at or near the surface (≤ 20 m or ≤ 25 m for the east Pacific) where whale sharks may be potentially susceptible to collision with an oncoming vessel.	A fraction between 0 and 1. Calculated spatially for average time spent near the surface in coastal and oceanic locations. See *Supplementary Methods* section 1.6 '*Whale shark collision zone use'*.	PSAT dive analysis
Potential collision exposure index	The number of vessels that a whale shark, if co-occurring within a given 0.25 × 0.25° grid cell with vessels, would be exposed to and therefore potentially susceptible to collision with when near the surface*.	Potential collision exposure index = traffic density × collision zone use. Unit is mean monthly number of vessels. See *Supplementary Methods* section 1.9 *'Potential collision exposure index'*.	Calculated based on previously described metrics
Collision risk index	The relative monthly susceptibility of individual whale sharks to potential collision with vessel traffic. Individuals will be at most risk when occupying regions with high vessel traffic density where occasions for interactions are also high. Collision estimates are based on the degree of spatio-temporal co-occurrence (hence susceptibility), rather than providing a probability estimate of an actual ship strike (vulnerability)*.	Potential collision exposure index scaled by whale shark spatial density. Given that the unit of shark spatial density is relative, the unit for collision risk index is arbitrary and is therefore used to indicate relative differences on spatio-temporal scales. Calculated on an individual, monthly basis. See *Supplementary Methods* section 1.10 *'Collision risk index'*.	Calculated based on previously described metrics

* For analyses involving lower accuracy PSAT tags (n = 92 tracks) cell smoothing and spatial averaging was used when creating maps and performing calculations to account for some of the potential bias related to the different error fields associated with PSAT and ARGOS tags (3, 15, 16) (see *Supplementary Methods*).

Table S2 | Satellite tracking summary information for 348 whale sharks tagged from 2005 to 2019 in the Atlantic, Indian, and Pacific oceans. Tag ratios denote ARGOS:PSAT tracks, sex ratios denote Male:Female:Unknown individuals, and total length refers to the median (mean ± s.d. (range)) size of individuals in metres (m).

(A) Track summary

Region	Total tracks	Tag type ratio	Sex ratio	Total length (m)	Tracking date range	Sum tracking duration (d)	Mean tracking duration (d)	Sum transmitting days (d)	Mean transmitting days (d)	Total distance travelled (km)	Mean distance travelled (km)	Mean speed (km d^{-1})
East Indian Ocean	74	74:0	44:17:13	6.2 (6.32 ± 1.61 (3.0-10.0))	2005-2019	11663	157.61	3216	43.46	143253.70	1935.86	19.70
East Pacific	89	75:14	5:38:46	10.0 (9.51 ± 2.37 (4.0-13.1))	2007-2018	9854	110.72	3611	40.57	184799.00	2076.39	25.18
North Atlantic	39	12:27	21:18:0	7.5 (7.36 ± 0.93 (4.9-9.0))	2005-2020	5425	139.10	1605	41.05	102607.16	2630.95	24.69
Northwest Indian Ocean	44	7:37	16:14:14	4.5 (4.97 ± 1.66 (3.0-8.0))	2009-2014	5777	131.30	752	17.09	35327.84	802.91	8.22
South Atlantic	14	5:9	7:7:0	9.0 (8.89 ± 1.50 (6.5-11.0))	2010-2019	1567	111.93	229	16.36	18414.60	1315.33	16.40
Southwest Indian Ocean	26	22:4	20:6:0	6.0 (6.18 ± 1.13 (4.0-8.7))	2006-2017	1596	61.38	834	32.08	34906.74	1342.57	28.42
West Pacific	62	61:1	52:6:4	5.5 (5.41 ± 1.03 (3.0-7.5))	2009-2020	16364	263.94	5261	84.85	164970.30	2660.81	12.96
Global	**348**	**256:92**	**165:106:77**	**6.5 (6.62 ± 2.13 (3.0 – 13.1))**	**2005-2020**	**52246**	**150.13**	**15508**	**44.56**	**684279.30**	**1966.32**	**19.53**

(B) Previously published literature using local track data included in this study.

Region	Track data primary literature
East Indian Ocean	Norman *et al.* (2016) (26) Sleeman *et al.* (2010) (27) Reynolds *et al.* (2017) (28)
East Pacific	Hearn *et al.* (2016) (29) Guzman *et al.* (2018) (30)
North Atlantic	Hueter *et al.* (2013) (31) Tyminski *et al.* (2015) (32) de la Parra *et al.* (2011) (33) Hazin *et al.* (2008) (34)
Northwest Indian Ocean	Robinson *et al.* (2017) (35) Berumen *et al.* (2014) (36) Rowat *et al.* (2007) (37)
South Atlantic	Perry *et al.* (2020) (38) Hazin *et al.* (2008) (34)
Southwest Indian Ocean	Diamant *et al.* (2018) (39) Rohner *et al.* (2018) (40) Rowat *et al.* (2007) (41)
West Pacific	Araujo *et al.* (2018) (42) Meyers *et al.* (2020) (43)

Table S3 | Collision zone use analysis summary performed using time-at-depth histogram files from 97 individuals. Significance column displays the Kolmogorov-Smirnov test results comparing median surface time between coastal and oceanic associated depth records.

Region	Total tracks	Depth records	Median surface time (%)	Mean (± s.d.) surface time (%)	Depth records with locations	Depth category	Depth records by category	Median surface time (%) by category	Mean (± s.d.) surface time (%) by category	Significance
North Atlantic	24	5691	64.30	60.33 (34.76)	3528	Coastal	877	63.90	60.57 (32.58)	<0.001***
						Oceanic	2651	73.70	65.34 (33.99)	
East Indian	9	1996	33.50	39.17 (27.35)	756	Coastal	715	42.50	45.79 (26.72)	<0.01**
						Oceanic	41	62.60	55.90 (30.58)	
Northwest Indian Ocean	18	2133	44.60	48.18 (30.92)	568	Coastal	486	55.70	53.66 (33.29)	0.3384^{ns}
						Oceanic	82	49.75	50.79 (30.17)	
Southwest Indian Ocean	4	701	65.60	62.62 (25.91)	490	Coastal	101	66.20	60.73 (25.47)	0.2015^{ns}
						Oceanic	389	67.20	64.15 (25.46)	
East Pacific Ocean	4	58	42.65	46.45 (30.54)	50	Coastal	0	-	-	-
						Oceanic	50	47.35	49.84 (29.51)	
West Pacific	38	28564	43.80	46.94 (28.41)	12118	Coastal	5968	55.90	56.46 (27.19)	<0.001***
						Oceanic	6150	47.60	49.74 (29.65)	
Global	**97**	**39143**	**45.7**	**48.84 (29.97)**	**17510**	**Coastal**	**8147**	**55.50**	**55.80 (28.40)**	**-**
						Oceanic	**9363**	**53.70**	**54.80 (31.60)**	

Table S4 | Summary of close passes, defined here as closest point-of-approach (CPA) time differences within 20 minutes at distances within 20 km, between two FastLoc® GPS tracked whale sharks in the Gulf of Mexico and high-resolution vessel tracking data obtained from https://coast.noaa.gov/.

(A) Tracking data summary where number of intersections refers to the total number of vessel track lines that intersected lines between whale shark locations within the same temporal range. Intersections per distance travelled relates to number of shark-vessel intersections per 1 km travel distance.

Shark ID	Sex	Total length (m)	Start date	End date	Tracking duration (d)	Transmitting days	Total distance travelled (km)	Speed (km d^{-1})	Number of locations	Number of locations per day (mean ± s.d. (range))	Number of intersecting vessel tracks	Vessel speed (m s^{-1}(knots))	Intersections per distance travelled
gsmp01792	M	4.90	14-Jun-18	29-Sep-18	107	21	2312.36	21.61	38	1.86 ± 1.15 (1-4)	696	5.98 (12)	0.30
gsmp01793	F	7.15	14-Jun-18	27-Aug-18	74	43	1851.71	25.02	213	4.98 ± 3.43 (1-12)	155	4.99 (10)	0.08

(B) Closest point-of-approach (CPA) summary where speeds relate to travelling speeds at CPA associated points. Where vessel draft information (which varies depending on load) was not available for the CPA, reported draft was obtained from the associated MMSI number from www.marinetraffic.com.

Shark ID	Vessel ID	CPA time difference (minutes)	CPA distance (km)	Vessel type	Draft (m)	Shark speed (m s^{-1})	Vessel speed (m s^{-1})	Vessel speed (knots)
gsmp01793	238294000	0.25	5.76	Tanker	8.0	0.50	6.06	11.78
gsmp01793	367612470	0.32	11.51	Cargo	6.0	0.49	4.88	9.49
gsmp01793	367659780	7.03	18.21	Passenger	7.0	0.65	0.61	1.19
gsmp01793	367659780	7.68	12.49	Passenger	7.0	0.50	0.28	0.54
gsmp01793	367691280	1.20	8.44	Cargo	3.5	0.24	0.03	0.06
gsmp01793	368001000	16.25	9.96	Other	6.0	0.50	5.62	10.93
gsmp01793	368009890	1.25	9.79	Dredger	2.0	0.20	2.20	4.28
gsmp01793	240990000	0.13	15.46	Tanker	13.3	0.50	5.24	10.19
gsmp01793	636015834	0.20	18.37	Tanker	14.5	0.49	7.04	13.69
gsmp01793	246456000	1.00	16.67	Cargo	10.7	0.24	6.58	12.79
gsmp01793	366989820	0.65	19.08	Tug	7.0	0.28	4.95	9.62
gsmp01793	366989820	1.50	3.77	Tug	7.0	0.27	4.68	9.10
gsmp01793	367527570	8.75	18.98	Other	1.9	0.08	2.93	5.70
gsmp01793	367570080	0.57	7.43	Tug	9.0	0.05	3.21	6.24
gsmp01792	366999703	0.58	17.26	Other	1.7	0.15	3.10	6.03
gsmp01792	367296000	0.40	8.57	Other	4.0	0.09	2.95	5.73
gsmp01792	367296000	0.88	10.30	Other	5.0	0.43	0.84	1.63
gsmp01792	367527750	0.45	11.29	Other	1.9	0.32	2.17	4.22
gsmp01792	368413000	0.03	17.24	Tug	6.9	0.30	6.02	11.70
gsmp01792	566256000	0.25	14.27	Cargo	10.8	0.15	5.54	10.77
gsmp01792	566256000	0.90	15.06	Cargo	10.8	0.02	5.61	10.91

Table S5 | Summary of quotes related to whale shark behavioural responses to vessels including a combination of informal anecdotes and formalised observations sourced from literature dating back to the first taxonomic description in 1829.

Year	Region	Quote	Context	Reference
1829	Cape, South Africa	*'At the time it was discovered, it was swimming leisurely near the surface of the water, and with a certain portion of its back above it. When approached, it manifested no great degree of fear, and it was not before a harpoon was lodged in its body that it altered its course and quickened its pace.'*	First ever formal taxonomic description of a whale shark	Smith (1829)
1870	Seychelles	*'…it now and then rubs itself against a large piroque, as a consequence upsetting it, but under such circumstances it never attacks or molests men.'*	Comments from one of the earliest authorities on whale sharks	Write (1870)
1915	Miami, Florida	*'I was surprised that the fish did not put up any fight. He proved to be a sluggish monster and seemed to fail to realize that anything particular was happening to him.'* *'…the second Florida specimen, at whose capture he was present, did not seem to be frightened at the approach of boats, made no resistance when harpooned, when shot, or when pulled to the surface…'*	In reference to captured whale sharks and events surrounding capture	Gudger (1915)
1927	Various	*'…all comment upon the fact that this shark in these waters shows no fear of boats or men. And even when attacked it makes no effort to retaliate, but solidly pursues its unchecked and for the most part undisturbed way.'*	Comments from five seamen	Gudger (1927)
1928	Cuba	*'The fish was sluggish and stupid, making no demonstration even when the boat was 'nosed' up against him.'*	In reference to a 32 ft shark estimated 9 tons in weight in Cuba	Gudger (1928)
1936	Bimini, Bahamas	*'The boat followed it around for about an hour, but the fish showed no fear of it whatever. The boat was 36 ft long and by getting as nearby alongside the shark as possible, the length of the fish was estimated as fully as great as that of the boat.'*	In reference to a whale shark followed by a 36 ft boat	Gudger (1936)
1936	Havana, Cuba	*'One of the party was fighting a marlin when the whale shark came swimming fearlessly up toward the stern of the yacht'*	In reference to a whale shark approaching a fishing yacht	Gudger (1936)
1938	Western Panama	*'…while a whale shark was lying at the surface to one side of the vessel. Suddenly, for some unknown reason, the great fish swam directly across the vessel's course and was caught on her bow.'*	In reference to a shark stuck and killed in the east Pacific	Gudger (1938)
1938	California	*'…it's desire to eat the bait thrown out by the fishing boats as 'chum' for tuna, lead it to 'hang around' these boats, and its sluggishness not infrequently leads to its getting 'bumped' by them. In the cases cited, the fish may have swum across the bow of the boat or may have lain inert in her course. I have record of a Rhincodon which swam so leisurely across the path of a vessel that it was missed by a few feet only.'*	In reference to multiple collisions being noted around fishing boats in California	Gudger (1938)

Table S5 | Continued

Year	Region	Quote	Context	Reference
1938	Various	*'It has been observed swimming so closely to vessels as to leave the impression that it was inspecting them.'*	Comment on species habit	Gudger (1938)
1939	Hawaii	*'..it was again seen swimming about under the stern amid slops and scraps thrown overboard from the ship's galley. "It swam leisurely around for about 20 minutes, bumping into the mooring lines a number of times…"…'*	Comments from ship captain and hydrographer	Gudger (1939)
1939	Gulf of Mexico	*'They were entirely unafraid, indeed one left the school and came alongside the ship and then went back again.'* *'They were not disturbed by the ships passing them at a distance (to the nearest) of about 20 ft but swam lazily along and "did not appear to be going anywhere."'* *'The fish were not afraid, though the vessel passes so closely that her wash broke over them. Mr. Parsons reports that had the nearest one been in the ship's path, it would have been rammed, so sluggish was its motion.'* *'They too were so sluggish they made no attempt to get away from the steamer.'*	In reference to the comments of seamen operating in the Gulf of Mexico	Gudger (1939)
1939	Bahamas	*'Being without fear these sharks swam so close to the boat that "We could easily have jumped astride their backs"'* *'"We ran into one fish, but he did not seem greatly upset, and his efforts to get clear were quite sluggish"'*	In reference to the comments from the Hydrographic Office, USA	Gudger (1939)
1940	Gulf of Papua	*'…the great shark – the "boomer" – "an enormous, mottled brute [at least 40 ft long] … came right underneath the bow and then floated quietly astern on the top of the water. We could have touched him with our hands by leaning over the bulwarks." Then the great shark swam all round the vessel as if inspecting it.'* *'One "for a while drifted around the ship in very close proximity. It must have struck the ship, for its head had rubbed some of the red paint off our ship"'*	In reference to the comments of seamen operating in the western Pacific	Gudger (1941)

Table S5 | Continued

Year	Region	Quote	Context	Reference
2007	Various	*'Whale sharks sometimes appear to avoid boats by diving slowly toward the seabed, usually without noticeably changing their speed (pers. obs.), this may be in response to the low-frequency sound signature of motors as discussed in the sensory biology section.'*	Within a review of the behavioural ecology of whale sharks	Martin (2007) (44)
2010	Tofo, Mozambique	*'The odds ratio for boat proximity shows that for each extra metre between the shark and boat, the shark was 0.882 times less likely to show an avoidance response. Similarly, larger sharks were less likely to avoid the boat, with each metre of length decreasing avoidance responses by 0.620 times. Specific testing of boat proximity effects found mean approach distances of 5.57± 4.97 m and 7.67± 6.08 m in cases of avoidance and no avoidance, respectively. No avoidance responses were noted at proximities >20 m.'*	Exploration of the behaviour of whale sharks during interactions with small boats and swimmers recorded during commercial snorkelling trips.	Peirce *et al.* (2010) (45)
2014	Oslob, Philippines	*'Non-provisioned individuals were observed swimming slowly and showing curiosity, approaching snorkelers and boats alike, possibly attracted by the large amount of food dispersed in the water during the provisioning activities.'*	Based on longitudinal data at a site where daily provisioning activities took place and whale sharks were present every day.	Araujo *et al.* (2014) (46)
2015	Oslob, Philippines	*'Sharks were most likely to show a response when they were free swimming, in which case their behaviour was not reinforced by provision of food, while they were least likely to show avoidance while they were vertically feeding.'*	Based on an investigation of whale sharks at a provisioning site exploring arrival time, avoidance and feeding behaviour using photo-identification and focal follows.	Schleimer *et al.* (2015) (47)
2016	Ningaloo, Australia	*'Whale sharks changed direction more often when vessels were present. The number of behavioural changes was also correlated to the interaction duration, with more changes observed for longer interactions.'* *'…it is possible that whale sharks may tolerate the presence of a vessel, thus maintaining their behaviour, if the need to thermoregulate or feed is critical, as observed in this study with the high number of 'neutral' behaviours.'*	Examination of whale shark behaviour using fixed-wing aerial surveys in Ningaloo Marine Park.	Raudino *et al.* (2016) (48)
2020	Oslob, Philippines	*'Our results also highlight that whale sharks are more likely to display avoidance in the event of a roadblock, wherein the animal's direction of travel is obstructed…Contrastingly, the individuals that were observed feeding (either vertically or horizontally) were less likely to display avoidance behaviours and react to external stimuli.'*	Based on in-water behavioural observations of whale sharks.	Legaspi *et al.* (2020) (49)

Table S6 | Mean monthly spatial overlap and collision risk index (CRI) for ocean region, sex and size class calculated at a 0.25 × 0.25° grid cell resolution scale. Mean CRI is the mean monthly collision risk whale sharks were exposed to within areas they occupied (*Supplementary Methods*). S.D., ± one standard deviation of the mean; S.E., ± one standard error of the mean. Ocean regions were selected based upon whale shark distribution, geographical features, and defined Food and Agriculture Organization major fishing area boundaries (Fig. S2*A*).

(A) Regional. Calculated mean monthly spatial overlap and collision risk index (CRI) globally and within the 7 defined ocean regions.

Region	Total tracks	Mean monthly spatial overlap (%)	Median	±.S.D.	± S.E.	Mean monthly CRI	Median	± S.D.	± S.E.
Global	348	92.44	100.00	14.13	0.76	1.89E-03	7.17E-04	3.93E-03	2.11E-04
East Indian Ocean	74	86.63	91.67	14.00	1.63	8.29E-04	6.65E-04	6.92E-04	8.04E-05
East Pacific	89	92.72	100.00	18.89	2.01	1.42E-03	3.11E-04	3.51E-03	3.74E-04
North Atlantic	39	98.27	100.00	2.82	0.45	2.77E-03	1.25E-03	4.45E-03	7.13E-04
Northwest Indian Ocean	44	96.89	100.00	5.84	0.88	6.68E-03	3.95E-03	7.08E-03	1.07E-03
South Atlantic	14	100.00	100.00	0.00	0.00	2.84E-04	1.64E-04	2.37E-04	6.34E-05
Southwest Indian Ocean	26	99.24	100.00	3.30	0.65	5.71E-04	2.77E-04	5.88E-04	1.15E-04
West Pacific	62	87.61	91.67	14.90	1.89	7.67E-04	5.74E-04	7.03E-04	8.93E-05

(B) Sex. Calculated mean monthly spatial overlap and CRI for all individuals and within each sex (and unknown sex).

Sex	Total tracks	Mean monthly spatial overlap (%)	Median	± S.D.	± S.E.	Mean monthly CRI	Median	± S.D.	± S.E.
All	348	92.44	100.00	14.13	0.76	1.89E-03	7.17E-04	3.93E-03	2.11E-04
Male	165	91.19	99.86	13.22	1.03	1.90E-03	6.70E-04	4.27E-03	3.33E-04
Female	106	95.04	100.00	10.48	1.02	1.34E-03	4.18E-04	2.90E-03	2.82E-04
Unknown	77	91.55	100.00	19.27	2.21	2.62E-03	8.59E-04	4.33E-03	4.97E-04

(C) Size class. Calculated mean monthly spatial overlap and CRI all individuals and within the 5 size classes (and unknown size).

Size class (m)	Total tracks	Mean monthly spatial overlap (%)	Median	± S.D.	± S.E.	Mean monthly CRI	Median	± S.D.	± S.E.
All	348	92.44	100.00	14.13	0.76	1.89E-03	7.17E-04	3.93E-03	2.11E-04
3	10	96.40	98.19	5.25	1.66	6.05E-03	3.02E-03	6.59E-03	2.09E-03
3-6	126	90.15	97.23	13.60	1.21	1.65E-03	6.61E-04	3.84E-03	3.42E-04
6-9	124	94.43	100.00	10.35	0.93	1.90E-03	8.32E-04	3.73E-03	3.35E-04
9-12	27	95.46	100.00	13.28	2.56	2.09E-04	1.71E-04	2.15E-04	4.13E-05
>12	4	87.63	96.68	20.40	10.20	3.87E-05	2.56E-05	3.86E-05	1.93E-05
Unknown	57	91.38	100.00	21.33	2.85	2.59E-03	8.47E-04	4.51E-03	6.03E-04

Table S7 | Effect of different vessel types on the mean monthly spatial overlap of whale sharks and vessels (%) and collision risk index (CRI) calculated at a 0.25 × 0.25° grid cell resolution scale.

		Vessel Type											
		All		Cargo		Fishing		Passenger		Tanker		Other	
		Mean	Median	Mean	Median	Mean	Median	Mean	Median	Mean	Median	Mean	Median
Global	%	92.44	100.00	82.31	94.44	34.70	30.00	47.79	47.50	73.66	85.26	85.25	92.43
	CRI	1.89E-03	7.17E-04	9.59E-04	3.08E-04	1.22E-05	3.56E-06	4.15E-05	1.00E-05	5.07E-04	8.29E-05	3.67E-04	1.20E-04
East Indian Ocean	%	86.63	91.67	82.87	90.00	46.76	50.00	39.70	37.12	72.42	80.28	77.09	84.67
	CRI	8.29E-04	6.65E-04	3.75E-04	2.29E-04	1.40E-05	7.56E-06	1.41E-05	4.52E-06	1.04E-04	6.14E-05	3.22E-04	2.18E-04
East Pacific	%	92.72	100.00	80.60	95.87	49.30	50.00	36.43	29.27	71.68	83.99	82.46	89.83
	CRI	1.42E-03	3.11E-04	7.69E-04	1.79E-04	2.15E-05	4.92E-06	5.63E-05	3.43E-06	2.34E-04	4.59E-05	3.39E-04	3.42E-05
North Atlantic	%	98.27	100.00	97.40	98.87	22.61	14.29	71.98	78.29	92.78	95.53	96.62	98.19
	CRI	2.77E-03	1.25E-03	1.50E-03	6.54E-04	4.31E-06	1.42E-06	8.36E-05	3.53E-05	8.16E-04	4.71E-04	3.60E-04	1.88E-04
Northwest Indian Ocean	%	96.89	100.00	83.69	92.96	31.20	24.63	52.42	53.85	72.83	85.21	95.31	99.44
	CRI	6.68E-03	3.95E-03	3.15E-03	1.90E-03	1.29E-05	2.92E-06	2.88E-05	1.75E-05	2.38E-03	1.02E-03	1.12E-03	7.87E-04
South Atlantic	%	100.00	100.00	99.88	100.00	24.21	25.60	55.23	59.82	63.09	62.70	87.02	86.38
	CRI	2.84E-04	1.64E-04	1.20E-04	9.55E-05	2.75E-06	1.70E-06	3.09E-05	1.08E-05	3.33E-05	1.84E-05	9.74E-05	3.35E-05
Southwest Indian Ocean	%	99.24	100.00	93.30	100.00	43.34	47.35	48.34	50.00	90.68	95.09	92.33	96.92
	CRI	5.71E-04	2.77E-04	4.20E-04	1.93E-04	6.50E-06	3.67E-06	8.10E-06	5.70E-06	7.58E-05	4.97E-05	6.06E-05	4.93E-05
West Pacific	%	87.61	91.67	65.05	73.51	8.38	0.00	53.18	52.12	61.75	68.89	81.26	83.33
	CRI	7.67E-04	5.74E-04	4.44E-04	3.00E-04	5.82E-06	0.00	5.24E-05	3.77E-05	1.43E-04	9.71E-05	1.23E-04	1.00E-04

Table S8 | Compiled global mortality database for lethal collisions between whale sharks and large vessels.

(A) Mortality database

Source (year published)	Year	Month	Closest location	Reported speed (knots)	Vessel name	Vessel type	Vessel journey (From > To)	Shark size (m)
E. Gudger: A second whale shark impaled on the bow of a steamer (1927)	1922	May	17° 57'S 38° 41'W	n/a	American Legion	Passenger		9
E. Gudger: A second whale shark impaled on the bow of a steamer (1927)	1924	July	4° 28'N 6° 24'W	n/a	Aba	Cargo		n/a
E. Gudger: A whale shark rammed by a vessel off the Pacific coast of Western Panama (1938)	1932	May	8° 14'N 82° 46'W	n/a	Talamanca	Cargo	Panama > Puerto Armuellas	5
E. Gudger: A whale shark rammed by a steamer off Colombo, Ceylon (1937)	1932	November	7° 5'N 77° 50'E	n/a	Johan van Oldebarnevelt	Passenger		n/a
E. Gudger: A whale shark rammed by a steamer off Colombo, Ceylon (1937)	1933	May	Port Sudan	n/a	Francesco Crispi	Destroyer	Port Sudan >	7.5
H. Delsman: Basking Shark in the Bab el Mandeb (1934)	1933	November	Island of Perim	n/a	Johan van Oldebarnevelt	Passenger		7
E. Gudger: A whale shark speared on the bow of a steamer in the Caribbean Sea (1937)	1934	April	South Caribbean Sea	18.5	Santa Lucia	Steamer	Cristobal > Cartagena	12
E. Gudger: A whale shark impaled on the bow of a steamer near the Tuamotus, South Seas (1937)	1934	September	13° 59'S 147° 46'W	16	Maunganui	Passenger		17
E. Gudger: Four whale sharks rammed by steamers in the Red Sea region (1938)	1936	January	14° 50'N 54° 44'E	15	President Wilson	Liner	Bombay > Suez Canal	14
E. Gudger: Four whale sharks rammed by steamers in the Red Sea region (1938)	1937	April	15° 31'N 41° 15'E	17	President Wilson	Liner	Colombo > Suez Canal	9
E. Gudger: Whale sharks struck by fishing boats off the coast of lower California (1938)	1938	May	24° 25'N 110° 13'W	n/a	Navigator	Schooner		9
D. Rowat: Personal observation (2000) referenced in Speed *et al.* (2008) (50)	2000	n/a	n/a	n/a	n/a	Warship	Seychelles >	n/a
El Telégrafo: Muere tiburón ballena que se había varado en Santa Marianita (2015) [The Telegraph: Whale shark that had been stranded in Santa Marianita dies]	2015	April	Santa Marianita	n/a	n/a	n/a		9
The Jakarta Post: Boat hits whale shark in Jayapura waters (2016)	2016	August	Jayapura waters	n/a	KM Labobar	Passenger	Serui > Jayapura	4
The Jordan Times: Aqaba whale shark 'died after getting stuck in vessel engine' (2017)	2017	July	Aqaba Port	n/a	n/a	n/a		n/a
Progreso Hoy: Aparece tiburón ballena durante el atraque de un buque en Puerto Progreso (2019) [Progreso Hoy: Whale shark appears during the docking of a ship in Puerto Progreso]	2019	July	Puerto de Altura	n/a	Polar Costa Rica	Cargo	Port of Altamira > Progreso	4
The Pattaya News: Dead whale shark found lying on front of cargo ship in Si Racha (2021)	2021	May	Laem Chabang Port	n/a	Mount Nicholson	Cargo	Hong Kong > Bangkok	n/a

(B) Mortality correlation outputs generated by re-running correlation tests after removing regions.

Region removed	*P-value*	r
East Indian Ocean	0.0154	0.896
East Pacific	0.0038	0.949
North Atlantic	0.0292	0.856
Northwest Indian Ocean	0.1733	0.637
South Atlantic	0.0346	0.843
Southwest Indian Ocean	0.0330	0.847
West Pacific	0.0266	0.863

Table S9 | Local-scale collision risk index (CRI) summary and corresponding scar occurrence (% of population with evidence of vessel related scarring) gathered from published sources.

Ocean region	Sub-region	Mean CRI	± S.D.	Scar occurrence (%)	Sample size	Putative scar cause	Reference
North Atlantic	Holbox, Mexico	1.87E-03	3.11E-03	25.0	350	*'Evidence of collisions'*	Ramírez-Macías *et al*. (2012) (51)
	Utila, Honduras	6.88E-04	4.84E-04	3.2	95	*'Propeller scars'*	Fox *et al.* (2013) (52)
Northwest Indian Ocean	Djibouti	3.24E-03	4.42E-03	65.0	23	*'Impacts with boats, propellers or possibly fishing gear'*	Rowat *et al.* (2006) (37)
	Shib Habil, Red Sea	7.36E-03	9.86E-03	15.0	136	*'Reasonably be attributed to collisions'*	Cochran *et al.* (2016) (53)
	Qatar, Arabian Gulf	6.07E-03	5.94E-03	14.3	14	*'Defined propeller marks'*	Robinson *et al.* (2013) (54)
Southwest Indian Ocean	Mahe, Seychelles	1.88E-04	1.36E-04	22.8	797	*'Lacerations'*	Speed *et al.* (2008) (50)
	Mozambique	5.34E-04	4.11E-04	2.8	180	*'Lacerations'*	Speed *et al.* (2008) (50)
East Indian Ocean	Ningaloo, Australia	7.21E-04	5.43E-04	3.6	913	*'Rows of parallel lacerations'*	Lester *et al.* (2020) (55)
West Pacific	Oslob, Philippines	8.83E-04	9.29E-04	47.0	158	*'Propeller scars'*	Araujo *et al.* (2014) (46)
	Southern Leyte, Philippines	8.20E-04	8.04E-04	45.0	93	*'Propeller cuts'*	Araujo *et al.* (2017) (56)

Table S10 | Statistical differences between collision risk exposure scores (calculated at a 0.25 × 0.25° grid cell resolution scale) for regional, sex, size classes and between enclosed geographical sub-regions. Red cells represent the percentage between 75 and 100% and orange cells between 50 and 75% of significant tests (at $\alpha < 0.05$ level of significance) from 1000 tests in total, and green cells <50% of tests (full statistical details given in *Supplementary Methods*).

(A) Regional. Statistical differences between CRI scores for individuals occupying different regions where subsets of 25 individuals were randomly selected for each run.

	North Atlantic	East Indian Ocean	Northwest Indian Ocean	Southwest Indian Ocean	East Pacific
East Indian Ocean	80.1				
Northwest Indian Ocean	20.9	96.2			
Southwest Indian Ocean	100.0	1.6	99.8		
East Pacific	76.0	6.1	95.0	0.0	
West Pacific	86.9	0.4	98.2	0.1	0.1

(B) Size class. Statistical differences between CRI scores for individuals of different size class where subsets of 10 individuals were randomly selected for each run and classes <10 individuals were removed from the analysis.

	3 m	3-6 m	6-9 m
3-6 m	12.5		
6-9 m	3.7	1.2	
9-12 m	100.0	38.3	61.6

(C) Sex. Statistical differences between CRI scores for individuals of different sex where subsets of 25 individuals were randomly selected for each run.

	Female
Male	18.2

(D) Sub-regions. Statistical differences between CRI scores for individuals occupying different subregions where subsets of 10 individuals were randomly selected for each run.

	Arabian Gulf	Gulf of Mexico
Gulf of Mexico	76.0	
Red Sea	10.5	2.8

Table S11 | Effect of different grid cell size on the mean monthly spatial overlap of whale sharks and vessels (%) and collision risk index (CRI).

(A) All tracked sharks. Values were calculated for all tracked sharks (ARGOS transmitter, n = 256, PSAT transmitter, n = 92) and global vessel activity.

		Grid Cell Size									
		2 × 2°		1 × 1°		0.75 × 0.75°		0.5 × 0.5°		0.25 × 0.25°	
		Mean	Median	Mean	Median	Mean	Median	Mean	Median	Mean	Median
Global	%	100.00	100.00	100.00	100.00	99.99	100.00	99.84	100.00	92.44	100.00
	CRI	5.82E-03	2.71E-03	4.80E-03	1.93E-03	3.21E-03	1.43E-03	2.68E-03	1.04E-03	1.89E-03	7.17E-04
East Indian Ocean	%	100.00	100.00	100.00	100.00	100.00	100.00	100.00	100.00	86.63	91.67
	CRI	3.62E-03	2.59E-03	3.40E-03	2.11E-03	1.96E-03	1.60E-03	1.32E-03	1.08E-03	8.29E-04	6.65E-04
East Pacific	%	100.00	100.00	100.00	100.00	100.00	100.00	99.63	100.00	92.72	100.00
	CRI	5.46E-03	1.59E-03	4.76E-03	8.96E-04	2.36E-03	6.44E-04	1.90E-03	5.29E-04	1.42E-03	3.11E-04
North Atlantic	%	100.00	100.00	100.00	100.00	99.97	100.00	99.99	100.00	98.27	100.00
	CRI	8.50E-03	5.55E-03	6.39E-03	2.99E-03	4.73E-03	2.10E-03	3.84E-03	1.72E-03	2.77E-03	1.25E-03
Northwest Indian Ocean	%	100.00	100.00	100.00	100.00	100.00	100.00	99.62	100.00	96.89	100.00
	CRI	1.55E-02	1.03E-02	1.31E-02	6.35E-03	9.88E-03	5.64E-03	9.36E-03	4.41E-03	6.68E-03	3.95E-03
South Atlantic	%	100.00	100.00	100.00	100.00	100.00	100.00	100.00	100.00	100.00	100.00
	CRI	4.38E-04	3.03E-04	3.61E-04	2.77E-04	4.01E-04	2.50E-04	3.22E-04	2.38E-04	2.84E-04	1.64E-04
Southwest Indian Ocean	%	100.00	100.00	100.00	100.00	100.00	100.00	100.00	100.00	99.24	100.00
	CRI	1.54E-03	1.02E-03	1.24E-03	7.02E-04	1.09E-03	5.76E-04	8.25E-04	4.77E-04	5.71E-04	2.77E-04
West Pacific	%	100.00	100.00	100.00	100.00	99.98	100.00	99.92	100.00	87.61	91.67
	CRI	3.47E-03	2.96E-03	2.15E-03	1.79E-03	1.76E-03	1.57E-03	1.28E-03	9.82E-04	7.67E-04	5.74E-04

(B) ARGOS tracked sharks. Values were calculated for all ARGOS transmitter tracked sharks (n = 256) and global vessel activity.

		Grid Cell Size									
		2 × 2°		1 × 1°		0.75 × 0.75°		0.5 × 0.5°		0.25 × 0.25°	
		Mean	Median	Mean	Median	Mean	Median	Mean	Median	Mean	Median
Global	%	100.00	100.00	100.00	100.00	100.00	100.00	99.85	100.00	90.53	100.00
	CRI	4.99E-03	2.47E-03	4.38E-03	1.71E-03	2.51E-03	1.26E-03	1.92E-03	9.22E-04	1.32E-03	5.65E-04
East Indian Ocean	%	100.00	100.00	100.00	100.00	100.00	100.00	100.00	100.00	86.63	91.67
	CRI	3.62E-03	2.59E-03	3.40E-03	2.11E-03	1.96E-03	1.60E-03	1.32E-03	1.08E-03	8.29E-04	6.65E-04
East Pacific	%	100.00	100.00	100.00	100.00	100.00	100.00	99.56	100.00	91.38	100.00
	CRI	6.21E-03	1.68E-03	5.45E-03	1.01E-03	2.60E-03	6.44E-04	2.14E-03	5.35E-04	1.60E-03	3.08E-04
North Atlantic	%	100.00	100.00	100.00	100.00	100.00	100.00	100.00	100.00	100.00	100.00
	CRI	1.47E-02	6.41E-03	1.32E-02	2.82E-03	9.13E-03	1.98E-03	7.52E-03	1.65E-03	5.41E-03	1.32E-03
Northwest Indian Ocean	%	100.00	100.00	100.00	100.00	100.00	100.00	100.00	100.00	100.00	100.00
	CRI	1.65E-02	3.79E-03	1.95E-02	2.56E-04	7.93E-03	7.25E-04	5.93E-03	2.48E-04	4.02E-03	7.34E-05
South Atlantic	%	100.00	100.00	100.00	100.00	100.00	100.00	100.00	100.00	100.00	100.00
	CRI	3.55E-04	2.88E-04	3.77E-04	2.87E-04	4.83E-04	5.15E-04	4.30E-04	4.21E-04	3.77E-04	2.57E-04
Southwest Indian Ocean	%	100.00	100.00	100.00	100.00	100.00	100.00	100.00	100.00	99.10	100.00
	CRI	1.73E-03	1.21E-03	1.41E-03	1.01E-03	1.25E-03	8.05E-04	9.38E-04	6.96E-04	6.48E-04	5.22E-04
West Pacific	%	100.00	100.00	100.00	100.00	99.98	100.00	99.92	100.00	87.41	91.67
	CRI	3.46E-03	2.95E-03	2.16E-03	1.81E-03	1.76E-03	1.56E-03	1.28E-03	9.75E-04	7.65E-04	5.65E-04

(C) PSAT tracked sharks. Values were calculated for all PSAT transmitter tracked sharks (n = 92) and global vessel activity.

		Grid Cell Size									
		2 × 2°		1 × 1°		0.75 × 0.75°		0.5 × 0.5°		0.25 × 0.25°	
		Mean	Median	Mean	Median	Mean	Median	Mean	Median	Mean	Median
Global	%	100.00	100.00	100.00	100.00	99.99	100.00	99.81	100.00	97.76	100.00
	CRI	8.15E-03	5.10E-03	5.99E-03	2.86E-03	5.16E-03	2.49E-03	4.81E-03	1.78E-03	3.47E-03	1.21E-03
East Indian Ocean	%	-	-	-	-	-	-	-	-	-	-
	CRI	-	-	-	-	-	-	-	-	-	-
East Pacific	%	100.00	100.00	100.00	100.00	100.00	100.00	100.00	100.00	99.85	100.00
	CRI	1.48E-03	1.53E-03	1.10E-03	7.60E-04	1.08E-03	6.91E-04	5.77E-04	4.71E-04	4.77E-04	3.34E-04
North Atlantic	%	100.00	100.00	100.00	100.00	99.96	100.00	99.98	100.00	97.50	98.08
	CRI	5.73E-03	5.55E-03	3.36E-03	3.00E-03	2.78E-03	2.10E-03	2.20E-03	1.72E-03	1.59E-03	1.25E-03
Northwest Indian Ocean	%	100.00	100.00	100.00	100.00	100.00	100.00	99.54	100.00	96.31	99.33
	CRI	1.53E-02	1.26E-02	1.19E-02	6.43E-03	1.02E-02	6.07E-03	1.00E-02	4.91E-03	7.19E-03	4.20E-03
South Atlantic	%	100.00	100.00	100.00	100.00	100.00	100.00	100.00	100.00	100.00	100.00
	CRI	4.84E-04	3.19E-04	3.52E-04	2.06E-04	3.56E-04	2.08E-04	2.62E-04	1.69E-04	2.33E-04	1.41E-04
Southwest Indian Ocean	%	100.00	100.00	100.00	100.00	100.00	100.00	100.00	100.00	100.00	100.00
	CRI	4.47E-04	4.14E-04	3.21E-04	2.13E-04	2.43E-04	1.83E-04	2.06E-04	1.56E-04	1.47E-04	1.30E-04
West Pacific	%	100.00	100.00	100.00	100.00	100.00	100.00	100.00	100.00	99.86	99.86
	CRI	3.88E-03	3.88E-03	1.78E-03	1.78E-03	1.58E-03	1.58E-03	1.33E-03	1.33E-03	9.15E-04	9.15E-04

Table S12 | Effect of different yearly subsets on the mean monthly spatial overlap of whale sharks and vessels (%) and collision risk index (CRI) calculated at a 0.25 × 0.25° grid cell resolution scale.

		Year range									
		2011-2014 Average		2011		2012		2013		2014	
		Mean	Median	Mean	Median	Mean	Median	Mean	Median	Mean	Median
Global	%	92.44	100.00	83.50	94.44	84.98	95.50	84.65	94.24	87.05	95.00
	CRI	1.89E-03	7.17E-04	1.37E-03	5.79E-04	1.85E-03	6.68E-04	2.07E-03	7.20E-04	2.23E-03	7.42E-04
East Indian Ocean	%	86.63	91.67	79.24	88.89	79.36	88.89	80.57	91.61	83.63	88.89
	CRI	8.29E-04	6.65E-04	7.38E-04	6.41E-04	7.60E-04	6.43E-04	8.43E-04	6.23E-04	9.29E-04	7.39E-04
East Pacific	%	92.72	100.00	82.48	96.49	83.96	97.52	85.37	95.27	84.67	96.60
	CRI	1.42E-03	3.11E-04	1.11E-03	2.92E-04	1.33E-03	3.09E-04	1.52E-03	3.27E-04	1.71E-03	3.30E-04
North Atlantic	%	98.27	100.00	97.74	99.56	97.65	99.77	97.38	99.11	97.57	99.56
	CRI	2.77E-03	1.25E-03	1.96E-03	8.45E-04	2.67E-03	1.26E-03	3.15E-03	1.53E-03	3.28E-03	1.41E-03
Northwest Indian Ocean	%	96.89	100.00	91.67	97.46	85.34	92.54	77.58	89.18	86.68	94.49
	CRI	6.68E-03	3.95E-03	4.44E-03	2.79E-03	6.86E-03	4.10E-03	7.46E-03	4.23E-03	7.95E-03	4.68E-03
South Atlantic	%	100.00	100.00	97.46	100.00	98.40	100.00	96.52	100.00	96.73	100.00
	CRI	2.84E-04	1.64E-04	2.31E-04	1.41E-04	2.54E-04	1.66E-04	3.02E-04	1.61E-04	3.37E-04	1.94E-04
Southwest Indian Ocean	%	99.24	100.00	90.44	97.22	93.67	100.00	95.21	100.00	95.67	100.00
	CRI	5.71E-04	2.77E-04	4.72E-04	2.44E-04	5.14E-04	2.44E-04	6.04E-04	2.58E-04	6.69E-04	3.57E-04
West Pacific	%	87.61	91.67	69.19	77.69	78.25	85.42	78.41	83.87	82.34	87.87
	CRI	7.67E-04	5.74E-04	5.83E-04	4.24E-04	7.12E-04	5.86E-04	8.42E-04	6.56E-04	8.64E-04	6.18E-04

Table S13 | Effect of different collision zone (surface) use scenarios on the mean monthly collision risk index (CRI) (see *Supplementary Methods*) calculated at a 0.25 × 0.25° grid cell resolution scale. Collision zone use scenarios refer to the surface use values fitted into the risk calculations and consist of: Main - empirical regional median by depth class (Table S3), Option 1 – overall regional median (Table S3), Option 2 – 0.45:0.45, Option 3 – 0.45:0.5625, Option 4 – 0.5625:0.45, Option 5 – 0.45:0.675, Option 6 – 0.675:0.45, Option 7 – 0.45:0.7875, Option 8 – 0.7875:0.45, Option 9 – 0.45:0.3375, Option 10 – 0.3375:0.45 (ratio coastal:oceanic) (see *Supplementary Methods*).

	Collision zone (surface) use scenario									
	Option1		Option2		Option3		Option4		Option5	
	Mean	Median	Mean	Median	Mean	Median	Mean	Median	Mean	Median
Global	1.59E-03	5.34E-04	1.56E-03	5.50E-04	1.77E-03	6.48E-04	1.73E-03	5.95E-04	1.98E-03	7.34E-04
East Indian Ocean	5.32E-04	4.39E-04	7.15E-04	5.90E-04	8.01E-04	6.52E-04	8.08E-04	6.52E-04	8.87E-04	7.10E-04
East Pacific	1.19E-03	2.73E-04	1.26E-03	2.88E-04	1.44E-03	3.51E-04	1.39E-03	2.97E-04	1.62E-03	4.21E-04
North Atlantic	2.56E-03	1.11E-03	1.79E-03	7.77E-04	2.05E-03	9.40E-04	1.98E-03	8.63E-04	2.31E-03	1.10E-03
Northwest Indian Ocean	5.64E-03	3.33E-03	5.69E-03	3.36E-03	6.39E-03	3.40E-03	6.43E-03	3.67E-03	7.08E-03	3.40E-03
South Atlantic	2.48E-04	1.43E-04	1.74E-04	1.00E-04	2.17E-04	1.25E-04	1.74E-04	1.00E-04	2.60E-04	1.50E-04
Southwest Indian Ocean	5.63E-04	2.72E-04	3.86E-04	1.87E-04	4.20E-04	2.07E-04	4.48E-04	2.14E-04	4.55E-04	2.28E-04
West Pacific	6.86E-04	5.27E-04	7.05E-04	5.42E-04	8.52E-04	6.45E-04	7.34E-04	5.50E-04	9.98E-04	7.51E-04
	Collision zone (surface) use scenario									
	Option6		Option7		Option8		Option9		Option10	
	Mean	Median	Mean	Median	Mean	Median	Mean	Median	Mean	Median
Global	1.91E-03	6.38E-04	2.19E-03	8.13E-04	2.09E-03	6.95E-04	1.35E-03	4.54E-04	1.38E-03	5.12E-04
East Indian Ocean	9.01E-04	7.29E-04	9.73E-04	7.56E-04	9.94E-04	8.05E-04	6.29E-04	5.06E-04	6.22E-04	5.06E-04
East Pacific	1.52E-03	3.05E-04	1.80E-03	4.69E-04	1.66E-03	3.31E-04	1.08E-03	2.25E-04	1.13E-03	2.81E-04
North Atlantic	2.17E-03	8.95E-04	2.57E-03	1.27E-03	2.36E-03	9.27E-04	1.53E-03	6.55E-04	1.60E-03	7.46E-04
Northwest Indian Ocean	7.16E-03	4.02E-03	7.77E-03	3.61E-03	7.89E-03	4.34E-03	5.00E-03	2.85E-03	4.96E-03	2.55E-03
South Atlantic	1.74E-04	1.00E-04	3.04E-04	1.75E-04	1.74E-04	1.00E-04	1.30E-04	7.51E-05	1.74E-04	1.00E-04
Southwest Indian Ocean	5.10E-04	2.41E-04	4.89E-04	2.50E-04	5.72E-04	2.68E-04	3.52E-04	1.67E-04	3.24E-04	1.60E-04
West Pacific	7.64E-04	5.79E-04	1.15E-03	8.57E-04	7.93E-04	6.22E-04	5.58E-04	4.17E-04	6.75E-04	5.10E-04

Table S14 | Effect of more recent yearly subsets on the mean monthly spatial overlap of whale sharks and vessels (%) and collision risk index (CRI) associated with cargo vessels calculated at a 0.25 × 0.25° grid cell resolution scale. Note that calculated values were similar between data providers and years with Exact Earth data marginally but consistently more conservative in spatial overlap and CRI estimations.

		Year range									
		Exact Earth		Global Fishing Watch							
		2011-2014		2017-2019		2017		2018		2019	
		Mean	Median	Mean	Median	Mean	Median	Mean	Median	Mean	Median
Global	%	82.31	94.44	83.68	95.45	71.64	80.00	72.94	82.50	74.32	84.29
	CRI	9.59E-04	3.08E-04	3.31E-03	9.64E-04	3.25E-03	9.35E-04	3.32E-03	8.94E-04	3.36E-03	9.27E-04
East Indian Ocean	%	82.87	90.00	83.95	87.66	73.32	75.00	74.27	78.29	60.87	65.83
	CRI	3.75E-04	2.29E-04	9.98E-04	6.12E-04	1.05E-03	5.71E-04	9.76E-04	5.77E-04	9.57E-04	4.90E-04
East Pacific	%	80.60	95.87	70.38	83.65	56.89	64.94	59.72	68.27	59.95	65.28
	CRI	7.69E-04	1.79E-04	1.68E-03	3.18E-04	1.84E-03	3.31E-04	1.50E-03	3.34E-04	1.66E-03	2.73E-04
North Atlantic	%	97.40	98.87	96.15	100.00	94.70	98.95	94.05	99.13	93.87	98.25
	CRI	1.50E-03	6.54E-04	5.72E-03	2.71E-03	5.01E-03	2.46E-03	6.22E-03	2.69E-03	5.91E-03	2.69E-03
Northwest Indian Ocean	%	83.69	92.96	77.06	88.30	73.21	83.19	70.67	82.71	73.94	83.69
	CRI	3.15E-03	1.90E-03	1.17E-02	8.21E-03	1.17E-02	8.34E-03	1.19E-02	8.54E-03	1.18E-02	8.28E-03
South Atlantic	%	99.88	100.00	99.40	100.00	70.27	74.07	76.83	86.53	88.34	92.34
	CRI	1.20E-04	9.55E-05	3.75E-04	3.00E-04	2.55E-04	2.12E-04	2.64E-04	1.82E-04	3.66E-04	2.93E-04
Southwest Indian Ocean	%	93.30	100.00	95.53	100.00	87.00	94.54	88.88	100.00	93.79	100.00
	CRI	4.20E-04	1.93E-04	8.87E-04	7.12E-04	9.36E-04	7.50E-04	7.69E-04	6.09E-04	9.43E-04	6.82E-04
West Pacific	%	65.05	73.51	90.56	100.00	68.82	75.76	70.87	80.48	87.40	95.75
	CRI	4.44E-04	3.00E-04	2.58E-03	1.58E-03	2.44E-03	1.58E-03	2.55E-03	1.66E-03	2.77E-03	1.61E-03

Table S15 | Summary of known whale shark aggregation sites depicted in Figure S2*B* and a primary reference.

Region	Known aggregation area	Reference
East Pacific	Bahía de Los Angeles, Mexico	Ramírez-Macías *et al*. (2012) (57)
	La Paz, Mexico	Ramírez-Macías *et al*. (2012) (57)
	Galapagos	Acuña-Marrero *et al.* (2014) (58)
North Atlantic	Azores	Afonso *et al.* (2014) (59)
	Yucatán Peninsula, Mexico	de la Parra *et al.* (2011) (33)
	Belize	Graham *et al.* (2007) (60)
	Utila, Honduras	Fox *et al.* (2013) (52)
	Rio de Janeiro, Brazil	Di Beneditto *et al.* (2021) (61)
	São Pedro and São Paulo, Brazil	Macena *et al.* (2016) (62)
South Atlantic	St. Helena	Perry *et al.* (2020) (38)
Northwest Indian Ocean	Shib Habil, Red Sea	Cochran *et al.* (2019) (63)
	Djibouti	Rowat *et al.* (2006) (37)
	Qatar	Robinson *et al.* (2013) (54)
	Gujarat, India	Pravin *et al.* (2000) (64)
	South Ari Atoll, Maldives	Riley *et al.* (2010) (65)
Southwest Indian Ocean	Tofo Beach, Mozambique	Rohner *et al.* (2018) (40)
	Mafia Island, Tanzania	Rohner *et al.* (2015) (66)
	Nosy Be, Madagascar	Diamant *et al.* (2018) (39)
	Mahe, Seychelles	Rowat *et al.* (2007) (41)
East Indian Ocean	Ningaloo, Australia	Meekan *et al.* (2006) (67)
West Pacific	Donsol, Philippines	McCoy *et al.* (2018) (68)
	Oslob, Cebu, Philippines	Araujo *et al.* (2014) (46)
	Palawan, Philippines	Araujo *et al.* (2019) (69)
	Southern Leyte, Philippines	Araujo *et al.* (2017) (56)
	Triton Bay, West Papua	Sianipar *et al.* (2019) (70)
	Saleh Bay, West Papua	Sianipar *et al.* (2019) (70)
	Cenderawasih Bay, West Papua	Meyers *et al.* (2020) (43)
Global	Other smaller scale areas	Norman *et al.* (2017) (71) Sequeira *et al.* (2013) (72) Sequeira *et al.* (2014) (1)

Table S16 | Summary of whale shark population trends and abundance estimates adapted from the International Union for the Conservation of Nature Red List assessment with the addition of relevant literature-based population estimates. The WildBook column refers to total number of individuals identified in Norman *et al.* (2017) (71) and the population column refers to region-specific population estimates where available and where not it gives number of individuals identified in the associated reference (§).

(A) Atlantic

		IUCN					Literature			GSMP	
Area (*tag site)	Description	Start index (year)	End index (year)	Data type	Inferred cause	References	WildBook	Population (§# identified)	References	Tags deployed	Percentage tagged
North Atlantic											
Azores	Expanding distribution due to climate change (1998 - 2013)	4 sharks per annum (1998)	90 sharks per annum (2013)	Sightings recorded from observers on pole-and-line tuna fishing vessels	Northward extension of 22°C isotherm	Afonso *et al*. (2014) (59)	-	-	-	39	2.82% (WildBook) 1.8% (WCA) 41.1% (Honduras) 5.86% (Mexico-Atlantic)
Belize	Anecdotal decrease in sightings by divers (1998 – 2015)	4-6 sharks per day (1998)	0 sharks per day (2015)	Daily whale shark sightings by dive guides at Gladden Spit	Unclear – poorly managed tourism?	Graham & Roberts (2007) (60)	47	2,167 (Western Central Atlantic Ocean - WCA)	McKinney *et al.* (2017) (73)		
Honduras	-	-	-	-	-	-	136	95§	Fox *et al.* (2013) (52)		
Mexico-Atlantic*	-	-	-	-	-	-	1101	521 – 809	Ramírez-Macías *et al*. (2012) (51)		
The United States-Gulf States (Florida*)	-	-	-	-	-	-	101	-	-		
South Atlantic											
St Helena*	-	-	-	-	-	-	-	277§	Perry *et al.* (2020) (38)	14	5.05% (St. Helena)
São Pedro and São Paulo*	-	-	-	-	-	-	-	-	-		
Western Africa	Broad-scale ~70% overall decrease in SPUE from tuna fleet (1980 - 2010)	~0.05 (1980)	~0.01 (2010)	SPUE from tuna fleet, and raw data	Unclear	Sequeira *et al.* (2014) (1)	-	-	-		

(B) Indian Ocean

		IUCN					Literature			GSMP	
Area (*tag site)	Description	Start index (year)	End index (year)	Data type	Inferred cause	References	WildBook	Population (§# identified)	References	Tags deployed	Percentage tagged
Northwest Indian Ocean											
Djibouti*	-	-	-	-	-	-	87	190§	Boldrocchi *et al.* (2020) (74)	44	6.72% (WildBook) 23.16% (Djibouti) 32.35% (Red Sea) 10.43% (Qatar & Oman) 49.43% (South Ari)
Red Sea*	-	-	-	-	-	-	57	136§	Cochran *et al.* (2016) (53)		
Qatar*	-	-	-	-	-	-	341	422§	Robinson *et al.* (2016) (75)		
Oman	-	-	-	-	-	-	69				
Maldives	National decrease in CPUE	30 caught per annum (single location) (1980)	20 or less (nationally) (1993)	Fishery catches	Overfishing	Anderson & Ahmed (1993) (76)	101	74 – 104 (South Ari)	Davies *et al*. (2012) (77)		
Southwest Indian Ocean											
Seychelles*	-	-	-	-	-	-	204	469 – 557	Brooks *et al*. (2010) (*78*)	26	2.95% (WildBook) 5.07% (Seychelles) 6.37% (Madagascar)
Mozambique*	Localised 79+% decline in SPUE	(2005)	(2016)	Modelled sighting data	Unclear	Rohner *et al*. (2013) (79)	676	-	-		
Madagascar*	-	-	-	-	-	-	-	408§	Diamant *et al.* (2021) (80)		
Western & Central Indian Ocean	Broad-scale increase in sightings to 2000; decrease to 2007. Significant decrease (~66%) overall	(1991)	(2007)	SPUE from tuna fleet, and raw data	Unclear	Sequeira *et al.* (2013) (81)	-	-	-		

(C) Indian Ocean continued

		IUCN					Literature			GSMP	
Area (*tag site)	Description	Start index (year)	End index (year)	Data type	Inferred cause	References	WildBook	Population (§# identified)	References	Tags deployed	Percentage tagged
East Indian Ocean											
Ningaloo, Australia*	Declining mtDNA diversity	(2007)	(2012)	Declining mtDNA diversity	Unclear	Vignaud *et al*. (2014) (82)	1082	319 – 436	Meekan *et al*. (2006) (67)	74	6.60% (WildBook) 19.60% (Ningaloo)
	(Controversial) 40% decline in SPUE; 1.6 m decline in mean TL	(1995)	(2004)	SPUE from tourism vessels	Unclear	Bradshaw *et al*. (2008) (83)					
	Small increase in number of 'returning' sharks over time. Decline in mean TL due to recruitment of smaller individuals	(1995)	(2008)	Individual data from mark-recapture models	Unclear	Holmberg *et al*. (2009) (84)					
Christmas Island*	-	-	-	-	-	-	40	-	-		

(D) Pacific

		IUCN					Literature			GSMP	
Area (*tag site)	Description	Start index (year)	End index (year)	Data type	Inferred cause	References	WildBook	Population (§# identified)	References	Tags deployed	Percentage tagged
West Pacific											
Thailand	Localised ~92% decline in SPUE (Andaman Sea)	1.58 (1992)	0.13 (2001)	Sightings per dive trip	Unclear	Theberge & Dearden (2006) (85)	184	-	-	62	6.02% (WildBook) 7.32% (Philippines) 49.21% (Indonesia)
Philippines*	Local ~60% decline in CPUE (Pamilican)	4.44 (1993)	1.7 (1997)	CPUE	Active fishery	Alava *et al*. (2002) (86)	775	479 (Donsol)§ 93 (Southern Leyte)§ 117 (Palawan)§ 158 (Cebu)§	McCoy *et al.* (2018) (68); Araujo *et al.* (2017) (56); Araujo *et al.* (2019) (69); Araujo *et al.* (2014) (46)		
	Local ~60% decline in CPUE (Guiwanon)	10 (1993)	3.8 (1997)	CPUE	Active fishery	Alava *et al*. (2002) (86)					
Taiwan	National ~50+% decrease in CPUE	272 sharks per annum (1997)	113 (over 15 months) (2002)	Fishery catches	Active fishery	Chen & Phipps (2002) (87)	-	-	-		
	Local ~80% decline in CPUE (Hongchun Harbour)	50-60 (1980)	>10 (1995)	Fishery catches	Active fishery	Chen & Phipps (2002) (87)					
	National decrease in mean TL of landed sharks	~4.6 m (2002)	~4.4 m (2007)	Decline in mean TL of landed sharks	Active fishery	Hsu *et al*. (2012) (88)					
Indonesia*	-	-	-	-	-	-	71	126§	Suruan *et al.* (2016) (89)		
Queensland, Australia*	-	-	-	-	-	-	-	-	-		
China*	National decrease in mean TL of landed sharks	8.27 m (prior 2004)	6.3 m (2008-2001)	Decline in mean TL of landed sharks	Active fishery	Li *et al*. (2012) (90)	-	-	-		

(E) Pacific continued

		IUCN					Literature			GSMP	
Area (*tag site)	Description	Start index (year)	End index (year)	Data type	Inferred cause	References	WildBook	Population (§# identified)	References	Tags deployed	Percentage tagged
East Pacific											
Western Central Pacific	Broad-scale 50% decrease in SPUE from tuna fleet	~1% (2003)	~0.5% (2012)	Occurrence in purse- seine sets	Unclear	Harley *et al*. (2013) (91)	-	-	-	89	12.57% (WildBook) 12.80% (The Galapagos) 94.68% (Bahía de Los Ángeles)
	Weak evidence for increasing SPUE from tuna fleet	0.003 (2000)	0.012 (2010)	SPUE from tuna fleet. Note - poor model performance.	Unclear	Sequeira *et al*. (2014) (1)					
The Galapagos*	-	-	-	-	-	-	141	695	Acuña-Marrero *et al*. (2014) (58)		
Mexico Pacific*	-	-	-	-	-	-	567	54 (2008) – 94 (2009) (Bahía de Los Ángeles)	Ramírez-Macías *et al*. (2012) (57)		
Panama*	-	-	-	-	-	-	-	-	-		

Table S17 | Summary of whale shark tag deployments per year.

Year	Tag count	Cumulative frequency	Cumulative %
2005	8	8	2.30
2006	12	20	5.75
2007	10	30	8.62
2008	6	36	10.34
2009	16	52	14.94
2010	38	90	25.86
2011	57	147	42.24
2012	33	180	51.72
2013	15	195	56.03
2014	5	200	57.47
2015	39	239	68.68
2016	36	275	79.02
2017	27	302	86.78
2018	33	335	96.26
2019	13	348	100.00

Table S18 | Effect of using Exact Earth or Global Fishing Watch datasets on the mean monthly spatial overlap of whale sharks and vessels (%) and collision risk index (CRI) associated with cargo vessels in 2014 calculated at a 0.25 × 0.25° grid cell resolution scale.

		Year range			
		Exact Earth		Global Fishing Watch	
		2014		2014	
		Mean	Median	Mean	Median
Global	%	71.87	81.94	75.93	87.18
	CRI	1.11E-03	2.84E-04	3.18E-03	8.35E-04
East Indian Ocean	%	73.24	80.24	75.37	86.50
	CRI	3.76E-04	2.17E-04	1.01E-03	5.55E-04
East Pacific	%	66.56	76.31	71.17	83.33
	CRI	8.22E-04	1.39E-04	2.30E-03	3.70E-04
North Atlantic	%	93.54	97.10	94.56	97.73
	CRI	1.78E-03	7.31E-04	5.68E-03	2.39E-03
Northwest Indian Ocean	%	71.16	82.16	74.15	84.52
	CRI	3.82E-03	2.33E-03	1.07E-02	7.58E-03
South Atlantic	%	80.86	82.74	81.32	83.00
	CRI	1.18E-04	9.86E-05	2.64E-04	2.03E-04
Southwest Indian Ocean	%	88.18	100.00	86.86	100.00
	CRI	5.01E-04	2.77E-04	1.14E-03	7.36E-04
West Pacific	%	55.75	54.66	67.08	71.93
	CRI	5.44E-04	3.41E-04	1.57E-03	1.05E-03

Table S19 | Collision zone use control analysis summary performed using time-at-depth histogram files from 24 individuals in the north Atlantic. Significance column displays the Kolmogorov-Smirnov test results comparing median surface time between males and females. Whale sharks of unknown sex were not considered in this analysis.

Sex	Total tracks	Depth records	Median surface time (%)	Mean (± s.d.) surface time (%)	Significance
Male	11	2129	37.50	47.11 (24.44)	0.2809^{ns}
Female	13	3562	54.50	59.98 (20.20)	

Table S20 | Collision zone use control analysis summary performed using time-at-depth histogram files from 38 individuals in the west Pacific.

Month	Depth records	Median surface time (%)	Mean (± s.d.) surface time (%)
JAN	2234	36.80	43.07 (27.66)
FEB	2238	38.75	44.95 (28.90)
MAR	2537	44.20	47.65 (28.00)
APR	2427	48.80	51.68 (30.11)
MAY	2591	50.30	53.23 (30.14)
JUN	2589	42.60	46.17 (30.31)
JUL	2563	46.80	46.32 (27.17)
AUG	2442	51.65	50.96 (26.43)
SEP	2261	45.00	46.54 (26.60)
OCT	2040	40.50	43.73 (27.09)
NOV	2382	40.40	43.34 (26.62)
DEC	2260	39.25	43.91 (28.75)

Table S21 | Mean (± s.d.) proportion of gaps within each category calculated for each individual as a total number of gaps within a track and summarised by region.

Region	Tag type	Count	≤ 3	3 -5	5 -10	10 -20	> 20
North Atlantic	ARGOS	12	0.55 (0.23)	0.11 (0.10)	0.11 (0.10)	0.09 (0.12)	0.14 (0.11)
	PSAT	27	0.69 (0.23)	0.11 (0.10)	0.12 (0.10)	0.05 (0.07)	0.04 (0.06)
South Atlantic	ARGOS	5	0.55 (0.31)	0.11 (0.09)	0.13 (0.11)	0.14 (0.13)	0.07 (0.08)
	PSAT	9	0.52 (0.20)	0.15 (0.13)	0.16 (0.18)	0.13 (0.09)	0.05 (0.07)
East Indian Ocean	ARGOS	74	0.61 (0.24)	0.10 (0.10)	0.13 (0.14)	0.08 (0.11)	0.07 (0.11)
Northwest Indian Ocean	ARGOS	7	0.25 (0.39)	0.06 (0.14)	0.00 (0.00)	0.39 (0.49)	0.31 (0.43)
	PSAT	37	0.41 (0.27)	0.12 (0.10)	0.17 (0.13)	0.14 (0.11)	0.15 (0.18)
Southwest Indian Ocean	ARGOS	22	0.83 (0.25)	0.01 (0.06)	0.06 (0.10)	0.005 (0.02)	0.09 (0.15)
	PSAT	4	0.70 (0.25)	0.08 (0.10)	0.03 (0.04)	0.14 (0.17)	0.04 (0.08)
East Pacific	ARGOS	75	0.60 (0.33)	0.07 (0.10)	0.12 (0.19)	0.12 (0.23)	0.09 (0.17)
	PSAT	14	0.61 (0.27)	0.10 (0.08)	0.14 (0.17)	0.06 (0.11)	0.08 (0.29)
West Pacific	ARGOS	61	0.65 (0.20)	0.11 (0.08)	0.12 (0.10)	0.08 (0.07)	0.04 (0.06)
	PSAT	1	0.82 (-)	0.00 (-)	0.18 (-)	0.00 (-)	0.00 (-)

Table S22 | Summary of the spatial coverage of whale sharks within each ocean region at a 1 × 1° cell resolution scale.

	Ocean Region						
	North Atlantic	South Atlantic	Northwest Indian Ocean	Southwest Indian Ocean	East Indian Ocean	West Pacific	East Pacific
Total no. of grid cells	2707	2383	668	1840	1919	4297	7514
No. of cells not occupied by sharks	2494	2303	597	1726	1659	3902	7053
No. of cells occupied by sharks	213	80	71	114	260	395	461
No. of shark locations within occupied cells	2072	2383	930	923	4049	6804	4187
% cells occupied by sharks	7.87	3.36	10.63	6.20	13.55	9.19	6.14
Total area of grid cells (million km^2)	31.37	26.95	8.13	20.67	22.49	50.77	84.95

3. Supplementary Figures

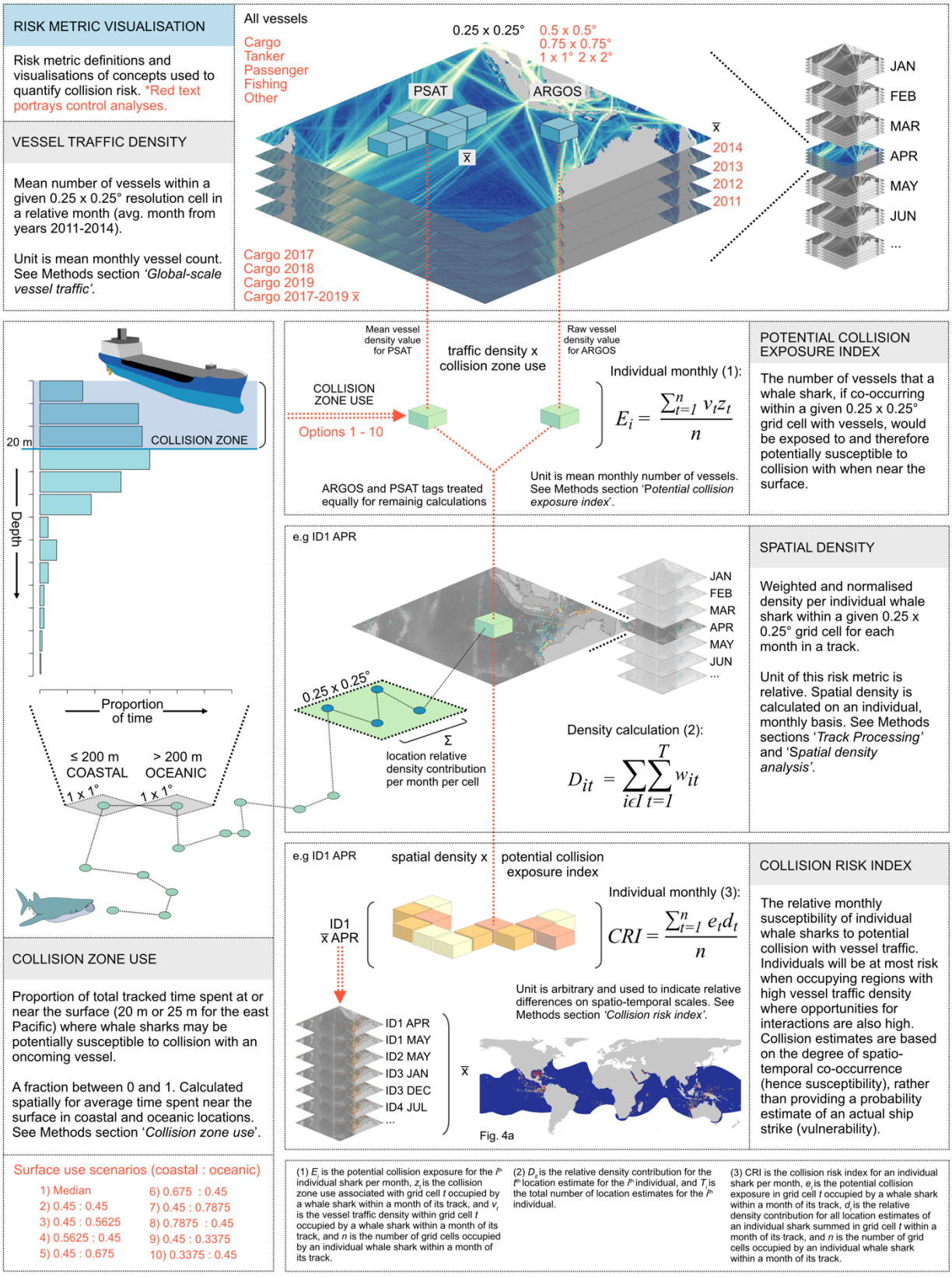

Figure S1 | Methods schematic. Risk metric definitions and visualisations of concepts used to quantify collision risk in whale sharks.

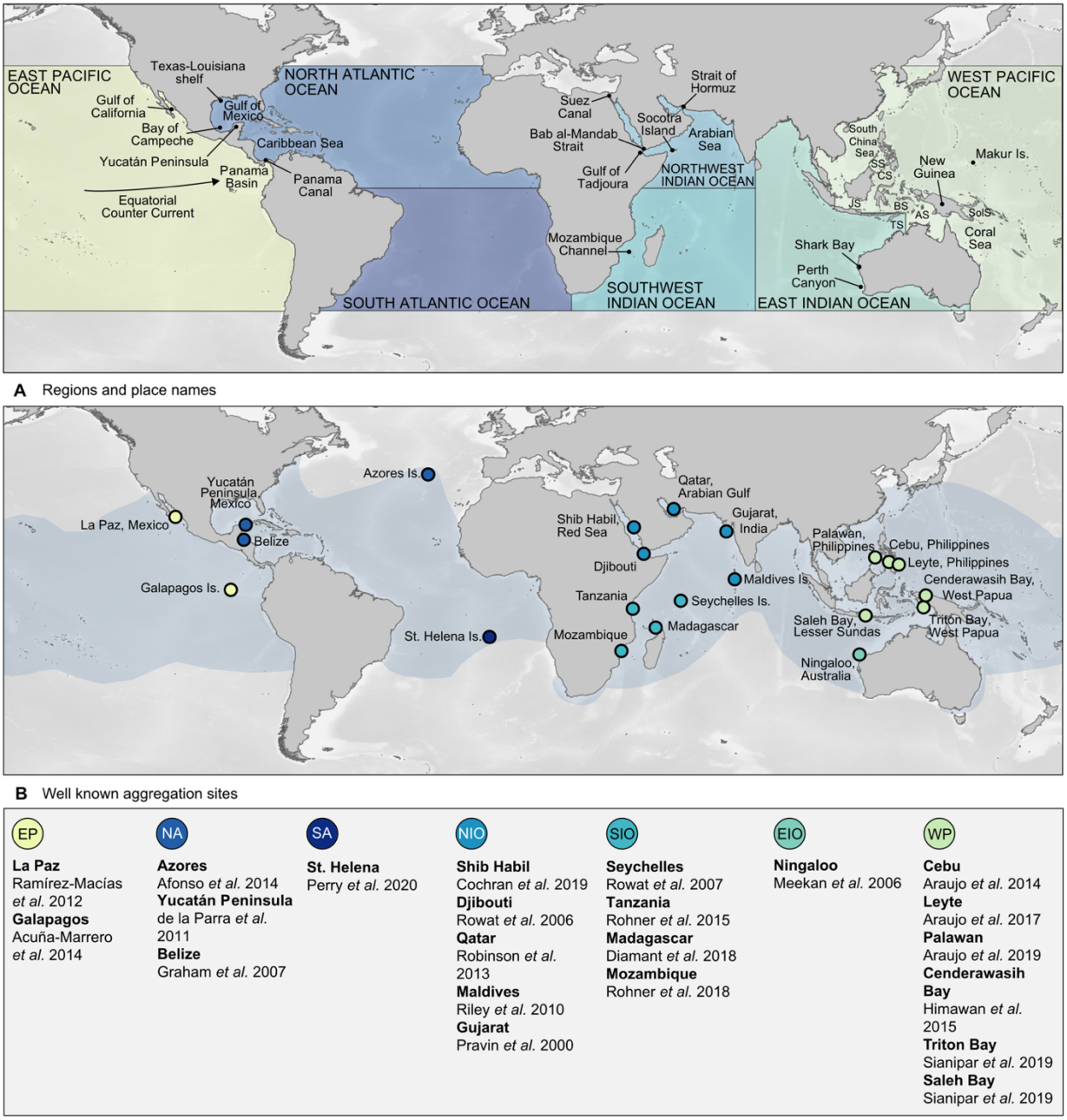

Figure S2 | Study regions and known aggregation sites. *(A)* Map of notable locations/ features referred to in the main paper overlaid with ocean regions. AS, Arafura Sea; BS, Banda Sea; CS, Celebes Sea; JS, Java Sea; TS, Timor Sea; SS, Sulu Sea; SolS, Solomon Sea. *(B)* Whale shark distribution (IUCN) overlaid with documented aggregation sites within each region. For full reference list see Table S15. EP, east Pacific; WP, west Pacific; EIO, east Indian Ocean; SIO, southwest Indian Ocean; NIO, northwest Indian Ocean; NA, north Atlantic; SA, south Atlantic.

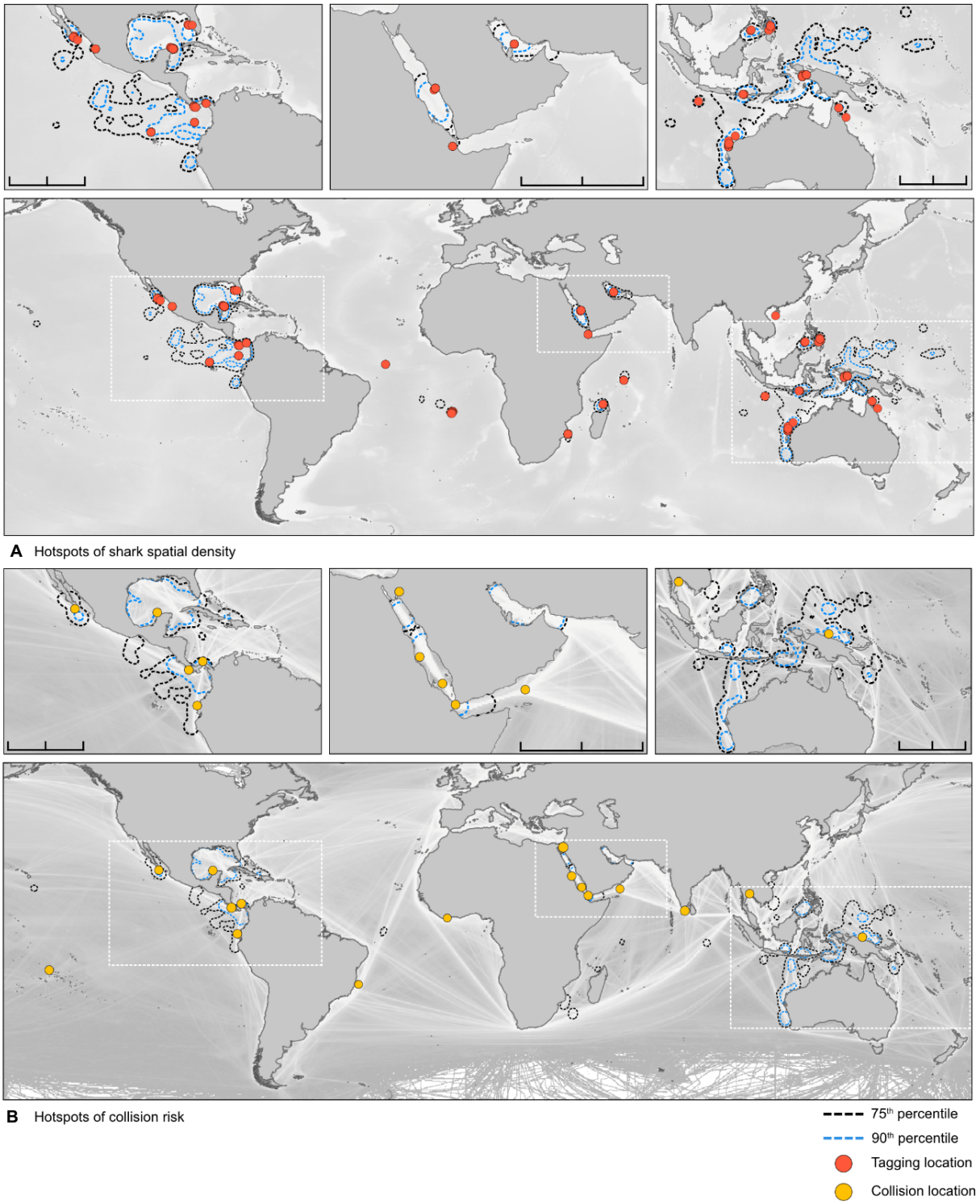

Figure S3 | The location of whale shark space-use hotspots and hotspots of risk. *(A)* Red circles denote the locations in which satellite transmitters were deployed on whale sharks. Space use hotspots are highlighted as the 75th (black dotted line) and 90th (blue dotted line) percentiles of the mean monthly relative density of estimated whale shark locations within 0.25 × 0.25° grid cells with a 2.5° radius applied. *(B)* Orange circles denote the locations where fatal collisions occurred or where bodies of fatally injured whale sharks were first noticed on the bow of vessels. Collision risk hotspots are highlighted as the 75th (black dotted line) and 90th (blue dotted line) of the mean monthly relative collision risk index within 0.25 × 0.25° grid cells given in Figure 4*A* with a 2.5° radius applied. Scale bars denote 1,000 km.

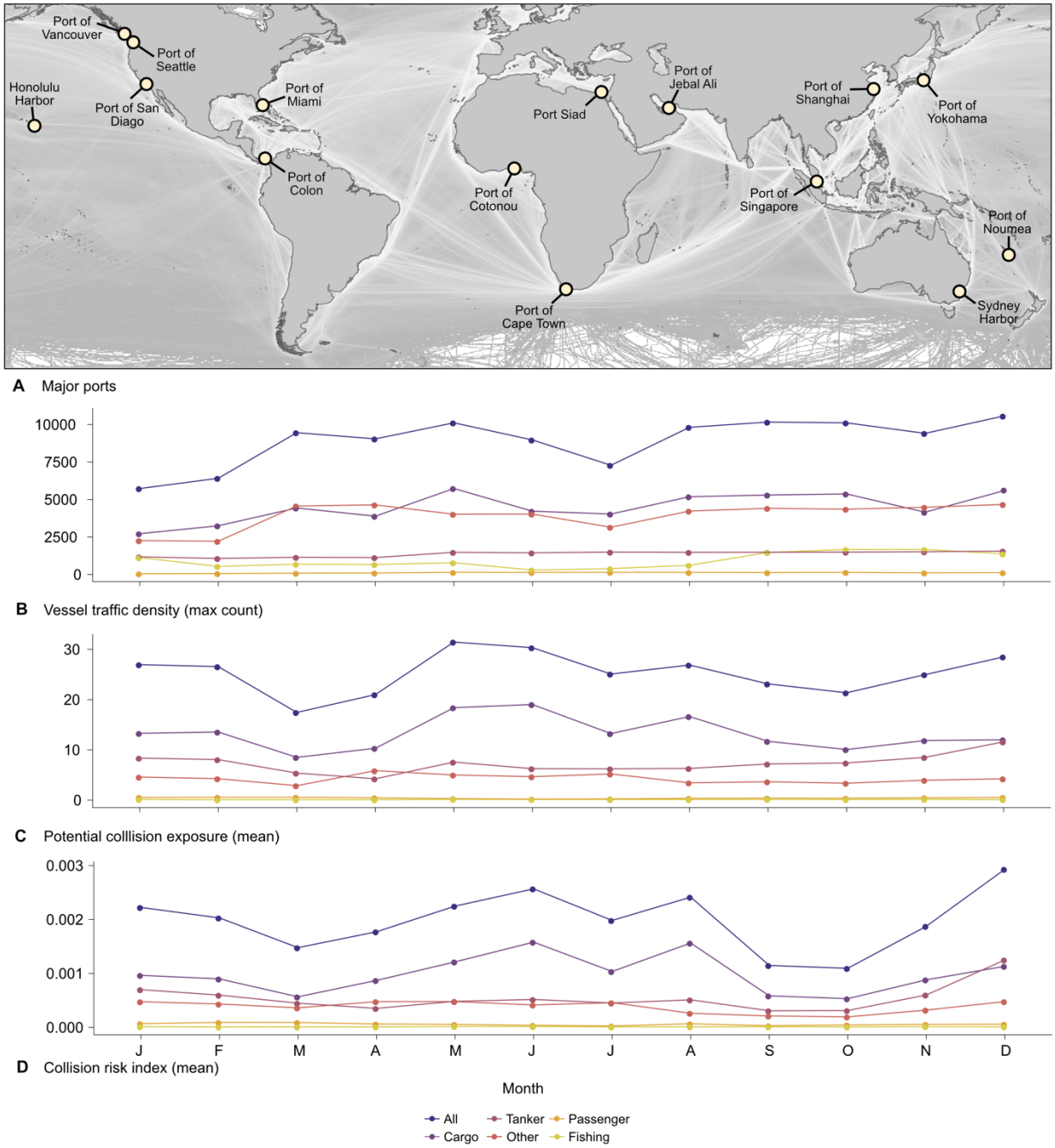

Figure S4 | Key ports and monthly patterns in unique vessel counts in relation to risk metrics. *(A)* Map displaying ocean ports. *(B)* Plot showing the maximum vessel density within a 0.25 × 0.25° resolution cell from the 2011-2014 average. *(C)* Plot showing mean potential collision exposure per individual per month by vessel type (unique vessel count). *(D)* Plot showing mean monthly collision risk index per individual per month by vessel type (relative units).

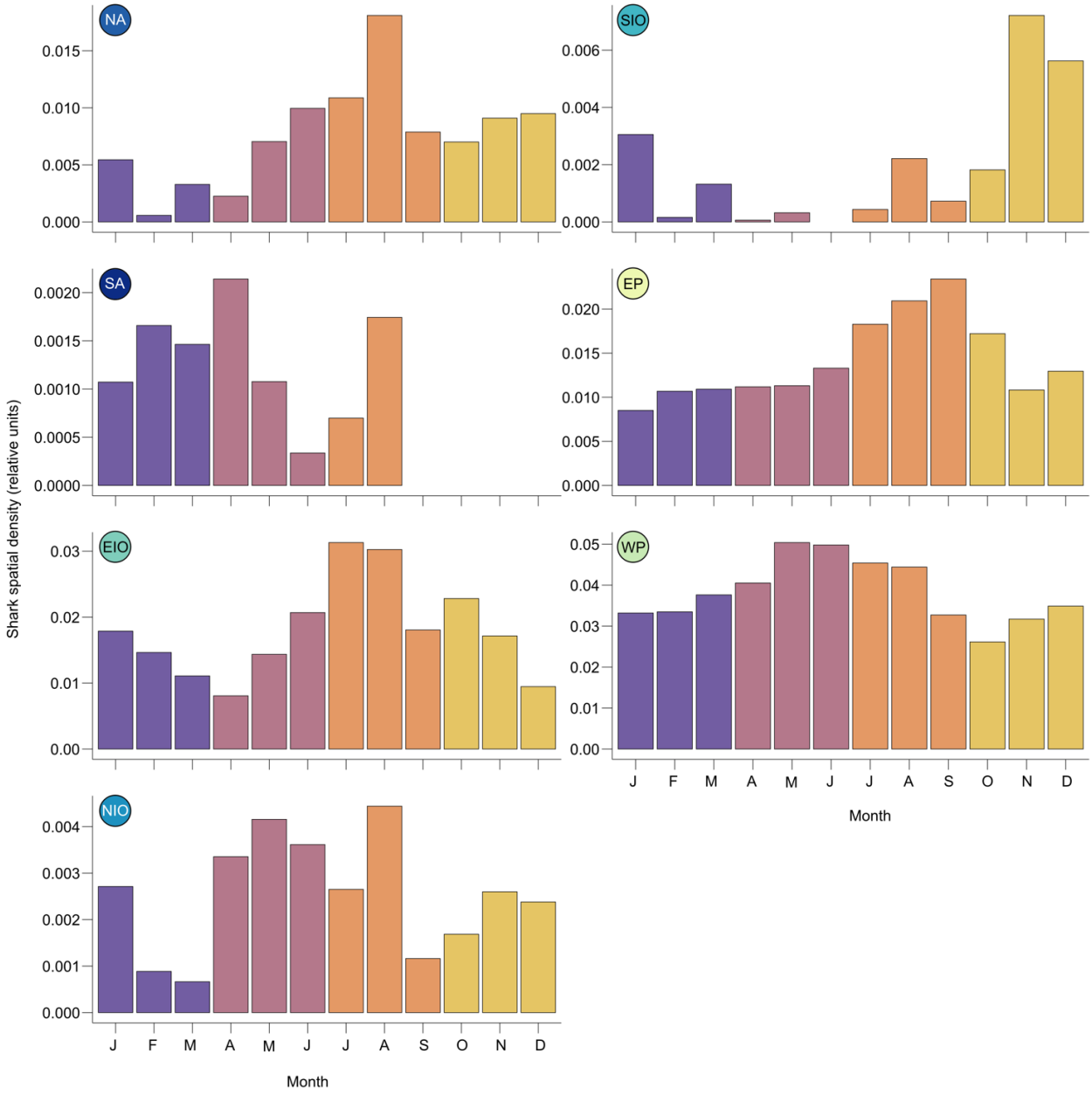

Figure S5 | Monthly patterns in spatial density across ocean regions. Plots showing the sum of individual spatial density within each ocean region across the year. Colours to aid comparison between regions. EP, east Pacific; WP, west Pacific; EIO, east Indian Ocean; SIO, southwest Indian Ocean; NIO, northwest Indian Ocean; NA, north Atlantic; SA, south Atlantic.

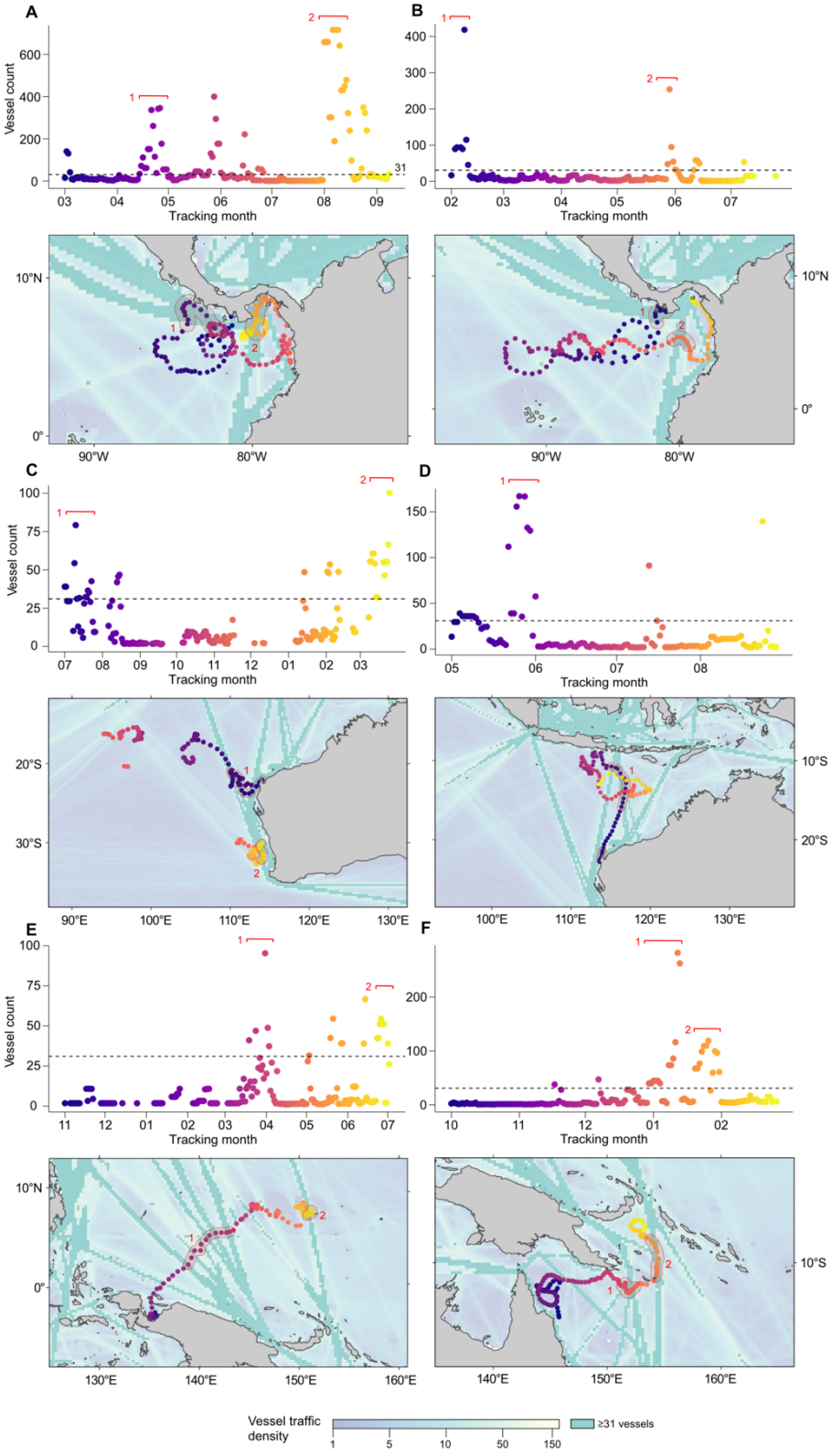

Figure S6 | Individual shark movements around busy routes. Examples of whale sharks tagged in the east Pacific *(A, B)*, east Indian Ocean *(C, D)* and west Pacific *(E, F)* regions that moved out from and, on occasion, back to known aggregation areas compared to the number of vessels encountered at each tracked location (*y* axis, 2011-2014 annual mean) with tracking month on the *x* axis (upper panels) and spatially (lower panels). Locations where individuals move through cells with busy traffic (defined as the top 90th percentile of vessel counts within a cell; 31 for the 2011-2014 annual mean, displayed as black dotted line in upper panels) are highlighted and numbered to display when and where the sharks pass through these areas during tracked movements. Cells with vessel counts with busy traffic have been coloured uniformly in maps to aid interpretation.

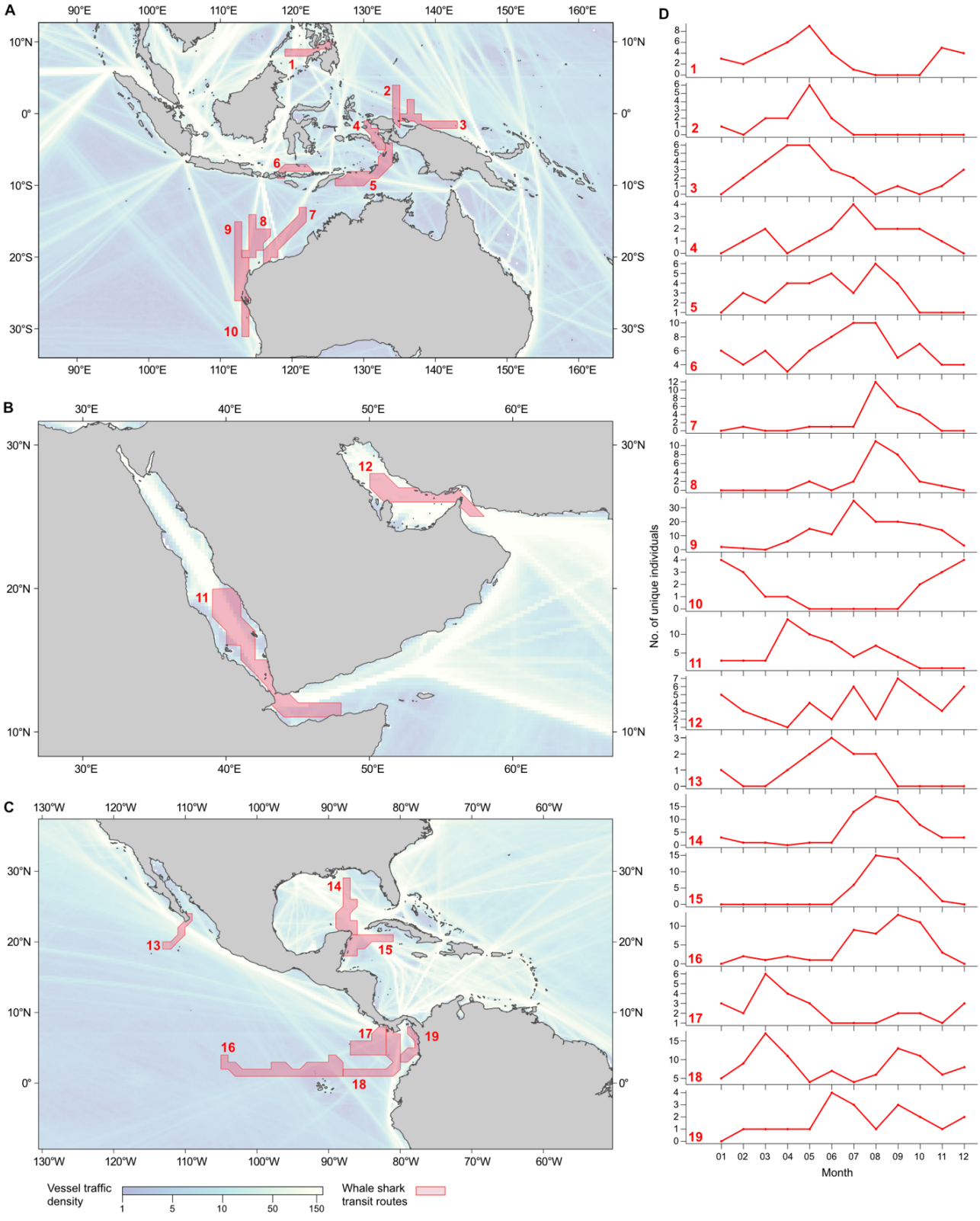

Figure S7 | Whale shark transit routes. *(A - C)* Transit routes (red polygons) used by multiple individuals constructed based on combined track paths and mapped on top of vessel traffic density (2011-2014 annual mean). Defined areas represent corridors into and away from aggregation sites used by the individuals tracked in this study. *(D)* Temporal variation on a monthly timescale of individuals located within each of the predefined transit routes. Numbers correspond to those mapped in the adjacent panels.

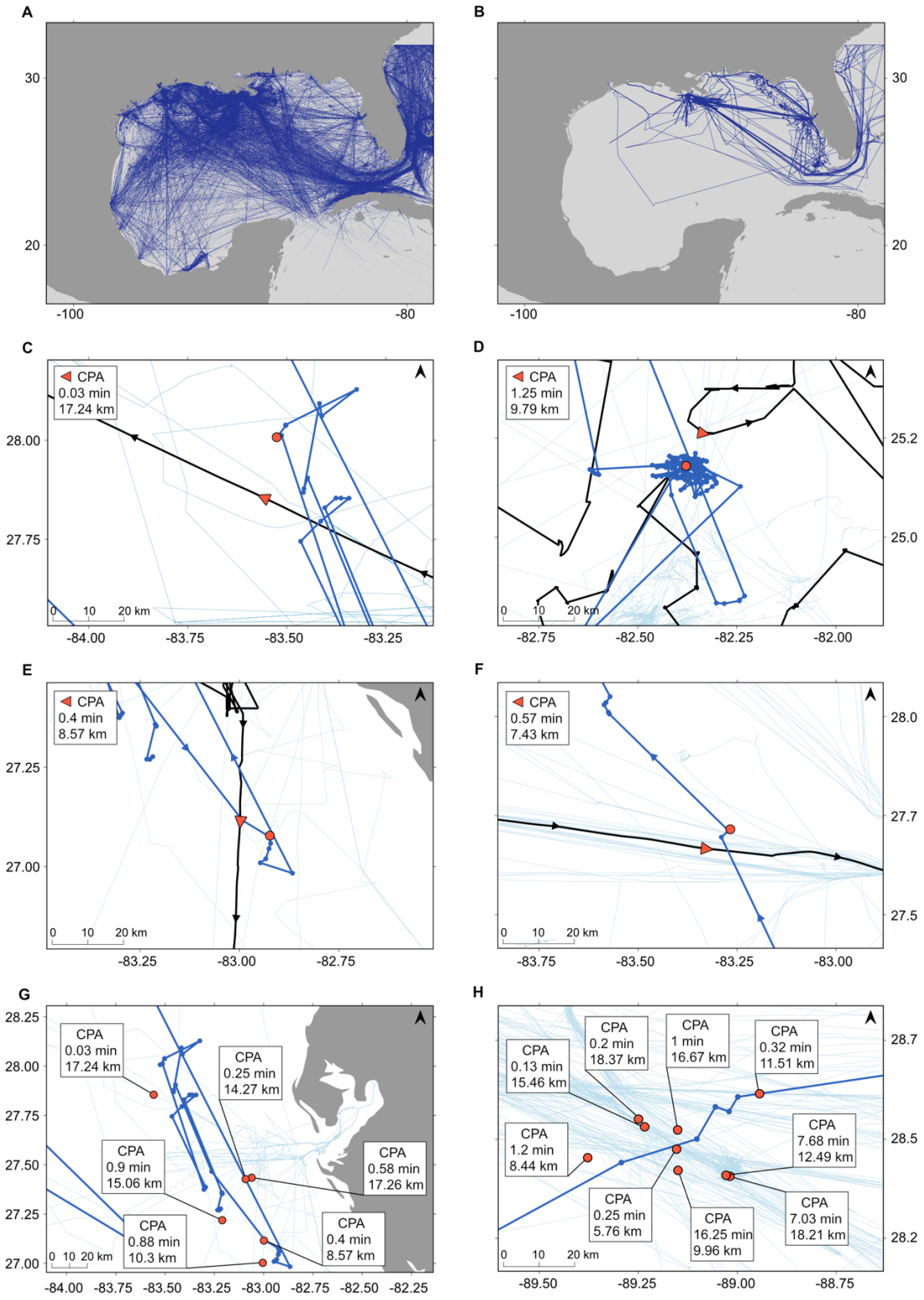

Figure S8 | Vessel tracking data and fine scale vessel-whale shark close approaches from within the Gulf of Mexico. *(A)* Tracks from the fine-scale dataset (obtained from https://coast.noaa.gov/) filtered to contain those that occur within the geographical and temporal extent of two FastLoc GPS® tracks and interpolated to one position per hour (see *Supplementary Methods*). *(B)* Shows high-resolution vessel tracks considered as containing a close pass (closest point of approach (CPA) within 20 minutes and 20 km) (see *Supplementary Methods*), with multiple positions per hour and no interpolation over timeframes with no recorded position. *(C - F)* Examples of CPAs where time difference (minute) and distance (km) at the vessel CPA are displayed. Red triangle denotes vessel CPA position, red circle denotes whale shark CPA position. *(G, H)* Multiple examples CPAs for whale shark gsmp01792 *(G)* and gsmp01793 *(F)* in areas where CPA occurrence was high (port entrances). Red circles denote vessel CPA where time difference (minute) and distance (km) is noted. Faded blue tracks in *C - F* display high-resolution vessel tracks considered as containing a close pass for each individual.

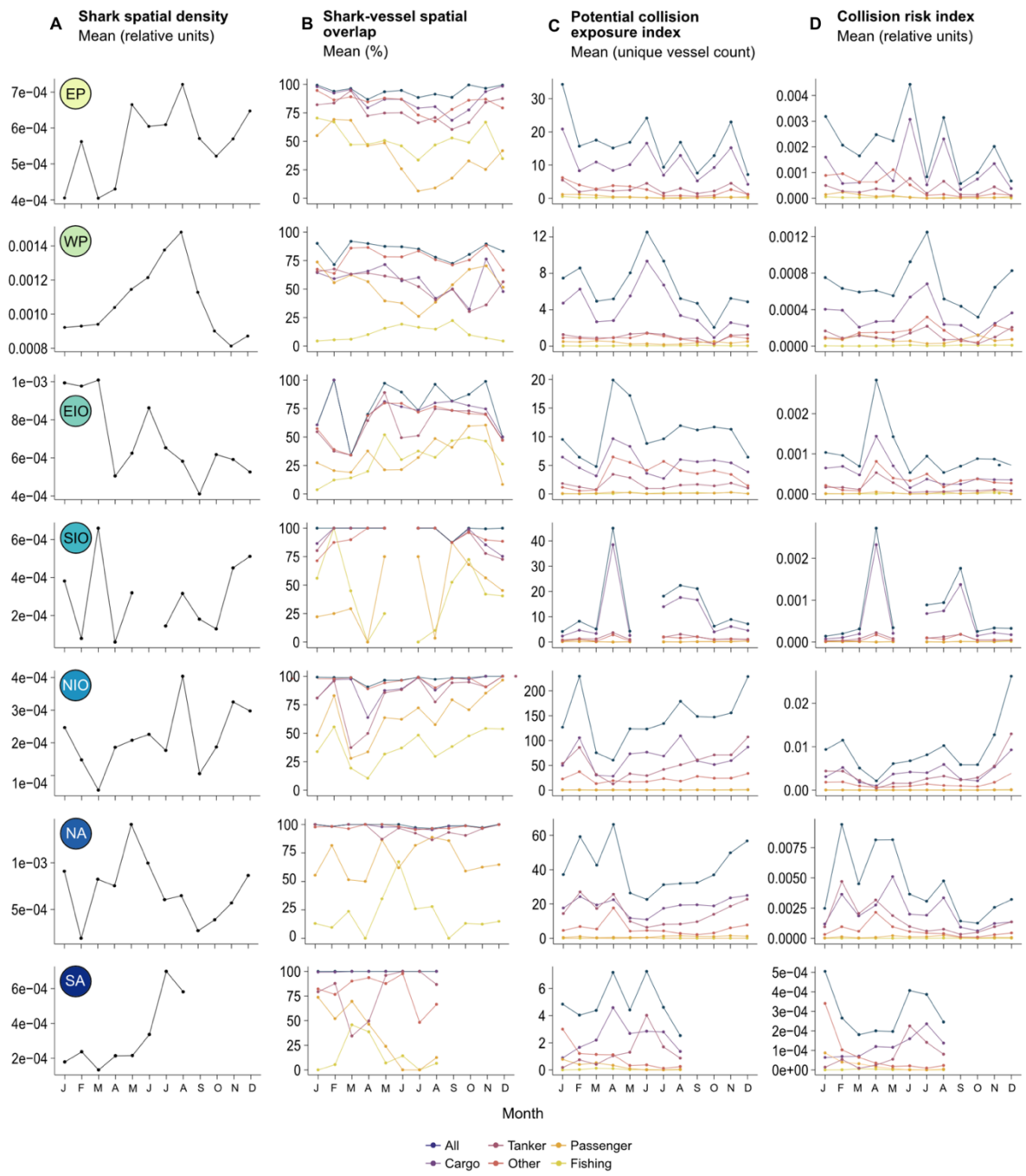

Figure S9 | Monthly patterns in risk metrics within each region by vessel type. *(A)* Plots showing the mean of summed spatial density (relative units) per individual per month summarised for each of the ocean regions within 1 × 1° resolution cells. *(B)* Shows the mean vessel-shark spatial overlap (%) per individual per month parsed into each of the 5 vessel types (cargo, fishing, other, tanker and passenger) and all types combined. *(C)* Shows the mean potential collision exposure (unique vessel count) per individual per month. *(D)* Shows the collision risk index (CRI) (relative units) per individual per month (panel four). EP, east Pacific; WP, west Pacific; EIO, east Indian Ocean; SIO, southwest Indian Ocean; NIO, northwest Indian Ocean; NA, north Atlantic; SA, south Atlantic.

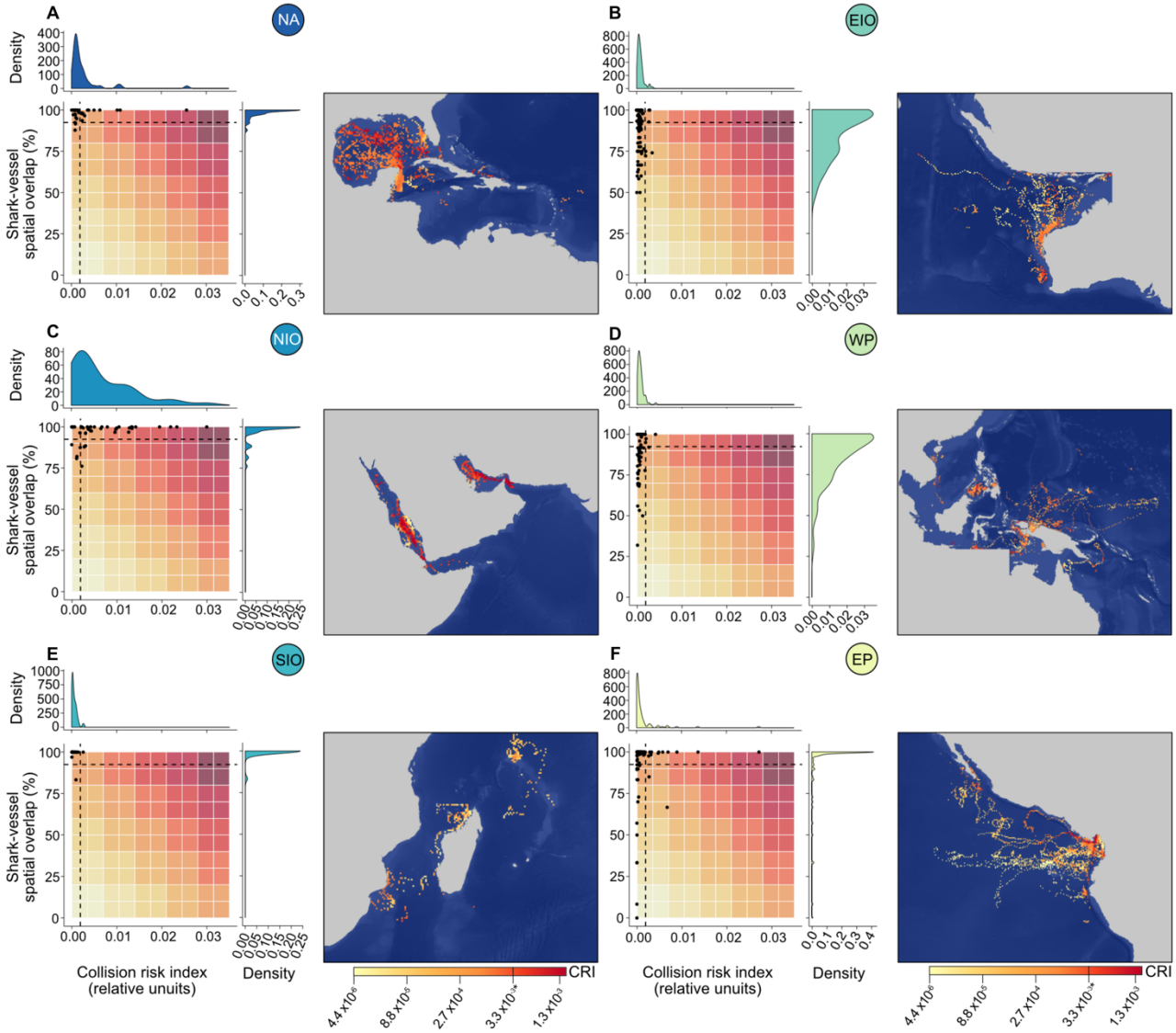

Figure S10 | Regional estimated collision risk index and overlap. *(A - F)* Collision risk index (CRI) plots (column 1 and 3) showing the spatial overlap between whale sharks and vessels and mean monthly CRI of individuals to indicate the distribution of overlap and risk within each region (higher- risk red zones indicate both high risk and high overlap and lower-risk yellow zones indicate low risk and overlap). Black dotted lines display global averages of overlap and risk indicating the distribution of individuals above and below these thresholds. For each region a map of the mean monthly CRI is given to the right of each plot (column 2 and 4). EP, east Pacific; WP, west Pacific; EIO, east Indian Ocean; SIO, southwest Indian Ocean; NIO, northwest Indian Ocean; NA, north Atlantic; SA, south Atlantic.

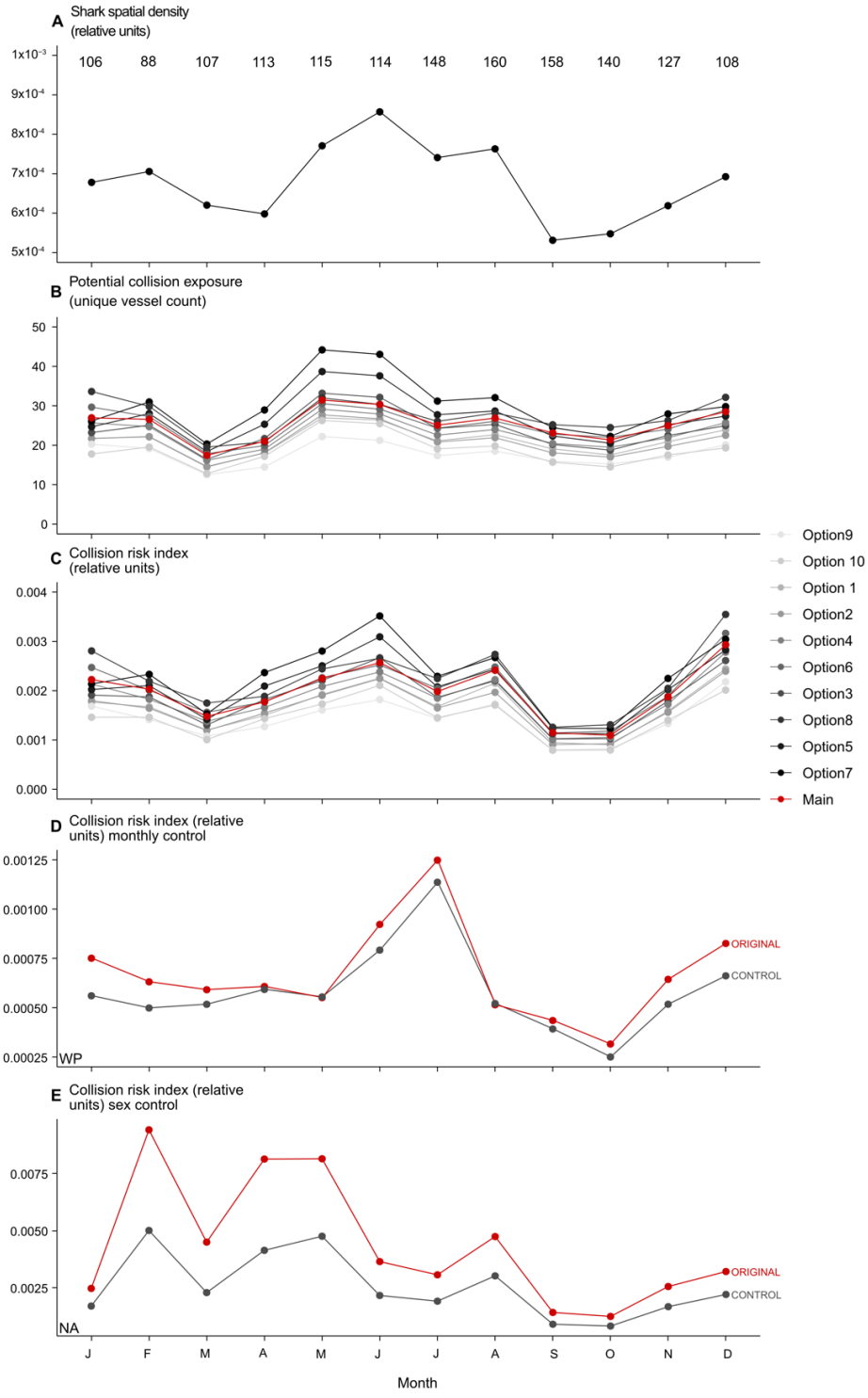

Figure S11 | Comparison of multiple collision-zone use scenarios. *(A)* Mean summed spatial density per individual per month within 1 × 1° resolution cells with sample size of individuals per month displayed. *(B)* Mean monthly potential collision exposure per individual per month within 0.25 x 0.25° resolution cells parsed by collision zone use scenarios. Red line depicts main analysis**.** *(C)* Mean monthly collision risk index per individual per month within 0.25 × 0.25° resolution cells parsed by collision zone use scenarios. Red line depicts main analysis. Collision zone use scenarios refer to the surface use values fitted into the risk calculations and consist of: Main - empirical regional median by depth class (Table S3), Option 1 – overall regional median (Table S3), Option 2 – 0.45:0.45, Option 3 – 0.45:0.5625, Option 4 – 0.5625:0.45, Option 5 – 0.45:0.675, Option 6 – 0.675:0.45, Option 7 – 0.45:0.7875, Option 8 – 0.7875:0.45, Option 9 – 0.45:0.3375, Option 10 – 0.3375:0.45 (ratio coastal:oceanic) (see *Supplementary Methods*). Options in the legend (excluding Main) are ordered (and coloured) by lowest (Option 9) to highest (Option 7) mean CRI. *(D)* Mean monthly collision risk index per individual per month within 0.25 × 0.25° resolution cells parsed by the original dataset (red) and monthly control (grey) (n = 38, Table S20). *(E)* Mean monthly collision risk index per individual per month within 0.25 x 0.25° resolution cells parsed by the original dataset (red) and sex control (grey) (n = 24, Table S19). WP, west Pacific; NA, north Atlantic.

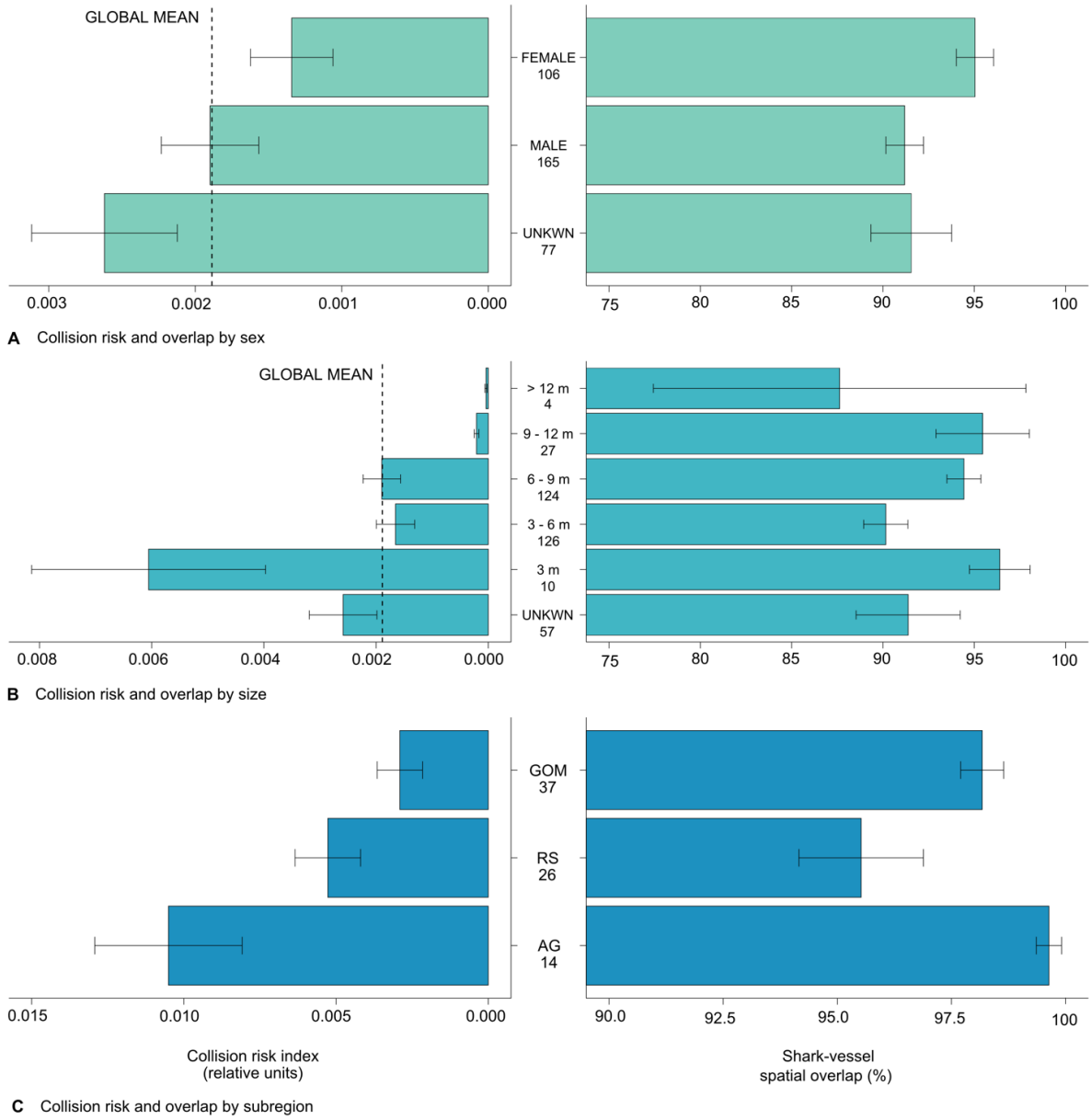

Figure S12 | Mean monthly spatial overlap and CRI. *(A)* Mean monthly CRI (left panel) and overlap (%) (right panel) experienced by female, male and unknown individuals (error bars denote ± one standard error of the mean (s.e.)). *(B)* Mean monthly CRI (left panel) and overlap (%) (right panel) experienced by individuals within each size class (error bars denote ± s.e.). *(C)* Mean monthly CRI (left panel) and overlap (%) (right panel) experienced by individuals within semi-enclosed subregions (error bars denote ± s.e.). Sample size displayed below group name. GOM, Gulf of Mexico; RS, Red Sea; AG, Arabian Gulf.

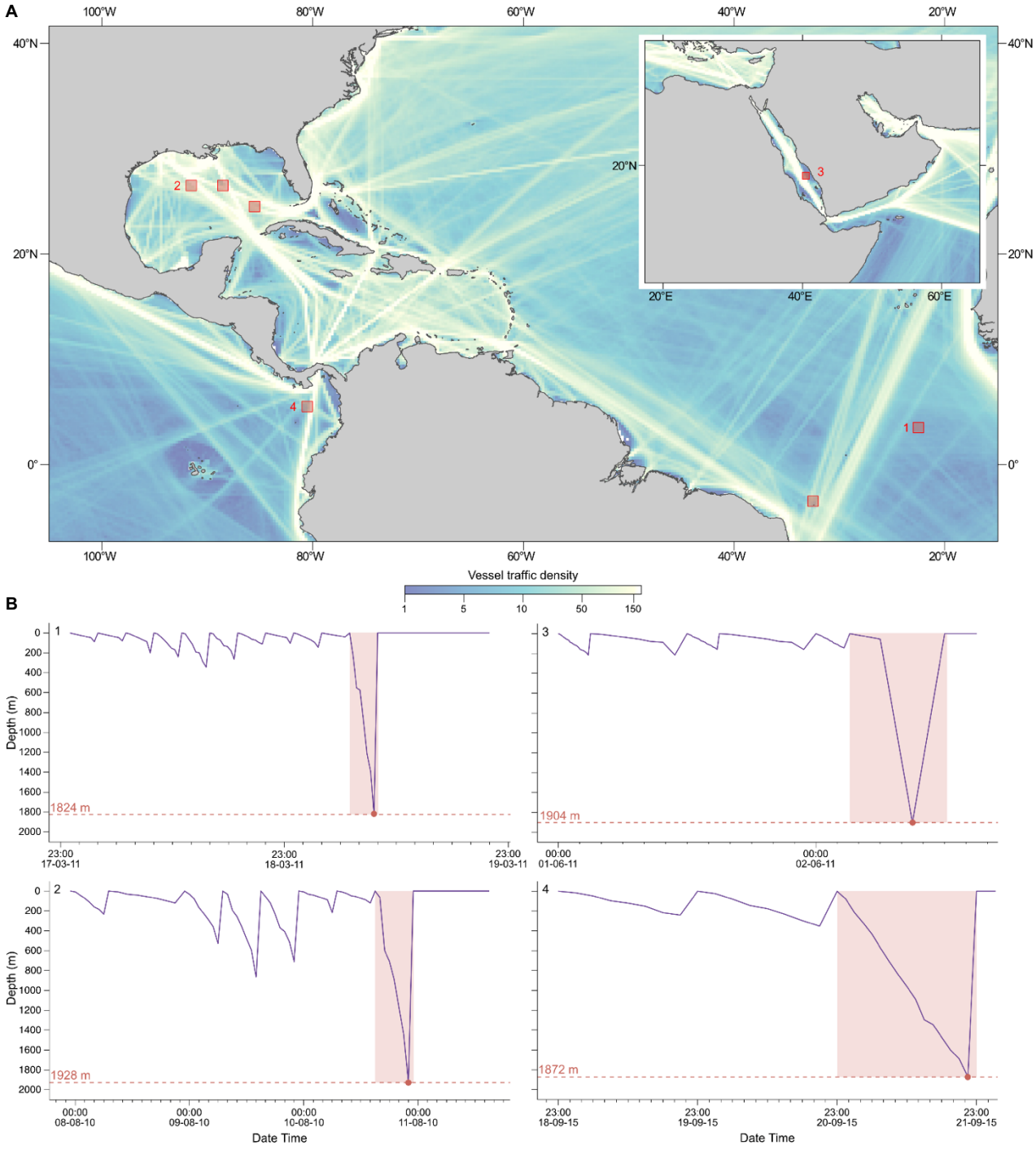

Figure S13 | Reconstructed depth profiles and mapped final locations. *(A)* Vessel traffic density (2011-2014 annual mean) overlaid with final locations of pop-up satellite archival tagged shark tracks where the tag dislodged due to depth limits being exceeded. Red polygons highlight the 1 × 1 ° resolution cells where the pop-up event occurred and the track ended. *(B)* Reconstructed depth profiles for 4 individual sharks where tag depth limits were exceeded. Red shaded areas highlight the final descent of the individuals and the red circle and dotted intercept denote the deepest depth recorded prior to the tag's maximum-depth triggered release. Numbers on plots link to those on the mapped polygons.

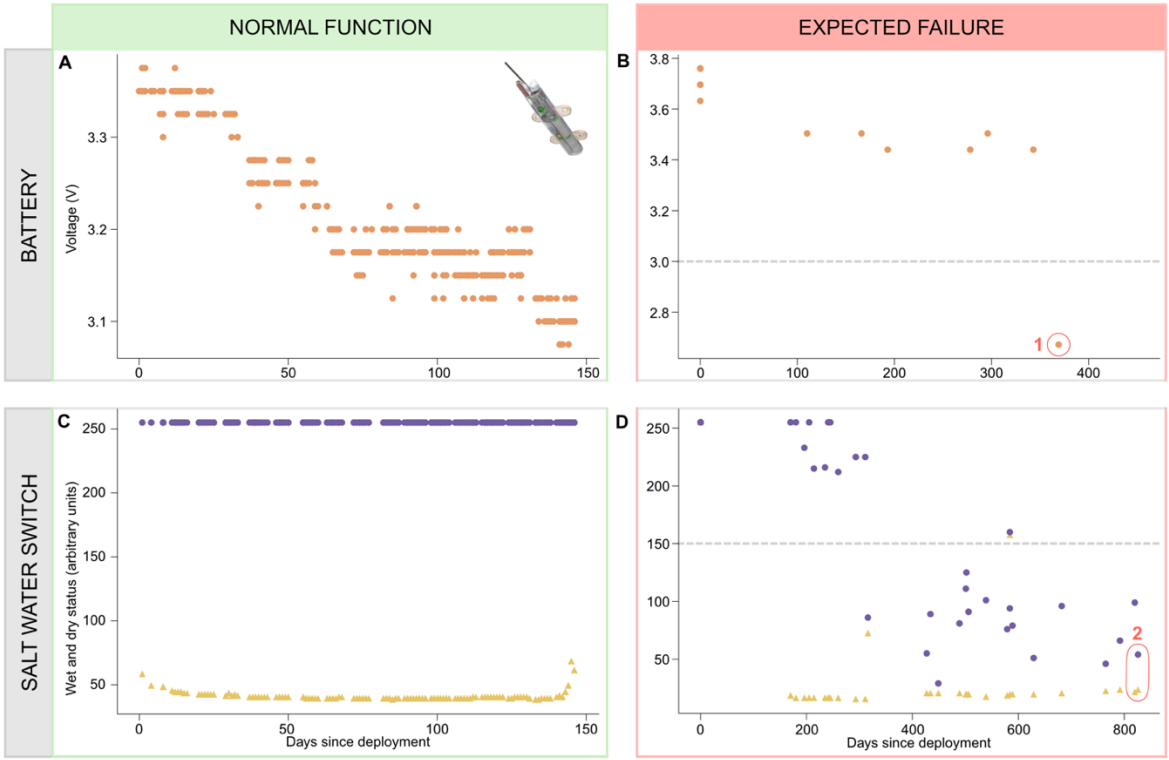

Figure S14 | Examples of ARGOS tag diagnostic indicators for normally functioning tags and those where failure was expected. *(A)* Voltage plotted over time (measured as days since deployment) for a tag which transmitted for approximately 150 days and showed no signs of battery exhaustion; although voltage dropped over time it remained above the threshold of 3 V. Image shows an example tag from Wildlife Computers (https://wildlifecomputers.com/). *(B)* An example of a drop in voltage in the final status transmissions indicative of battery exhaustion where voltage drops below 3 V (1). *(C)* Maximum 'dry' state of the tag (purple circles) and minimum dry state (yellow triangles) or 'wet' state of the saltwater switch plotted over time (measured as days since deployment) with no signs of biofouling; there is always a clear difference between the 'wet' and 'dry' states. *(D)* An example of progressive biofouling where the 'dry' and 'wet' states converge and the 'dry' drops below 150 on final transmission (2) suggesting biofouling was the reason for the cessation of transmission.

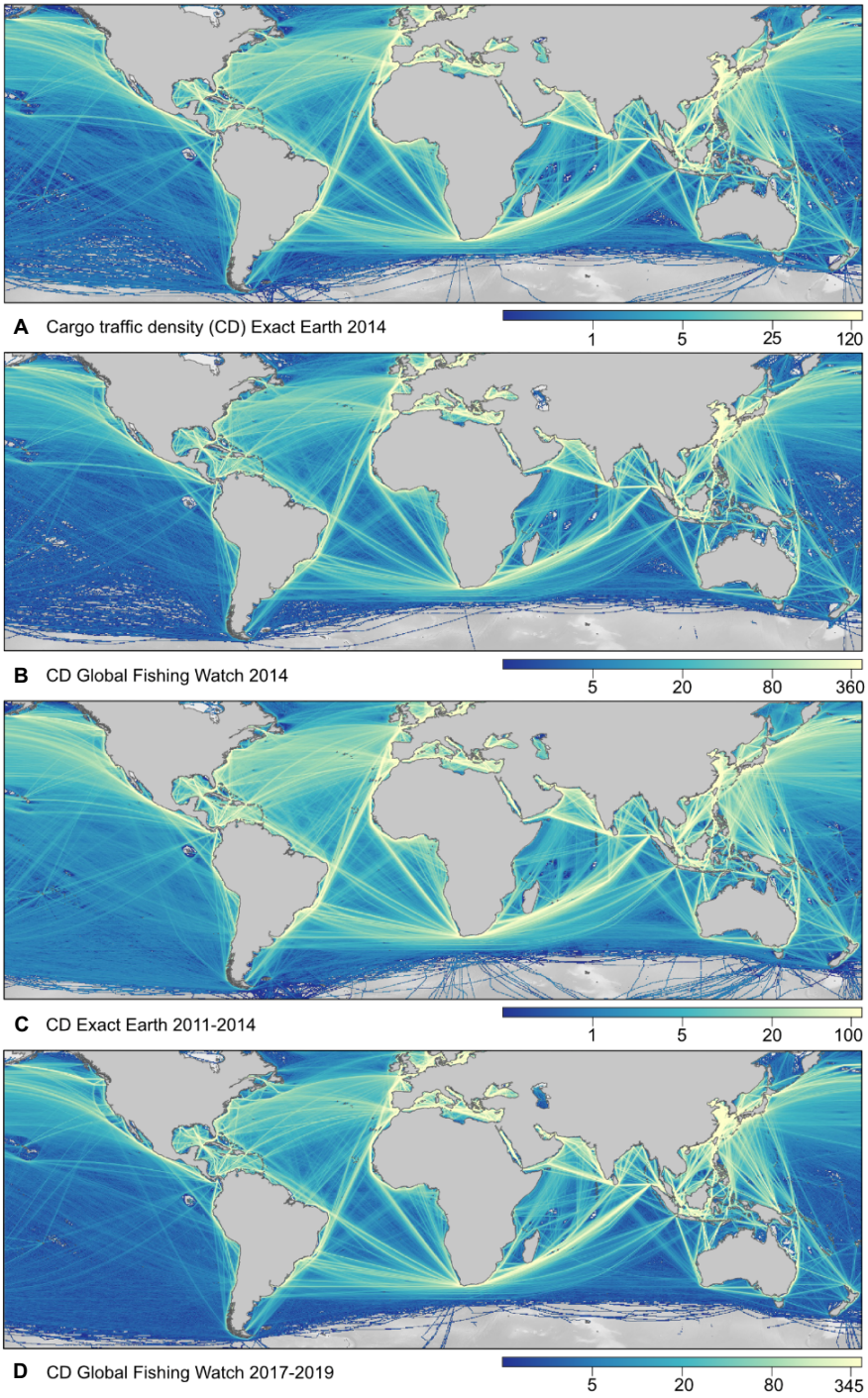

Figure S15 | Exact Earth and Global Fishing Watch vessel datasets. *(A)* Cargo vessel traffic density (total count of vessels within 0.25 × 0.25° resolution cells) from Exact Earth, where mean monthly total number of AIS-tracked vessels is averaged for the year 2014. Lighter colours reflect higher densities of vessels. *(B)* Cargo vessel traffic density (total count of vessels within 0.25 × 0.25° resolution cells) from Global Fishing Watch, where mean monthly total number of AIS-tracked vessels is averaged for the year 2014. Lighter colours reflect higher densities of vessels. *(C)* Cargo vessel traffic density (total count of vessels within 0.25 × 0.25° resolution cells) from Exact Earth, where annual total number of AIS-tracked vessels is averaged for the years 2011-2014. Lighter colours reflect higher densities of vessels. *(D)* Cargo vessel traffic density (total count of vessels within 0.25 × 0.25° resolution cells) from Global Fishing Watch, where annual total number of AIS-tracked vessels is averaged for the years 2017-2019. Lighter colours reflect higher densities of vessels.

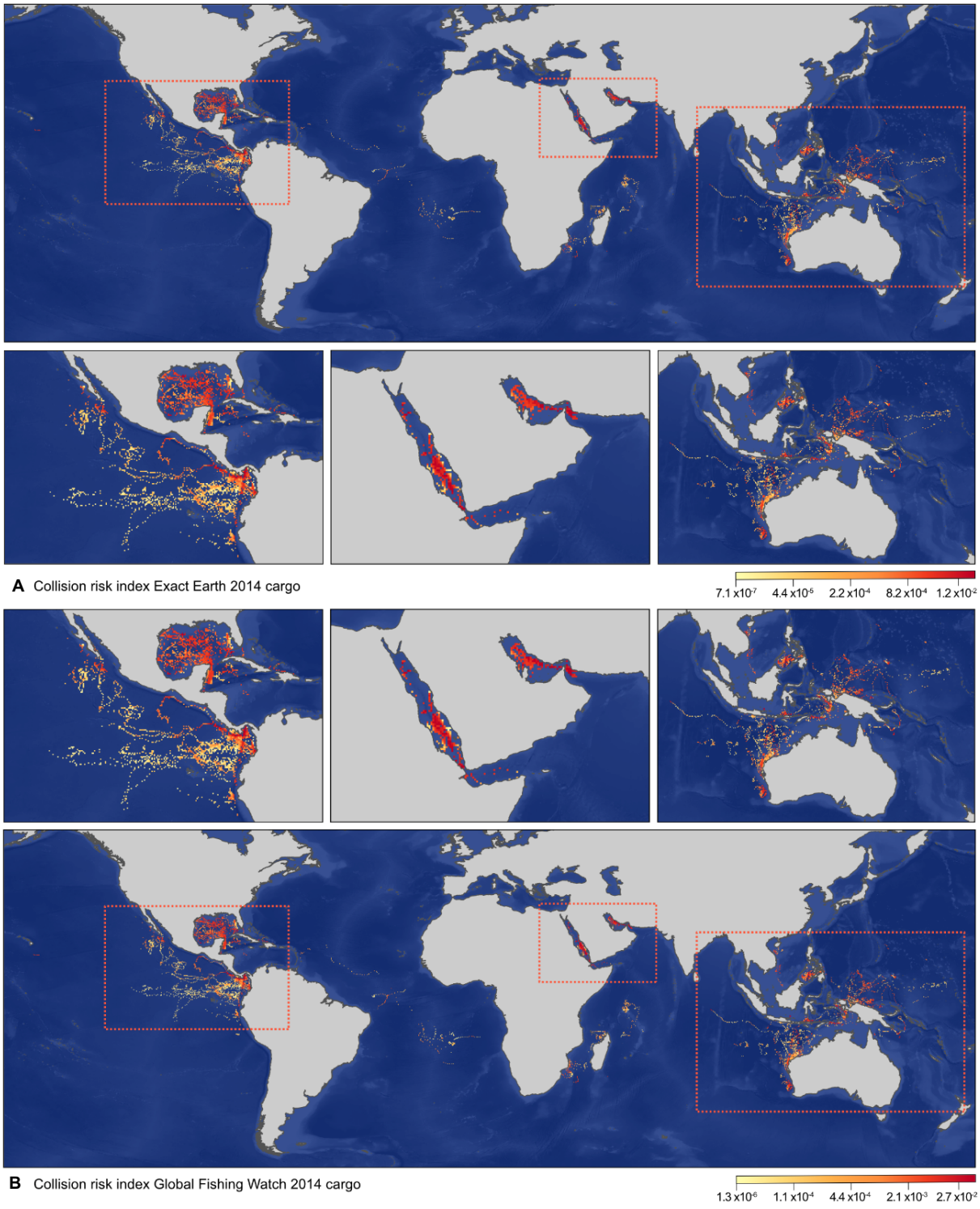

Figure S16 | Comparison of risk between vessel datasets. *(A)* Collision risk index (CRI). Distribution of the mean monthly overlap and CRI that whale sharks are exposed to in overlapping areas within each 0.25 × 0.25° resolution cell in 2014 calculated from the Exact Earth dataset. Red cells represent higher relative CRI than yellow cells. *(B)* Collision risk index (CRI). Distribution of the mean monthly overlap and CRI that whale sharks are exposed to in overlapping areas within each 0.25 × 0.25° resolution cell in 2014 calculated from the Global Fishing Watch dataset. Red cells represent higher relative CRI than yellow cells.

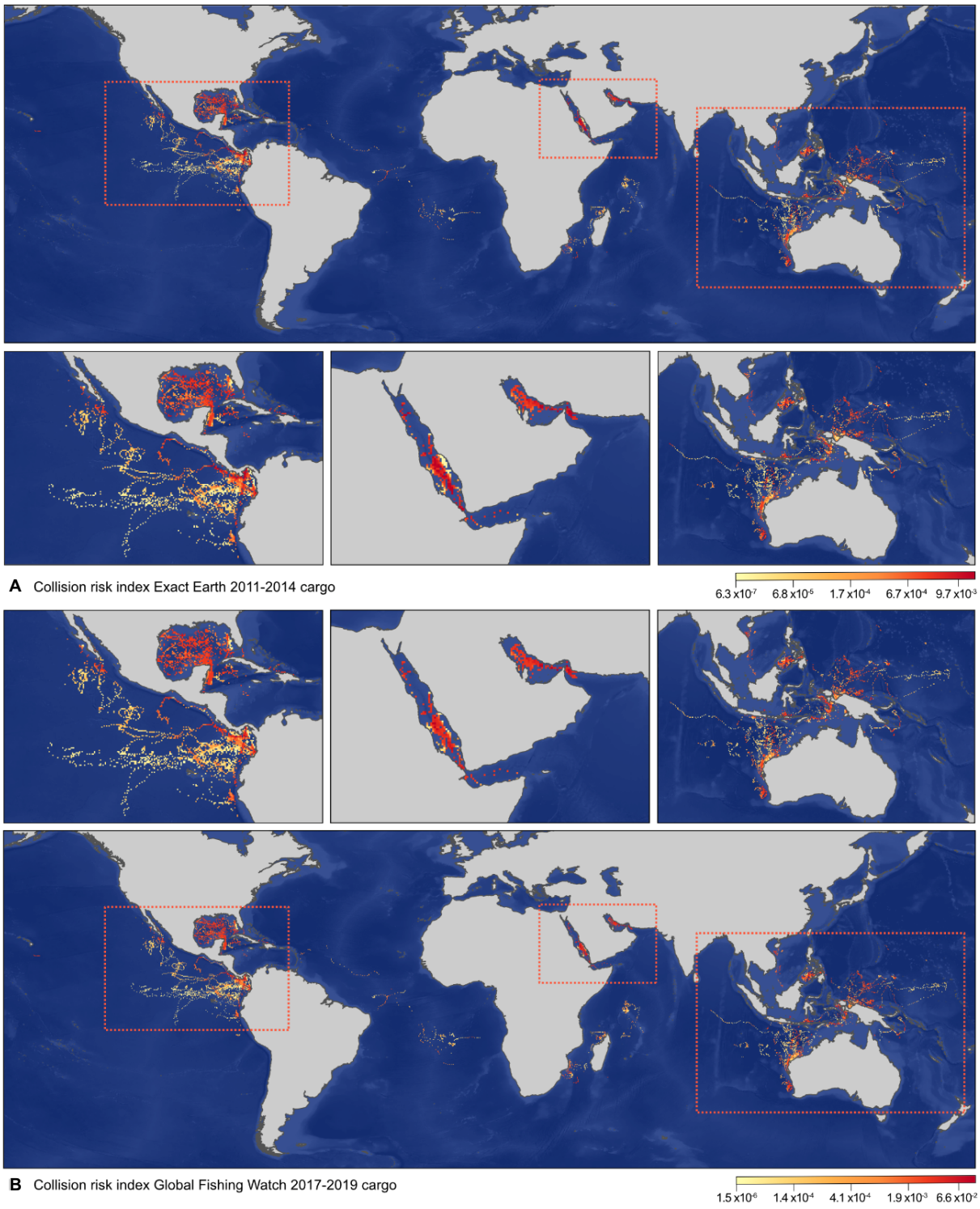

Figure S17 | Comparison of risk between years. *(A)* Collision risk index (CRI). Distribution of the mean monthly overlap and CRI that whale sharks are exposed to in overlapping areas within each 0.25 × 0.25° resolution cell calculated from the 2011-2014 average Exact Earth dataset. Red cells represent higher relative CRI than yellow cells. *(B)* Collision risk index (CRI). Distribution of the mean monthly overlap and CRI that whale sharks are exposed to in overlapping areas within each 0.25 × 0.25° resolution cell calculated from the 2017-2019 average Global Fishing Watch dataset. Red cells represent higher relative CRI than yellow cells.

4. Supplementary Results and Discussion

4.1 Whale shark-vessel collision reports and analysis

We collated as many reports of fatal collisions between whale sharks and large vessels as were available from searches of the published literature and news reports (Table S8). There were surprisingly few, likely due to the absence of a centralised global database of fatal collisions or a shipping-industry reporting mechanism for collating data. Although the number of fatal collisions available in this study was relatively few, many of them provided detailed accounts. For example, in the mid-1900s a number of anecdotal collision reports were published, primarily by the author E.W Gudger, in which whale sharks were described as being struck by ships in regions including the Gulf of Mexico and the Red Sea (92-94). One incident occurred near Socotra Island, where the Gulf of Aden meets the northwest Indian Ocean with a vessel travelling at 15 knots (7.7 m s^{-1}) on passage from Bombay to the Suez Canal (95), and early anecdotes from the Gulf of Mexico described whale sharks as unafraid of vessels, despite their close passing (92) (Table S5). These reports provide some of the best descriptive records of the threats posed by large vessel traffic to date, and highlighted several cases of confirmed mortality, where struck whale sharks did not survive the impact force (94) (Table S8). However, aside from these early anecdotes, explicit collision accounts have rarely been documented and modern collision reports are largely limited to unpublished observations (50). For example, in 2000 an unpublished report of a whale shark struck and killed by a large vessel was recorded off the Seychelles (50). In another case researchers speculated that dive data revealed a potential collision where a tagged whale shark travelling at the surface along a busy shipping route on the northwest shelf of Australia suddenly descended to 900 m, where it remained for 12 h (50, 96). Other accounts have occasionally appeared in local news articles (97-99) (Table S8).

The lack of formal collision records may be due to the vast size and speed of modern vessels (100), making collisions with marine life more difficult to detect by onboard observers (50). Whale sharks are also negatively buoyant, which suggests that following a lethal vessel collision the body

would, in most cases, sink and remain hidden from detection (50). Consequently, recent collision-related data for whale sharks are limited to monitoring injuries on individuals *surviving* a collision. Vessel-related injuries have been reported for whale sharks surviving collisions at several aggregation sites worldwide (37, 46, 50, 51), and in some areas the frequency of scars from presumed interactions with vessels have increased (55, 101). However, using these data to estimate collision risk may underestimate the threat, given the rapid rates of injury healing in elasmobranchs that can mask sub-lethal impacts (102, 103), or prevent accurate determination of collision risk among regions. These difficulties likely explain why collision risks for whale sharks have received relatively little attention compared to marine mammals, where direct links to collision-induced mortality are determined through necropsies of stranded and recovered floating carcasses (104, 105). Further, estimates based on surviving individual sharks with scarring suggest that injuries are mostly linked to interactions with smaller vessels (see references in Table S9), which have little or no impact on regional mortality (55) (for potential sub-lethal impacts of small vessel collisions see discussions in 101 and 103). Collisions with large commercial vessels are not included in any assessments to date.

Using the available fatal collision reports as a first step, we found a positive correlation between CRI regional estimates and frequency of reported whale shark mortality due to ship strike per region (Fig. 4*D*), indicating that the areas with greatest overlap intensity between whale sharks and AIS-monitored traffic were also those with highest reported whale shark mortalities from collisions with large vessels. We acknowledge that the number of reported shark mortalities due to ship strike available to us in this study were limited (n = 17), precluding a more detailed statistical analysis. To explore the robustness of the correlation in the light of the low number of points, we removed each data point sequentially and re-calculated the correlation. The analysis showed that the correlation was robust to individual data point removal for all regions except the NIO region, which had the greatest CRI and highest reported mortalities (Table S8*B*). This correlation remained positive however, indicating that although non-significant there was a trend for higher mortality with greater CRI values when all regions except NIO were considered together. This trend is also supported by our result showing that 50% of

reported mortalities occurred within the 75th percentile of CRI, indicating that half the mortalities were centred in the relatively spatially limited CRI hotspots. Therefore, although there was sparse mortality data to validate more thoroughly the CRI estimates, the results possible with the limited data available do suggest CRI summarises spatial overlap and intensity as an important driver of ship strike mortality of whale sharks.

4.1.1. Using tracking data to infer mortality

Although published accounts of confirmed mortality cases are limited, satellite transmitters attached to animals that are involved in a lethal event can potentially relay a detectable trace of the animal's fate in the collected data. Here, pop-off satellite archival transmitter (PSAT) tag depth profiles were reconstructed to search for potential indicators of individual mortality (Fig. S13). Depth profiles over time provide information on the vertical behaviour of whale sharks and are regularly used to make inferences about the species use of the water column (106). Although whale sharks make deep dives into the bathypelagic zone (>1000 m depth) (32), when the animal dives too deep the tag is released and floats to the surface in order to avoid damage leading to failure. Tracks where maximum tag depth limits were reached were examined for indicators of mortality. Indicators of potential mortality include the tag popping off when at 1504 m or 1924 m depths (depending on tag manufacturer) due to the tag's depth limit being reached, a slow final vertical descent rate relative to other descent rates recorded during the track, and the pop-off location occurring in an area of high vessel traffic density. Collectively, these factors allude to a sinking dead whale shark as opposed to the normal use of the water column by a living shark. For tracks where the tag had released due to exceeding tag depth limits, we calculated the vessel traffic density within the cell where the track ended (Fig. 5*A*, Fig. S13). We found that the mean of vessel traffic per 0.25 × 0.25° grid cell was 78.50 vessels (± 53.99 s.d., n = 7 individuals, 2011-2014 annual mean). On average, the grid cells within which tags indicated potential mortality contained more than double the number of vessels than those defined as having busy marine traffic (characterised as ≥90th percentile of unique vessel counts within grid cells; 31 vessels for 2011-2014 annual mean).

Therefore, the potential mortality of whale sharks occurred in locations where shipping density was among the highest recorded within the entire AIS dataset.

4.2 Risk quantification challenges

The assessment of where animals are at risk of collision is an essential step towards more in-depth studies to quantify collision-induced shark mortality directly, and, where necessary, pursue the implementation of appropriate mitigation measures in relevant geographical areas (107). Global whale shark distribution studies have revealed large-scale movements and habitat suitability (1, 72), however, there are no collision risk analyses based on vessel movements. Due to a lack of basic information, it is difficult to assess the true scale and scope of the threat posed by large vessels to whale sharks, and as a result, not only may there be cryptic mortality in relation to collisions, but also, any effort to quantify associated risk presents several unique challenges.

In marine mammal research, spatial risk models have been developed based typically on the horizontal co-occurrence of vessels and whales (108-111). Using this approach, models can define collision risk as the spatially explicit feasibility of an interaction between a vessel and whale, but this may not account for vertical space use or other factors (13). More recently, whale depth behaviours (i.e., the average time whales occupy various depths) have been incorporated in vessel collision studies (13, 112). Since putative collision risk is only realised when animals are within or near surface waters, where collision is feasible, depth use is considered a critical parameter (13). Other risk modelling approaches have incorporated further complexity by considering factors such as the likelihood of whale avoidance (12, 113), expected rates of collision (111, 114), and the lethality of collision (111, 115, 116). Quantification of these factors usually requires detailed information of both whale (e.g., behavioural responses) and vessel (e.g., type, hull draft size and speed) behaviour and characteristics. For whale sharks, for which no collision risk assessment yet exists, the importance of these factors remains unknown. However, there is evidence to suggest that whale sharks show limited avoidance to oncoming vessels at close range (Table S5) (45), and it is well known that individuals spend large portions of time

in surface waters (32, 117), which may vary dependent on coastal and oceanic habitats (32, 39, 117). Considering the limited knowledge concerning what factors contribute to ship collisions with whale sharks, we considered identifying regions where the potential risk of vessel interactions was high to be an important first step in exploring collision risk for this species. Therefore, in this study we considered spatial and temporal co-occurrence of whale sharks and vessels, where shark surfacing time was quantified directly and explicitly incorporated.

4.3 Shark movement by sex and size class

Both sexes of whale shark were tracked within each of the seven ocean regions (Table S2). However, the west and east Pacific regions were highly segregated with biases towards male and female individuals, respectively (Fig. 1*A*). Tracked sharks with total length measurements of 3-9 m (classes 3-6 m and 6-9 m) accounted for 71.8% of total tracks (n = 348 tracks). The majority of smaller individuals (3 m) were tracked in the region of the Red Sea and larger individuals (>12 m) were tracked solely in the east Pacific region, which also accounted for 81.5% of individuals with a total length of 9-12 m (n = 348 tracks, Table S2). Individuals with a total length of 3-6 m spent the most time in coastal areas (56.5% of locations in waters ≤200 m, n = 7,969 locations) compared to smaller and larger individuals which spent more time in oceanic waters (3 m, 16.9% of locations in waters ≤200 m, n = 431 locations; 9-12 m, 9.3% of locations, n = 890 locations; >12 m, 0% of locations, n = 96 locations).

4.4 Oceanic vs. coastal sea surface use

In some regions, whale sharks spent significantly more time in the upper water column (collision risk zone, ≤20 m or ≤25 m for the east Pacific) when transiting oceanic waters than when in coastal regions (K.S. test, Table S3). The proportion of total tracked time spent in surface waters in oceanic locations was significantly greater than in coastal locations in the north Atlantic (K.S. test = 0.14, n = 3,528 locations, $p < 0.001$) and east Indian Ocean (K.S. test = 0.28, n = 756 locations, $p <$

0.01), while the opposite was true for the west Pacific (K.S. test = 0.12, n = 12,118 locations, $p < 0.001$) (Table S3). No difference in surface use was recorded between males and females in the north Atlantic (K.S. test = 0.406, n = 24 individuals, $p = 0.209$) (Table S19), and the west Pacific region showed relatively consistent monthly surface use with values ranging from 36.8% (median for January, n = 2,234 records) to 51.75% (median for August, n = 2,442 records) (Table S20).

4.5 Vessel density and closest point of approach

In the main analysis, the highest overall traffic density for all vessel types was in March to May and August to December peaking in December (Fig. S4). Fishing vessels exhibited the broadest spatial variation with the highest overall traffic density occurring from September to January. Several large-scale areas were used heavily, including the central equatorial and northwest regions of the Pacific and the southwest Indian Ocean. Passenger vessel routes occurred between tourist locations such as San Diego and Honolulu, between Miami and Caribbean Sea ports, and between Sydney and Noumea in New Caledonia, with maximum vessel counts being highest from May to October (Fig. S4). Cargo vessel movements in the more recent dataset (2017-2019) were spatially and temporally similar to those used in the main analysis (2011-2014) in relative terms, however, higher numbers of vessels within a cell were apparent across all regions (Fig. S15).

For the fine scale analysis, a total of 6,847 vessel tracks occurred within the temporal and geographical extent of the two FastLoc GPS® tracked whale sharks in the Gulf of Mexico (25°N 90°W, Table S4). Most tracks in the filtered dataset made journeys within the Gulf, travelling between U.S. ports including Port Arthur, Texas, Tampa Port, Florida, Port Fourchon and Port of South Louisiana, Louisiana, and Port of Mobile, Alabama (Fig. S8 *A* and *B*). The vessel–whale shark interactions involved six vessel types (tanker, cargo, passenger, tug, dredger and 'other' type vessels; the 'other' class included law enforcement, fishery patrol and offshore supply vessels). For example, the minimum closest point-of-approach (CPA) distances recorded for this small sub-sample of tagged sharks involved a tanker vessel travelling at 6 m s^{-1} and a tug vessel at 5 m s^{-1}, which passed estimated whale shark

positions at distances of 3.8 km (time difference of 1.5 min) and 5.8 km (time difference of 15 seconds), respectively (Fig. 3 *D* and *E*). CPA filtered tracks were also inspected to locate instances where time difference increased and distance decreased to determine if a second CPA was apparent (i.e. the closest point in space but not time). The closest second CPA distances within a reasonable time frame were 262.42 m within 40 minutes and 814.64 m within 14 minutes. The FastLoc GPS tracked whale sharks experienced an average of 0.19 (n = 2 tracks) vessel intersections per 1 km travelled, where an intersection was defined as an instance where lines joining points crossed within the same temporal time frame (Table S4*A*). Based on the fine-scale tracking analysis, the theoretical kinetic energy brought to collisions by ships may be 150 times greater than the energy brought by the sharks (KE = ½ mv^2, e.g. 3.84^2 / 0.31^2 = 153, Table S4).

4.6 Spatial overlap and collision risk index

We made several assumptions needed for working with global scale AIS-tracked large vessel movements and shark satellite transmitters of varied spatial accuracy, coupled with the paucity of information available on whale shark behavioural responses to vessels. Primarily, the global AIS data was summarised into mean monthly values to facilitate comparison with concurrent monthly space use of individual whale sharks and to accommodate the range of whale shark tracking years used. Further, data constraints posed by our global tracking approach precluded the incorporation of behavioural factors of both sharks and vessels that contribute to determining whether a collision will take place (vulnerability risk), in addition to the potential outcome of the event (i.e., mortality or major injury). Instead, our study focussed on the susceptibility of whale sharks to large vessel collisions, which evidence suggests are more likely to be lethal (107) (Table S8), by estimating the potential collision risk based upon spatial and temporal co-occurrence of whale sharks and large vessels within each region.

4.6.1 North Atlantic

In the north Atlantic mean monthly CRI was lowest for five months of the year, from September to January where the maximum extent of individuals occupying the Gulf of Mexico (GOM) was broad. CRI was higher from February to August where positions were distributed more centrally in the GOM around vessel routes connecting ports on the north coast (such as Port of Galveston, Texas) to those in the Caribbean Sea (such as Port of Colon at the entrance of the Panama Canal) (Fig. S9). One 7.5 m female shark made a long-distance movement from the tagging site (northeast Yucatán Peninsula) into the mid-Atlantic Ocean. This individual was most at-risk during September and October whilst moving through the Caribbean Sea, and less susceptible to collision when moving through the open Atlantic during the later months of the track. Although studies to date have not explored overlap between whale sharks and vessel activity in this heavily trafficked region, the GOM has been highlighted as an area of collision concern for other megafauna species such as manta rays (118), turtles (119) and marine mammals (104, 120), which can occupy areas close to busy vessel routes (118). A whale shark was also photographed having been struck by the bow of a large vessel in 2019 (98) (Table S8). Studies in the region of Holbox, which is on the southern coast of the GOM on the Yucatán Peninsula, found that 13 - 33% of whale sharks encountered between 2005 and 2008 had significant scarring attributable to boat strikes (51), and the GOM was the focus of many early collision related anecdotes (93) (Table S5). The high CRI identified in the present study and the fact that high-resolution vessel data is freely available (https://coast.noaa.gov/) make the GOM well suited for further research related to vessel and whale shark interactions, potentially incorporating collision mitigating factors (such as vessel transiting speed) into calculations that were not possible on a global scale. This area would also benefit from management focussed at reducing whale shark-vessel conflict within collective shark transit routes (Fig. S7), and perhaps also within smaller scale aggregation hotspots (Fig. 2*A*) that are close to busy routes (Fig. 2*B*), such as the site off the coast of the Yucatán Peninsula (Fig. S2*B*). Local efforts by the National Commission for Protected Natural Areas in Mexico to establish a Particularly Sensitive Sea Area (PSSA) have not yet been successful. With a number of potentially vulnerable species in this region

(118, 119), selection of effective mitigation measures likely requires a multi-species approach and active interactions between relevant stakeholders so that individual priorities can be identified and addressed (121).

4.6.2 South Atlantic

In the south Atlantic region, CRI was lowest from February to May and peaked in January (Fig. S9) when one whale shark traversed the shipping route connecting ports in South America (such as Rio de Janeiro Port, Brazil), across the Atlantic to ports in northern Africa and Europe (such as Port of Vigo in Spain) (Fig. 2*B*). Throughout most of the year, sharks in the south Atlantic region made movements in mid-Atlantic oceanic waters, often occupying areas far from known shipping routes where susceptibility to collision is lower due to lower vessel traffic density. Despite being far from heavily used marine traffic areas, which explains the low mean monthly CRI in the region, the sharks tracked in the south Atlantic experienced the highest overlap with vessels (mean monthly overlap 100.0%, n = 14, Table S6*A*, Fig. 4*B*, Fig. S9). Vessel use in the Atlantic Ocean was the most spatially extensive among the defined regions in this study, and was primarily used by cargo vessels, with very few cells lacking traffic on monthly timescales (Fig. 2*B*), increasing the opportunities for overlap. However, because the vessel traffic density within the overlapping cells was generally lower than other regions, mean monthly CRI was also lower during tracked months (Fig. S9). Although the south Atlantic region is one of the lesser-known areas in terms of whale shark movement and ecology included in this study, St. Helena has recently been highlighted as an important reproductive habitat, with the first reliable eyewitness accounts of mating behaviour reported for whale sharks (38). It is crucial that known ecologically important areas for this species are identified and protected where necessary in the South Atlantic and globally. Given the high reported overlap values in the region, collisions should be a key consideration in marine management and planning policy. Because there are also whale shark hotspots on the west African coast, in areas such as the Gulf of Guinea (1) and the waters of Gabon (122), there is potential for region wide connectivity where whale sharks visiting St. Helena move eastward to feed in coastal

waters (72). If this is the case, transiting sharks will cross several busy shipping routes in oceanic waters and may also be susceptible to collision in coastal areas (Fig. 2*B*). Indeed, the Gulf of Guinea contains one of the largest ports in west Africa (Port of Cotonou), and has been noted as a concern for other species in the area due to vessel movements around the Bight of Benin (123). Similarly, vessels travelling to and from Santos Port, the largest port in Brazil (São Paulo), will pose a collision threat to whale sharks occupying the coastal feeding locations on the eastern Brazilian coast, as well as those occupying the offshore platforms positioned along the Campos Basin (61).

4.6.3 Northwest Indian Ocean

CRI in the northwest Indian Ocean was relatively high all year round, which is not surprising given that previous studies on whale sharks have shown movements (63) and aggregating activity (54) within areas also heavily used by vessels (Fig. 2 *A* and *B*). Mean monthly CRI in the region was higher than any other region for every month of the year except April and May when individuals in the north Atlantic experienced a higher mean monthly CRI (Fig. S9). Mean monthly CRI in the region peaked in December, when there was a hotspot of high spatial density in the Gulf of Oman at the entrance of the Strait of Hormuz. Vessel density was extremely high in this area throughout the year, where vessels moved through a narrow waterway linking the Arabian Gulf to the Gulf of Oman and the Arabian Sea. At its narrowest point, this pass is 55 km wide and the shipping lanes in each direction are just over 3 km wide (124). CRI estimates for individual sharks during December were higher for tanker vessels than for any other vessel type and represented one of the few instances in which tankers presented a greater potential threat than cargo vessels (Fig. S9). We identified distinct CRI hotspots within the Red Sea and the Arabian Gulf. This region was also found to have the highest number of reported fatal collisions (Fig. 4*D*, Fig. S3*B*), presumably driven by the close proximity of shark aggregations and large vessels shown in our analysis. Both regions were also explored in the local CRI and scarring comparison analysis. In Shib Habil (Red Sea), 15% of identified individuals from a sample size of 136 had scarring that was reasonably attributed to collision with mainly smaller sized vessels that were not included in

this study (Table S9). Similar frequencies were recorded in Qatari waters (Arabian Gulf), where 14.3% of individuals had distinctive propeller marks, although this value was based on a much smaller sample of 14 identified individuals. These values are not as high as expected (relative to other local areas) which may reflect lower numbers of smaller vessels co-occurring with shark space use in these gulf regions. It is more likely that large vessel collisions result in severe and fatal injuries that were not recorded in these preliminary scarring assessments that largely record sharks surviving from collisions with smaller vessels.

In the Gulf of Tadjoura, Djibouti, south of the Bab al-Mandab Strait where the Red Sea meets the Gulf of Aden, vessel related scars were observed on 65% of identified sharks (37), based on a sample size of 23 (Table S9). In this case local vessel activity was highlighted as a concern for injury inducing collisions (37). Individuals from the Djibouti aggregation have been shown to travel north into the Red Sea, through the Bab al-Mandab Strait, and back again, where they may be susceptible to collision (Fig. 1*A*) (36, 63). Whale sharks tracked in this region in the present and previous studies are slightly biased towards juvenile sharks, and the Red Sea may be an important foraging ground for late-stage juveniles and sub-adults (63). Further, a presumed pregnant female shark was tagged in the region of the Arabian Gulf and travelled through the Strait of Hormuz on a south-westerly trajectory before the tag detached close to the Socotra Islands (Yemen), likely crossing a number of busy vessel routes (Fig. 2*B*). It may be the case, therefore, that this region is ecologically important for a range of life stages, and collisions should be considered a key concern for these groups. In 2017 a local news article reported on a lethal collision in the Jordanian Gulf of Aqaba, in which a whale shark was struck and became lodged in a large propeller, disabling the engine (Table S8) (97). Anecdotal accounts of other species being killed by collisions with large vessels have emerged from the region (104), but there are few published accounts. Although likely to protect many species occupying these narrow and enclosed waters, mitigation strategies explored in these areas will have to consider complex political, economic, and environmental factors because they are bordered by many countries. Traffic Separation Schemes (TSS) are already in place in some of these areas, and re-routing around important whale shark habitats may not be possible due to the limited space and safety concerns. However, mandated reductions in vessel

speed in areas identified as collective whale shark transit routes (Fig. S7) and aggregation areas could help to reduce collision risk in this region which we estimate to be among the highest globally.

4.6.4 Southwest Indian Ocean

Mean monthly CRI in the southwest Indian Ocean saw a peak in April, when one location on the eastern side of Madagascar overlapped with a shipping route from Port of Cape Town to Port of Singapore, and a lesser peak in September, when all locations were situated in coastal waters off the coast of Mozambique, many of which overlapped with vessels travelling to and from East Africa to Port of Cape Town (Fig. 2*B*, Fig. S9). Most sharks tracked in this region made movements within the Mozambique Channel (Fig. 1*A*), which is transected by one primary vessel route connecting ports in South Africa to the north Indian Ocean via the Comoro Islands. Although some shark locations overlapped with this route, the greatest risk area in the southwest Indian Ocean was the dense vessel route south of Madagascar that connects the West to the East via Port of Cape Town. One location overlapped with this route where a high CRI was recorded, but further tagging studies are needed in the region to establish potential movements around this area. Studies on inter-ocean connectivity of whale sharks suggest that there is the potential for individuals to travel along the South African coast and through the Cape of Good Hope from the Indian Ocean into the Atlantic (72). Although this has not been confirmed through tagging, stranded whale sharks on the east coast of South Africa have been recorded, and might be associated with the changes in temperature during movements around the continent (125). If this is the case, sharks may be susceptible to collision when traversing the busy shipping route off the southern coast of South Africa which has been highlighted as a key area for collision concern for other species based on stranding records and vessel interactions (126, 127). The sharks tagged around the Seychelles (Fig. 1*A*) did not traverse any specific heavily used vessel routes and thus were associated with a lower mean monthly CRI and a single reported fatal collision with a large vessel (Fig. S3, Table S8). However, reported scarring frequency determined from a multi-site assessment of laceration wounds, likely inflicted by small coastal vessels, across the Indian Ocean (50)

was higher in the Seychelles compared to other Indian Ocean sites (excluding Djibouti), and further investigation into the threats presented by other types of vessel in this area are needed. Individuals were not tracked moving further north than the equator; however, studies suggest links with the north Indian Ocean to be possible (72), where collision risk identified here was much higher. Studies in Tanzania have acknowledged vessel strike as a primary conservation concern in the region (128). In this case seasonal, area-specific go-slow zones were put forward as a potential mitigation option due to the relatively small size and predictability of the home-range of aggregating individuals (128).

4.6.5 East Indian Ocean

During December, January and March, mean monthly overlap in the east Indian Ocean region was lowest in the dataset (50%, 61% and 34%, respectively, Fig. S9) compared to the north and southwest Indian Ocean regions, where individuals experienced much higher overlap in the same months (mean monthly spatial overlap ~99% for December, January and March) (Fig. S9). Mean monthly CRI in the east Indian Ocean region peaked in April when all estimated shark locations were less than ~200 km from shore and overlapped with shipping routes connecting Perth to the northern coast of Australia and across the open ocean to ports in Southeast Asia (Fig. *2B* and Fig. S9). We identified several seasonal transit routes used by multiple whale sharks off northwest and western Australia (Fig. S7*A*), indicating persistent shipping and shark movement patterns co-occur in this region. This regional example also suggests that although in some regions collision zone use was greater in oceanic waters (Table S3), the higher vessel density in coastal/ shelf areas means whale sharks are generally more at risk of collision when in coastal/ shelf waters, despite spending less time in the upper 20 m where susceptibility to collision is greater. In this region, the majority of oceanic movements occurred in the latter half of the year (from July to December) which is when many tracks overlapped with shipping routes connecting ports in Australia to those in Southeast Asia. However, mean monthly CRI values appeared lower than in peak months as positions were also recorded in the less dense vessel areas that surround distinct routes. Overlap with fishing vessels in the east Indian Ocean was the second highest region in the dataset

(mean monthly overlap 46.8%, n = 74). Catch and bycatch risk has been highlighted as a concern for whale sharks in the Indian Ocean associated with purse seine fishing practices (129, 130).

The CRI hotspot identified in the Perth Canyon area, where whale sharks gathered (n = 6) off the shelf from November to April (Fig. 2*A*) may represent an important feeding habitat for this species, although more fine-scale tracking analyses are needed to confirm the importance of this area. In recent years, whale sharks have been anecdotally sighted in this region (131, 132), and sharks tracked in this study were only observed in this area (approximately 29°S to 33°S) in later years (2017 onward) which may be linked to climatic changes and increased frequency of marine heat waves recorded in Western Australia (131). Variations in wind and insolation, influencing seasonal changes and mesoscale features within the region, have been linked to enhancing both pelagic production (133) and a physical aggregation of plankton that also attracts pygmy blue whales (134, 135). Whale sharks may be susceptible to collision whilst exploiting these features. Given the long-standing whale shark tourism industry based in Western Australia, where strict Codes of Conduct have been established to protect sharks from human impacts (136), this region may be well suited to developing mitigations with a strong foundation of positive public perception and stakeholder compliance. Vessels travelling to and from Perth and ports on the south coast of Australia (such as Port of Adelaide) could be instructed to avoid the oceanic waters off the shelf during the months where the whale shark hotspot was identified. Alternatively, if vessel operators identify multiple individuals aggregating, then a Dynamic Management Area (DMA) approach, whereby passing vessels reduce speeds and avoid the area, may reduce the risk of collision (107). Similar approaches have protected important dugong habitats in Queensland (Australia) on a year-round basis and seasonally around loggerhead and green turtle habitats in the U.S. Florida Coast (137, 138). Further research into the applicability and success of these techniques for whale sharks is warranted.

4.6.6 West Pacific

In the west Pacific region, mean monthly CRI peaked in June and July, when there was an area of high shark density along collective shark transit routes near the Makur Islands that overlapped with a distinct shipping route connecting ports in Australia, through the Solomon Sea to the Port of Yokohama in Japan (Fig. S9). In the months of May to July, tracked whale sharks also spent time in the Sulu Sea with positions overlapping with a number of shipping routes connecting ports on the China mainland, such as Port of Fuzhou, to those in Indonesia (Fig. 2*B*, Fig. S9). From January to June, tracks along the northern coast of the island of New Guinea overlapped with vessel routes connecting ports in Australia to ports in East Asia. Throughout the year, a number of shark tracks overlapped with the distinct route that transits the Arafura Sea from the tip of Queensland (Australia) to the island of Timor-Leste. A hotspot of potential collision risk was identified in the Sulu Sea in the Philippines. Published accounts of propeller scars were observed on 47% (based on a sample size of 158) of the whale sharks sighted in Oslob, near Cebu Island in the Philippines (46), which is one of the islands east of the Sulu Sea where sharks must cross the Western Nautical Highway when moving into the region from the Cebu Strait and Bohol Sea. Scars were noted as most likely caused by small outrigger boats with propeller diameter between 5 and 20 cm, or from larger commercial-vessel collisions (propeller diameter, 21–50 cm) (46) that were not the subject of the current study. Similar vessel-related scar frequencies were recorded in the region of Southern Leyte (56) (Table S9). In 2016 a local news article reported on a lethal collision in Jayapura waters off Papua, Indonesia, in which a 4 m whale shark was hit by a large vessel where the captain apparently could not avoid the collision (Fig. S3*B*, Table S8) (99). This confirms that lethal collisions with vessels occur in the region as predicted from the shark – AIS vessel derived CRI estimates we present, in addition to injuries inflicted on whale sharks by smaller vessels.

Overlap with fishing vessels in the west Pacific was surprisingly low (mean monthly overlap 8.4%, n = 62) given reports of whale shark capture in the region (Table S16) (139). It is likely this discrepancy is related to small coastal fishing vessels, without AIS receivers, that operate in the west Pacific which

have been known to make illegal catches of whale sharks (72). This region, in particular, would benefit from fine-scale assessments that incorporate smaller vessel sizes into risk quantification studies in order to fully represent the threat of collision presented by all boat traffic operating around whale sharks. Further, behavioural assessments that explore how sharks respond to vessels, perhaps considering those that are provisioned with food (with potential habituation) (140), and those at other sites, would provide valuable insight as to how individual shark behaviours might factor into the probability of collisions occurring in heavily trafficked areas. In 2017, Tubbataha Reefs Natural Park (http://tubbatahareefs.org) in the central Sulu Sea was approved by the International Maritime Organisation (IMO) as a Potential Sensitive Sea Area (PSSA) and designated as an Area to Be Avoided (ATBA). The protected area covers almost 100,000 hectares (1000 km^2) of high-quality marine habitats containing three atolls and a large area of deep sea which large vessels must avoid. Whale sharks in this study were tracked near to this site where spatial CRI was high around the route passing though the Sulu Sea (Fig. S7*A*). Fine-scale vessel and whale shark tracking assessments could be explored in this area to quantify potential interactions inside and outside of the park and evaluate the success of mitigation strategies.

4.6.7 East Pacific

In contrast to the west Pacific, CRI in the east Pacific region was higher in the first half of the year (January to June) where sharks were exposed to persistent potential risk of collision when occupying the area (Fig. S9), and particularly when travelling along collective transit routes (Fig. S7*C*). For instance, although shark spatial density in this region was focussed around the entrance of a major port in the Panama Basin, yielding high CRI values year-round, in the first 6 months of the year a number of tracks moved northward from the Panama Basin along the west coast of Panama and Costa Rica, following the same trajectory of vessels travelling to and from Port Colon and ports in North America. This route comprises hundreds of vessels with >1000 unique vessels present within a cell at its most dense (2011-2014 annual mean), indicating that whale sharks occupying the area may have greater

potential for collision (greater susceptibility). Studies suggest this area is also a concern for whale species (141).

During the latter 6 months of the year, more tracks occupied oceanic waters in the region of the South Equatorial Current, where vessel activity was much lower. Movements of adult females in this area have been linked to thermo-biological frontal systems (142), where preferential occupancy has been indicated in areas with strong thermal gradients driven by divergence in the current systems along the equator and the west coast of South America (142). Fishing vessels' space use has also been linked to thermo-biological frontal systems (3). Whale sharks in the east Pacific overlapped with fishing vessels more than any other region (mean monthly overlap 49.3%, n = 89) which aligns with expectation given that fishing activity was widespread in this region (Fig. 2*B*). The Inter-American Tropical Tuna Commission (IATTC) bans the setting of purse seines around whale sharks in the east Pacific (143), however fishing related conflict is not uncommon in the area. There was no published scarring information available from any aggregation site in the east Pacific, so no comparison with local CRI could be made in the present study, however four reported fatal collisions are known for the region (Table S8). We suggest that monitoring projects should aim to gather data on fatal collisions and on preliminary scarring assessments, if possible, based on standardised terminology (103).

The Galapagos has been highlighted as an important area for mature female whale sharks (29). The IMO granted PSSA status to the Galapagos in 2004 and this status helps protect the islands and surrounding waters from traditional freedom of passage of international marine traffic. The designation boundary is apparent on vessel density maps (Fig. 2*B*) and reduces susceptibility to collision around the islands (particularly on the northern side) where CRI was low. TSS have also been implemented by the IMO within the Panama Canal. These designations limit speed and dictate the route of passing vessels and have reduced the risk of collisions with whales in the area (141).

4.6.8 Sex and size

Across sex and size classes, average monthly spatial overlap varied from 91.2% for males to 95.0% for females (91.6% for unknown sex, Fig. S12, Table S6*B*), and from 87.6% for individuals with a total length >12 m to 96.4% for individuals with a total length of 3 m (Fig. S12, Table S6*C*). Differences in the overlap patterns between space use and vessel traffic among ocean regions, sex and size class were not driven by the number of tags that were deployed in each group (ocean region, Pearson's r = -0.32, n = 7, $p = 0.45$; sex, Pearson's r = -0.12, n = 3, $p = 0.88$; size class, Pearson's r = -0.35, n = 6, $p = 0.94$). Smaller individuals (3 m) had a significantly greater mean monthly CRI than larger individuals (9-12 m) (Fig. S12, Table S6*C*; K.W Test, Table S10*B*). This may be driven by smaller whale sharks occupying enclosed coastal areas, which may also be foraging grounds for late-stage juveniles and sub-adults (e.g. Red Sea (63)) where vessel activity was high (Fig. 2*B*). Larger individuals tended to occupy more open ocean regions where vessel density was more dispersed and concentrated along discrete traffic highways between which there were relatively lower densities of AIS-tracked vessels (Fig. 2*B*). No significant trend was observed when comparing the mean monthly CRI of male sharks (n = 165 tracks) to females (n = 106 tracks) (Fig. S12, Table S10*C*), although CRI was generally higher in males which may be explained by their use of preferred coastal regions where nearby ports lead to convergence in traffic.

4.7 Collision risk index and scar frequency analysis

Several regions with a high reported frequency of individuals with vessel-related injuries were associated with low values of estimated potential collision risk (e.g. west Pacific) (Table S9). The majority of vessel-related injuries observed on whale sharks in previous studies appear to be inflicted by smaller vessels (46), which indicates that whale sharks are vulnerable to collisions with smaller vessels that are not fitted with AIS receivers and so were not included in the vessel dataset we used. We found several coastal study sites where high estimated CRI corresponded with a relatively low

frequency of individuals with vessel related injuries (e.g. two sites in the northwest Indian Ocean) (Table S9). This suggests that evidence for injuries on surviving sharks inflicted by large vessels equipped with AIS receivers may not be evident in regional monitoring studies and are therefore likely to be missing from regional risk quantification estimations. Given that we found an increase of reported fatal collisions with higher CRI estimates on a regional basis, this indicates larger vessels are more likely to be the cause of direct mortality than smaller vessels, which in turn likely inflict most of the injuries comprising the scarring frequency data. Further, whale sharks with injuries remain within localised areas (101), which could explain the lack of correlation of vessel-related injuries and CRI, since CRI is relevant only to large AIS-tracked vessel movements. The near absence of injuries to whale sharks that are estimated to have been inflicted by large AIS-tracked vessels (50) (Table S9) implies that when there are collisions with large vessels they are likely to lead to mortality, as reported in early anecdotes and published records (Table S8) (94) and supported by our results. Mortality inflicted by large vessels will lead to subsequent sinking of the individual sharks, and will therefore go unreported in population assessments.

4.8 Collision risk index sensitivity analyses

Although the grid cell size selected for spatial analyses can potentially alter overlap values (3, 7), analysis of grid cell size here showed that spatial patterns of whale shark occurrence with higher or lower CRI remained consistent, as did the patterns of mean overall risk values on a monthly basis, irrespective of the spatial scale used (Table S11). This was evident for both ARGOS (n = 256) and PSAT (n = 92) tags (Table S11), so varying spatial accuracy of different tag types had no impact on the CRI results. Similarly, these patterns remained the same irrespective of the subset of years of vessel AIS positions that were analysed (Table S12). We used sensitivity analyses to determine effects of variations in surface depth use on risk estimates. At finer scales, changes in risk were spatially apparent when sharks were moving throughout coastal or oceanic waters, however regional patterns of risk remained constant as did temporal fluctuations (Table S13, Fig. S11). This confirms that had we chosen

a shallower collision zone value (i.e. ≤10 m), relative patterns of risk would reflect those reported here and that time at depth is an important consideration locally but less so when comparing regions on global scales. Applying different depth-use values derived from sex and monthly differences did not alter CRI patterns on broad spatial or temporal scales (Fig. S11). Analysis of whale sharks in the western Pacific (where we had a large sample size of sharks with both horizontal and vertical data available, n = 46), revealed that collision zone use (proportion of time spent ≤20 m) within the highest collision risk hotspots (defined here as ≥90th percentile of relative CRI) differed to outside hotspots by no more than 2% (median inside 90th percentile 41.15%, 43.12 mean ± s.d. 23.28; median outside 43.1%, 48.67 mean ± s.d. 28.13), and that there was no difference in collision zone use when whale sharks were occupying the busiest vessel areas (characterised as 31 vessels for 2011-2014 annual mean) compared to others (K.S. test = 0.121, p = 0.104). This suggests that, on the scale of the present analysis (0.25 × 0.25°), the time spent in surface waters where whale sharks are susceptible to collision remains consistent irrespective of the number of vessels and associated risk, which corroborates observations of their limited avoidance (Table S5). However, at finer resolutions, we acknowledge that there is potential for whale sharks to respond to vessels under certain (as yet unstudied) scenarios, and future studies should attempt to address this area of research through use of more detailed simultaneous shark and vessel tracking (12).

When we compared the datasets used in the main analysis (2011-2014) with more recent (2017-2019) AIS shipping data for cargo vessels (Fig. S17), the global overlap values were within 2% of one another (mean monthly overlap 2011-2014, 82.3%, 2017-2019, 83.7%) (Table S14). Although global CRI was considerably higher in the more recent years, the broad spatial distribution of risk remained similar, as did and regional patterns of risk compared to the main analysis (2011-2014). The primary differences were that mean monthly overlap in the west Pacific region increased to above that of the east Pacific and northwest Indian Ocean, and that mean monthly CRI in the east Indian Ocean became marginally higher than the southwest Indian Ocean in later years. Overall, these outcomes suggest that here we provide a more conservative estimate of risk given that overall risk was higher in the later years.

Furthermore, our results represent a conservative estimate of risk as we did not analyse small vessel movements, given that they do not use AIS and no other global data of movements or routes used by small vessels are available. A lack of data on the global distribution patterns of small vessels prohibits the identification of collision risk estimates likely to result in injuries but not necessarily direct mortality, which was the focus of our study, particularly in coastal areas where whale sharks use aggregation sites (37, 46, 50). Small vessel collisions can lead to injuries and compromise individual fitness, reduce movements or affect behaviours (101, 103), which may exacerbate vessel threat in regional populations where there is also risk of collision with large vessels. CRI hotspot areas may also be subject to high levels of small vessel use that further increases risk to this species.

4.9 Identifying whale shark hotspots

In this study we used global-scale data on the dynamic spatial patterns of both whale sharks and marine traffic from satellite tracking and AIS vessel monitoring. This approach has the advantage of describing the actual locations occupied by sharks and vessels for estimating overlap and collision risk for individual whale sharks. The horizontal and vertical space use of whale sharks presented here (Fig. 1 *A* and *B*) reflects observations from other studies where this species has been shown to occupy surface waters for substantial portions of time (32, 41, 44, 96, 117, 144, 145), make long distance movements through coastal and oceanic waters (29-31, 59, 146) and aggregate in distinct coastal regions often on a seasonal basis (33, 37, 39, 51, 52, 54, 63, 67) (see references in Table S2*B* and Table S15) . The identified hotspots (Fig. S3*A*) and seasonal shifts in spatial density on local scales (Fig. S5) follow a similar trend to previous region-based whale shark distribution analyses (1, 72). Several global hotspots that have been identified previously for whale sharks, through use of species distribution modelling (1), were not apparent in the present study. This may be due to limitations of empirical track data (i.e. tracks representing only a portion of a whale shark's life and tagged individuals representing a fraction of an entire population (Table S16)), or equally to the limitations of models to describe accurately the locations of highly heterogenous distributions of sharks exemplified by seasonal

aggregations in localized areas. Other global hotspot areas (1) not identified here are experiencing unclear population declines and may also pose a collision risk to whale sharks (Table S16), but further research is needed to quantify risk across predicted distributions. Furthermore, ocean-basin scale movements that may not be picked up in tracking datasets are possible for whale sharks (72), and individuals will be susceptible to collision whilst moving across vessel routes that transect ocean basins (Fig. 2*A*).

4.10 Further research and mitigation

Research aimed at improving our understanding of the behavioural responses of whale sharks to vessels will greatly enhance future risk quantification studies. Although some baseline information related to how the species may respond to small vessels does exist (45, 48, 147), these assessments could be enhanced with an increased research focus on the impacts of large vessels. For example, behavioural assessments incorporating factors such as vessel detection and avoidance (12), responses to alerting stimuli (148-152), area specific responses (153), and activity specific responses (154, 155) can have very important outcomes in this field and assist in the determination of appropriate management (107). Further, small-scale local studies that consider the high-resolution temporal aspects of whale shark movement and vessel tracking (156) will allow for specific evidence-based mitigations to be developed, however these will not extend across an entire species distributional range where overlap with marine traffic occurs. Studies that take a global scale, species range approach coupled with high-location-accuracy animal tracking (e.g. using GPS tags) will be capable of extending the estimation of collision risk from 10s of metres to 1000s of kilometres.

On a global scale we were unable to incorporate small vessels into the risk calculations, as there are currently no large-scale datasets available that monitor smaller craft. Our CRI estimates, therefore, only highlight risk posed by large vessels and should be considered a conservative estimate when taking into account the total collision risk faced by this species within each of the high-risk areas identified. Collisions with small vessels, which can reach higher speeds than those of larger size, have been

highlighted as a key concern for whale sharks in many coastal areas where known aggregations occur seasonally (37, 46, 50, 51, 55) (Table S15). In fact, the discrepancy between small and large vessel datasets has been a primary hurdle in studies attempting to quantify collision risk for marine taxa (107, 157). Here, we explored the correlations between our reported CRI and reported direct mortality from ship strikes on a regional scale, and on a localised scale with published rates of vessel related scarring. It was evident from our results, as expected when using large vessel AIS-monitoring to derive CRI, that CRI more closely reflects direct mortality with large vessels than injuries (scarring) inflicted by smaller vessels. However, our analyses of CRI and direct mortality were based on relatively few reported records of fatal collisions of whale sharks with large vessels. In addition, the comparison of CRI with local scarring data was based on several assumptions. Firstly, while it is possible that recorded scars were inflicted within the defined local regions, it is also possible that this damage occurred in some other part of the whale sharks' range, given the long-distance movements of this species (Fig. 1*A*). Secondly, the data we used to represent regional scarring frequency came from a range of published sources, which were not standardised across monitoring sites (most notably in terms of injury classification and sample sizes). Collectively, our analyses relating CRI to mortality and scarring highlight that there is presently no system in place to reliably record the impact of large vessels on whale sharks and that further research into the generation of evidence of mortality related to vessel strikes is vital. A research approach that could be used to investigate the potential scale of the 'cryptic' mortality of whale sharks due to large vessel collisions suggested here could include fitting several vessels on busy shipping routes with surface infra-red detectors or forward-looking subsurface sonar to record frequencies of large marine animals passing ahead of the bow. Alternatively, a forensic approach could also be taken by swabbing the bows of large vessels in busy ports near whale shark aggregation sites for whale shark tissue for DNA analysis to quantify directly any collisions taking place.

Results showing the temporal patterns and spatial maps of estimated overlap and potential collision risk provide the basis for further research leading to conservation initiatives for this species in the light of predicted increases in marine traffic (100) and can be used to inform both regional and broad scale collision risk management. To protect whale sharks successfully from the threat of collision, a

combination of both locally focused conservation initiatives and international agreements would be required to minimise collision risk and protect animals during movements through coastal waters within national jurisdictions as well as in the international high seas, which were both highlighted as key movement areas where risk hotspots can occur. The high-risk areas identified in our study may be well suited to developing mitigations and as sites for further study incorporating finer-scale, dynamic assessments of risk (156). IMO designations (e.g. PSSAs, TSSs, ATBAs) (107, 110, 121, 158, 159) aimed at managing international traffic may be suitable mitigation options for this species and our results identify potential conservation targets that could be area-focused on collective whale shark transit routes in high CRI areas. For example, TSSs (i.e. shipping lanes) can reduce the risk of lethal encounters between vessels and whales when compliance with a routing measure is high (141, 159, 160). However, in the case of the high potential risk areas identified in this study for whale sharks, re-routing may not always be feasible. We identified the Strait of Hormuz as a collision risk hotspot but, given the narrow entrance to the Arabian Gulf (124), there are limited options for re-routing vessels whilst ensuring safe transits. Further, re-routing shipping lanes may not be possible in coastal regions where whale shark-vessel overlap occurred around port entrances, such as in the Panama Basin at the entrance to the Panama Canal. Vessel traffic exclusion zones, which aim to reduce the number of vessels in an area, may provide a suitable alternative for whale sharks, especially in areas where individuals aggregate in large numbers, along collective movement routes (Fig. S7) or in space use hotspots (Fig. S3*A*). Exclusion zones can operate as permanent voluntary ATBAs (161) or DMAs (107) and have been used to protect whale species (107, 159-161). PSSAs, which are areas that are recognised as being in need of special protection through action by the IMO, may also be suitable in regions where whale sharks are highlighted as vulnerable to damage by vessels (Fig. 4*A*, Fig. S7). Alternatively, speed restrictions, which can be implemented within IMO designated areas or independently, have been suggested as a way of providing animals and vessel operators with prolonged potential detection periods, offering a greater chance of whale sharks and vessels avoiding a collision event (116, 162-164). Collisions with vessels travelling at high speeds may result in a greater impact and increase the risk of mortality or serious injury (165). When the relationship between vessel speed and probability of lethal collision was modelled in large whale populations, the probability of lethal injury decreased to

<50% when vessels travelled at speeds ≤10 knots (~5 m s^{-1}) (115). Here, vessel speeds at the closest point of approach often exceeded this threshold (Table S4*B*). Although this approach may be effective for protecting whales, the relationship between actual collision risk and vessel speed remains unknown for whale sharks and requires further research.

In dense whale shark hotspots, large vessels have a higher chance of causing damage due to greater likelihood of encountering individuals. Similarly, in areas with high levels of both large vessel collision risk and small vessel traffic the likelihood of shark-vessel interactions will be greater. We suggest these areas to be the focus of management efforts, which will require clear relay and communication of important whale shark areas to decision makers. This approach has been shown to be successful in other impacted groups (107) where imposing local regulations such as speed limits (116, 162) are the preferred measure when vessels cannot be safely re-routed (163, 164, 166). Although management approaches may be effective with protecting other species (107), the relationship between collision risk and mitigating factors remain unknown for whale sharks and further research needs to better understand the potential implications of management efforts on both local and international scales.

5. Supplementary References

1. A. M. M. Sequeira, C. Mellin, D. A. Fordham, M. G. Meekan, C. J. Bradshaw, Predicting current and future global distributions of whale sharks. *Glob. Chang. Biol.* **20**, 778-789 (2014).

2. R. L. Delong, B. S. Stewart, R. D. Hill, Documenting migrations of northern elephant seals using day length. *Mar. Mamm. Sci.* **8**, 155-159 (1992).

3. N. Queiroz *et al.*, Global spatial risk assessment of sharks under the footprint of fisheries. *Nature* **572**, 461-466 (2019).

4. C. H. Lam, A. Nielsen, J. R. Sibert, Improving light and temperature based geolocation by unscented Kalman filtering. *Fish. Res.* **91**, 15-25 (2008).

5. T. Sippel, J. Holdsworth, T. Dennis, J. Montgomery, investigating behaviour and population dynamics of striped marlin (*Kajikia audax*) from the southwest pacific ocean with satellite tags. *PLOS ONE* **6**, e21087 (2011).

6. D. S. Johnson, J. M. London, M.-A. Lea, J. W. Durban, Continuous-time correlated random walk model for animal telemetry data. *Ecology* **89**, 1208-1215 (2008).

7. D. A. Kroodsma *et al.*, Tracking the global footprint of fisheries. *Science* **359**, 904-908 (2018).

8. V. M. Eguíluz, J. Fernández-Gracia, X. Irigoien, C. M. Duarte, A quantitative assessment of Arctic shipping in 2010–2014. *Sci. Rep.* **6**, 1-6 (2016).

9. A. M. Dujon, R. T. Lindstrom, G. C. Hays, The accuracy of Fastloc-GPS locations and implications for animal tracking. *Methods Ecol. Evol.* **5**, 1162-1169 (2014).

10. A. D. Lowther, C. Lydersen, M. A. Fedak, P. Lovell, K. M. Kovacs, The Argos-CLS Kalman Filter: Error structures and state-space modelling relative to FastLoc GPS data. *PLOS ONE* **10**, e0124754 (2015).

11. E. Bryant, 2D location accuracy statistics for FastLoc® cores running firmware versions 2.2 & 2.3. *Wildtrack Telemetry Systems Ltd* **6**, (2007).

12. M. F. McKenna, J. Calambokidis, E. M. Oleson, D. W. Laist, J. A. Goldbogen, Simultaneous tracking of blue whales and large ships demonstrates limited behavioral responses for avoiding collision. *Endanger. Species Res.* **27**, 219-232 (2015).

13. E. M. Keen *et al.*, Night and Day: diel differences in ship strike risk for fin whales (*Balaenoptera physalus*) in the california current system. *Front. Mar. Sci.* **6**, 730 (2019).

14. G. K. Silber, J. Slutsky, S. Bettridge, Hydrodynamics of a ship/whale collision. *J. Exp. Mar. Biol. Ecol.* **391**, 10-19 (2010).

15. A. Nielsen, K. A. Bigelow, M. K. Musyl, J. R. Sibert, Improving light-based geolocation by including sea surface temperature. *Fish. Oceanogr.* **15**, 314-325 (2006).

16. S. L. Teo *et al.*, Validation of geolocation estimates based on light level and sea surface temperature from electronic tags. *Mar. Eco. Prog. Ser.* **283**, 81-98 (2004).

17. R. Core Team. (R Foundation for Statistical Computing, Vienna, Austria., 2019).

18. N. Barve *et al.*, The crucial role of the accessible area in ecological niche modeling and species distribution modeling. *Ecol. Modell.* **222**, 1810-1819 (2011).

19. B. A. Block *et al.*, Tracking apex marine predator movements in a dynamic ocean. *Nature* **475**, 86-90 (2011).

20. QGIS Development Team. (Open Source Geospatial Foundation Project, 2020).

21. G. C. Hays, Tracking animals to their death. *J. Anim. Ecol.* **83**, 5-6 (2014).

22. G. C. Hays, J. O. Laloë, A. Rattray, N. Esteban, Why do Argos satellite tags stop relaying data? *Ecol. Evol.* **11**, 7093-7101 (2021).

23. G. C. Hays, C. J. A. Bradshaw, M. C. James, P. Lovell, D. W. Sims, Why do Argos satellite tags deployed on marine animals stop transmitting? *J. Exp. Mar. Biol. Ecol.* **349**, 52-60 (2007).

24. H. S. Horn, Measurement of "overlap" in comparative ecological studies. *Am. Nat.* **100**, 419-424 (1966).

25. A. D. Rijnsdorp, A. M. Buys, F. Storbeck, E. G. Visser, Micro-scale distribution of beam trawl effort in the southern North Sea between 1993 and 1996 in relation to the trawling frequency of the sea bed and the impact on benthic organisms. *ICES J. Mar. Sci.* **55**, 403-419 (1998).

26. B. M. Norman, S. Reynolds, D. L. Morgan, Does the whale shark aggregate along the Western Australian coastline beyond Ningaloo Reef? *Pac. Conserv. Biol.* **22**, 72-80 (2016).

27. J. C. Sleeman *et al.*, To go or not to go with the flow: Environmental influences on whale shark movement patterns. *J. Exp. Mar. Biol. Ecol.* **390**, 84-98 (2010).

28. S. D. Reynolds, B. M. Norman, M. Beger, C. E. Franklin, R. G. Dwyer, Movement, distribution and marine reserve use by an endangered migratory giant. *Divers. Distrib.* **23**, 1268-1279 (2017).

29. A. R. Hearn *et al.*, Adult female whale sharks make long-distance movements past Darwin Island (Galapagos, Ecuador) in the Eastern Tropical Pacific. *Mar. Biol.* **163**, (2016).

30. H. M. Guzman, C. G. Gomez, A. Hearn, S. A. Eckert, Longest recorded trans-Pacific migration of a whale shark (*Rhincodon typus*). *Mar. Biodivers. Rec.* **11**, 8 (2018).

31. R. E. Hueter, J. P. Tyminski, R. de la Parra, Horizontal movements, migration patterns, and population structure of whale sharks in the Gulf of Mexico and northwestern Caribbean sea. *PLOS ONE* **8**, e71883 (2013).

32. J. P. Tyminski, R. De La Parra-Venegas, J. González Cano, R. E. Hueter, Vertical movements and patterns in diving behavior of whale sharks as revealed by pop-up satellite tags in the eastern Gulf of Mexico. *PLOS ONE* **10**, e0142156 (2015).

33. R. de la Parra Venegas *et al.*, An unprecedented aggregation of whale sharks, *Rhincodon typus*, in Mexican coastal waters of the Caribbean Sea. *PLOS ONE* **6**, e18994 (2011).

34. F. Hazin, T. Vaske Júnior, P. Oliveira, B. Macena, F. Carvalho, Occurrences of whale shark (*Rhincodon typus* Smith, 1828) in the Saint Peter and Saint Paul archipelago, Brazil. *Braz. J. Biol.* **68**, 385-389 (2008).

35. D. P. Robinson *et al.*, Some like it hot: Repeat migration and residency of whale sharks within an extreme natural environment. *PLOS ONE* **12**, e0185360 (2017).

36. M. L. Berumen, C. D. Braun, J. E. M. Cochran, G. B. Skomal, S. R. Thorrold, Movement patterns of juvenile whale sharks tagged at an aggregation site in the Red Sea. *PLOS ONE* **9**, e103536 (2014).

37. D. Rowat, M. G. Meekan, U. Engelhardt, B. Pardigon, M. Vely, Aggregations of juvenile whale sharks (*Rhincodon typus*) in the Gulf of Tadjoura, Djibouti. *Environ. Biol. Fishes* **80**, 465-472 (2007).

38. C. T. Perry *et al.*, St. Helena: An important reproductive habitat for whale sharks (*Rhincodon typus*) in the central south Atlantic. *Front. Mar. Sci.* **7**, 576343 (2020).

39. S. Diamant *et al.*, Movements and habitat use of satellite-tagged whale sharks off western Madagascar. *Endanger. Species Res.* **36**, 49-58 (2018).

40. C. A. Rohner *et al.*, Satellite tagging highlights the importance of productive Mozambican coastal waters to the ecology and conservation of whale sharks. *PeerJ* **6**, e4161 (2018).

41. D. Rowat, M. Gore, Regional scale horizontal and local scale vertical movements of whale sharks in the Indian Ocean off Seychelles. *Fish. Res.* **84**, 32-40 (2007).

42. G. Araujo *et al.*, Satellite tracking of juvenile whale sharks in the Sulu and Bohol Seas, Philippines. *PeerJ* **6**, e5231 (2018).

43. M. M. Meyers, M. P. Francis, M. Erdmann, R. Constantine, A. Sianipar, Movement patterns of whale sharks in Cenderawasih Bay, Indonesia, revealed through long-term satellite tagging. *Pac. Conserv. Biol.* **26**, 353-364 (2020).

44. R. A. Martin, A review of behavioural ecology of whale sharks (*Rhincodon typus*). *Fisheries Research* **84**, 10-16 (2007).

45. S. J. Pierce, A. Méndez-Jiménez, K. Collins, M. Rosero-Caicedo, A. monadjem, Developing a Code of Conduct for whale shark interactions in Mozambique. *Aquat. Conserv.* **20**, 782-788 (2010).

46. G. Araujo *et al.*, Population structure and residency patterns of whale sharks, *Rhincodon typus*, at a provisioning site in Cebu, Philippines. *PeerJ* **2**, e543 (2014).

47. A. Schleimer *et al.*, Learning from a provisioning site: code of conduct compliance and behaviour of whale sharks in Oslob, Cebu, Philippines. *PeerJ* **3**, e1452 (2015).

48. H. Raudino *et al.*, Whale shark behavioural responses to tourism interactions in Ningaloo Marine Park and implications for future management. *Conservation Science W. Aust.* **10**, 2 (2016).

49. C. Legaspi *et al.*, In-water observations highlight the effects of provisioning on whale shark behaviour at the world's largest whale shark tourism destination. *R. Soc. Open Sci.* **7**, 200392 (2020).

50. C. W. Speed *et al.*, Scarring patterns and relative mortality rates of Indian Ocean whale sharks. *J. Fish. Biol.* **72**, 1488-1503 (2008).

51. D. Ramírez-Macías *et al.*, Patterns in composition, abundance and scarring of whale sharks *Rhincodon typus* near Holbox Island, Mexico. *J. Fish. Biol.* **80**, 1401-1416 (2012).

52. S. Fox *et al.*, Population structure and residency of whale sharks *Rhincodon typus* at Utila, Bay Islands, Honduras. *J. Fish. Biol.* **83**, 574-587 (2013).

53. J. E. M. Cochran *et al.*, Population structure of a whale shark *Rhincodon typus* aggregation in the Red Sea. *J. Fish. Biol.* **89**, 1570-1582 (2016).

54. D. P. Robinson *et al.*, Whale sharks, *Rhincodon typus*, aggregate around offshore platforms in Qatari waters of the Arabian Gulf to feed on fish spawn. *PLOS ONE* **8**, e58255 (2013).

55. E. Lester *et al.*, Multi-year patterns in scarring, survival and residency of whale sharks in Ningaloo Marine Park, Western Australia. *Mar. Ecol. Prog. Ser.* **634**, 115-125 (2020).

56. G. Araujo *et al.*, Population structure, residency patterns and movements of whale sharks in Southern Leyte, Philippines: results from dedicated photo-ID and citizen science. *Aquat. Conserv.* **27**, 237-252 (2017).

57. D. Ramírez-Macías, A. Vázquez-Haikin, R. Vázquez-Juárez, Whale shark *Rhincodon typus* populations along the west coast of the Gulf of California and implications for management. *Endanger. Species Res.* **18**, 115-128 (2012).

58. D. Acuña-Marrero *et al.*, Whale shark (*Rhincodon typus*) seasonal presence, residence time and habitat use at Darwin Island, Galapagos Marine Reserve. *PLOS ONE* **9**, e115946 (2014).

59. P. Afonso, N. McGinty, M. Machete, Dynamics of whale shark occurrence at their fringe oceanic habitat. *PLOS ONE* **9**, e102060 (2014).

60. R. T. Graham, C. M. Roberts, Assessing the size, growth rate and structure of a seasonal population of whale sharks (*Rhincodon typus* Smith 1828) using conventional tagging and photo identification. *Fish. Res.* **84**, 71-80 (2007).

61. A. P. M. Di Beneditto, S. C. Moreira, S. Siciliano, Endangered whale sharks in southeastern Brazil: Records and management issues. *Ocean Coast. Manag.* **201**, 105491 (2021).

62. B. C. L. Macena, F. H. V. Hazin, Whale shark (*Rhincodon typus*) seasonal occurrence, abundance and demographic structure in the mid-equatorial Atlantic Ocean. *PLOS ONE* **11**, e0164440 (2016).

63. J. E. M. Cochran *et al.*, Multi-method assessment of whale shark (*Rhincodon typus*) residency, distribution, and dispersal behavior at an aggregation site in the Red Sea. *PLOS ONE* **14**, e0222285 (2019).

64. P. Pravin, Whale shark in the Indian coast – Need for conservation. *Curr. Sci.* **79**, 310-315 (2000).

65. M. J. Riley, M. S. Hale, A. Harman, R. G. Rees, Analysis of whale shark *Rhincodon typus* aggregations near South Ari Atoll, Maldives Archipelago. *Aquat. Biol.* **8**, 145-150 (2010).

66. C. A. Rohner *et al.*, Whale sharks target dense prey patches of sergestid shrimp off Tanzania. *J. Plankton Res.* **37**, 352-362 (2015).

67. M. G. Meekan *et al.*, Population size and structure of whale sharks *Rhincodon typus* at Ningaloo Reef, Western Australia. *Mar. Ecol. Prog. Ser.* **319**, 275-285 (2006).

68. E. McCoy *et al.*, Long-term photo-identification reveals the population dynamics and strong site fidelity of adult whale sharks to the coastal waters of Donsol, Philippines. *Front. Mar. Sci.* **5**, 271 (2018).

69. G. Araujo *et al.*, Photo-ID and telemetry highlight a global whale shark hotspot in Palawan, Philippines. *Sci. Rep.* **9**, 17209 (2019).

70. A. Sianipar, M. V. Erdmann, A. Hassan, I. Alaydrus, A tale of three bays: comparison of movement patterns of three whale shark populations in eastern Indonesia in *5th International Whale Shark Conference*. (Ningaloo, Australia, 2019).

71. B. M. Norman *et al.*, Undersea Constellations: The global biology of an endangered marine megavertebrate further informed through citizen science. *BioScience* **67**, 1029-1043 (2017).

72. A. M. M. Sequeira, C. Mellin, M. G. Meekan, D. W. Sims, C. J. Bradshaw, Inferred global connectivity of whale shark Rhincodon typus populations. *J. Fish. Biol.* **82**, 367-389 (2013).

73. J. A. McKinney *et al.*, Long-term assessment of whale shark population demography and connectivity using photo-identification in the Western Atlantic Ocean. *PLOS ONE* **12**, e0180495 (2017).

74. G. Boldrocchi, M. Omar, A. Azzola, R. Bettinetti, The ecology of the whale shark in Djibouti. *Aquat. Ecol.* **54**, 535-551 (2020).

75. D. P. Robinson *et al.*, Population structure, abundance and movement of whale sharks in the Arabian Gulf and the Gulf of Oman. *PLOS ONE* **11**, e0158593 (2016).

76. R. C. Anderson, H. Ahmed, The shark fisheries of the Maldives. FAO, Rome, and Ministry of Fisheries, Male, Maldives. (1993).

77. T. K. Davies, G. Stevens, M. G. Meekan, J. Struve, J. M. Rowcliffe, Can citizen science monitor whale-shark aggregations? Investigating bias in mark–recapture modelling using identification photographs sourced from the public. *Wildl. Res.* **39**, 696-704 (2012).

78. K. Brooks, D. R. L. Rowat, S. J. Pierce, D. Jouannet, M. Vély, Seeing Spots: Photo-identification as a regional tool for whale shark identification. *West. Indian Ocean J. Mar. Sci.* **9**, 185-194 (2010).

79. C. Rohner *et al.*, Trends in sightings and environmental influences on a coastal aggregation of manta rays and whale sharks. *Mar. Ecol. Prog. Ser.* **482**, 153-168 (2013).

80. S. Diamant *et al.*, Population structure, residency, and abundance of whale sharks in the coastal waters off Nosy Be, north-western Madagascar. *Aquat. Conserv.* **31**, 3492-3506 (2021).

81. A. M. M. Sequeira, C. Mellin, S. Delean, M. G. Meekan, C. J. A. Bradshaw, Spatial and temporal predictions of inter-decadal trends in Indian Ocean whale sharks. *Mar. Ecol. Prog. Ser.* **478**, 185-195 (2013).

82. T. M. Vignaud *et al.*, Genetic structure of populations of whale sharks among ocean basins and evidence for their historic rise and recent decline. *Mol. Ecol.* **23**, 2590-2601 (2014).

83. C. Bradshaw, B. Fitzpatrick, C. C. Steinberg, B. Brook, M. Meekan, Decline in whale shark size and abundance at Ningaloo Reef over the past decade: The world's largest fish is getting smaller. *Biol. Conserv.* **141**, 1894-1905 (2008).

84. J. Holmberg, B. Norman, Z. Arzoumanian, Estimating population size, structure, and residency time for whale sharks *Rhincodon typus* through collaborative photo-identification. *Endanger. Species Res.* **7**, 39-53 (2009).

85. P. Dearden, Detecting a decline in whale shark *Rhincodon typus* sightings in the Andaman Sea, Thailand, using ecotourist operator-collected data. *Oryx* **40**, 337-342 (2006).

86. M. Alava, E.R.Z. Dolumbaló, A.A. Yaptinchay, R.B. Trono, Fishery and trade of whale sharks and manta rays in the Bohol Sea, Philippines. pp. 132-148. *In: S.L. Fowler, T.M. Reed & F.A. Dipper (eds), Elasmobranch Biodiversity, Conservation and Management. Proceedings of the International Seminar and Workshop, Sabah, Malaysia, July 1997.* (2002).

87. V. Y. Chen, M. J. Phipps, T. E. Asia, David, L. P. Foundation, Management and Trade of Whale Sharks in Taiwan. Traffic East Asia-Taipei (2002).

88. H.-H. Hsu, S. Joung, K.-M. Liu, Fisheries, management and conservation of the whale shark *Rhincodon typus* in Taiwan. *J. Fish. Biol.* **80**, 1595-1607 (2012).

89. S. Suruan, B. Pranata, C. Tania, M. Kamal, Photo ID-based assessment of the whale shark (*Rhincodon typus*) population in Kwatisore, Wondama Bay, West Papua, Indonesia in *4th International Whale Shark Conference*. (Doha, Qatar, 2016).

90. W. Li, Y. Wang, B. Norman, A preliminary survey of whale shark *Rhincodon typus* catch and trade in China: an emerging crisis. *J. Fish. Biol.* **80**, 1608-1618 (2012).

91. S. Harley, P. Williams, J. Rice, Spatial and temporal distribution of whale sharks in the western and central Pacific Ocean based on observer data and other data sources. *Western and Central Pacific Fisheries Commission, Pohnpei.* (2013).

92. E. W. Gudger, The whale shark in the Caribbean Sea and the Gulf of Mexico. *Sci. Mon.* **48**, 261-264 (1939).

93. E. W. Gudger, The whale shark unafraid the greatest of the sharks, *Rhincodon typus*, fears not shark, man nor ship. *Am. Nat.***75**, 550-568 (1941).

94. E. W. Gudger, Whale sharks rammed by ocean vessels: how these sluggish leviathans aid in their own destruction. *New England Naturalist* **7**, 1–10. (1940).

95. E. W. Gudger, Four whale sharks rammed by steamers in the Red Sea region. *Copeia* **1938**, 170-173 (1938).

96. S. Wilson, J. Polovina, B. Stewart, M. Meekan, Movements of whale sharks (*Rhincodon typus*) tagged at Ningaloo Reef, Western Australia. *Mar. Biol.* **148**, 1157-1166 (2006).

97. Namrouqa, H, 'Aqaba whale shark 'died after getting stuck in vessel engine'' in *The Jordan Times* (2017) https://www.jordantimes.com/news/local/aqaba-whale-shark-died-after-getting-stuck-vessel-engine Accessed 25 January 2022.

98. P. Hoy, 'Aparece tiburón ballena durante el atraque de un buque en Puerto Progreso [Whale shark appears during the docking of a ship in Puerto Progreso]' in *Progreso Hoy* (2019) https://progresohoy.com/noticias/aparece-tiburon-ballena-durante-el-atraque-de-un-buque-en-puerto-progreso-10114053/ Accessed 25 January 2022.

99. K. McMurray, 'A sad day for whale sharks' in *Tracking Sharks* (2016) https://www.trackingsharks.com/sad-day-whale-sharks/ Accessed 25 January 2022.

100. United Nations Conference on Trade and Development (UNCTAD). *Review of Maritime Transport 2019* (2019) https://unctad.org/system/files/official-document/rmt2019_en.pdf Accessed 25 January 2022.

101. J. Harvey-Carroll *et al.*, The impact of injury on apparent survival of whale sharks (*Rhincodon typus*) in South Ari Atoll Marine Protected Area, Maldives. *Sci. Rep.* **11**, 937-937 (2021).

102. F. McGregor, A. J. Richardson, A. J. Armstrong, A. O. Armstrong, C. L. Dudgeon, Rapid wound healing in a reef manta ray masks the extent of vessel strike. *PLOS ONE* **14**, e0225681 (2019).

103. F. Womersley, J. Hancock, C. T. Perry, D. Rowat, Wound-healing capabilities of whale sharks (*Rhincodon typus*) and implications for conservation management. *Conserv. Physiol.* **9**, (2021).

104. D. W. Laist, A. R. Knowlton, J. G. Mead, A. S. Collet, M. Podesta, Collisions between ships and whales. *Mar. Mamm. Sci.* **17**, 35-75 (2001).

105. A. S. Jensen, G. K. Silber, J. Calambokidis, Large whale ship strike database. *US Department of Commerce. National Oceanic and Atmospheric Administration*. Technical Memorandum NMFS-OPR (2003).

106. D. Rowat, K. Brooks, A review of the biology, fisheries and conservation of the whale shark *Rhincodon typus*. *J. Fish Biol.* **80**, 1019-1056 (2012).

107. R. P. Schoeman, C. Patterson-Abrolat, S. Plön, A global review of vessel collisions with marine animals. *Front. Mar. Sci.* **7**, 292 (2020).

108. C. J. Fonnesbeck, L. P. Garrison, L. I. Ward-Geiger, R. D. Baumstark, Bayesian hierarchichal model for evaluating the risk of vessel strikes on North Atlantic right whales in the SE United States. *Endanger. Species Res.* **6**, 87-94 (2008).

109. R. Williams, P. rsquoHara, Modelling ship strike risk to fin, humpback and killer whales in British Columbia, Canada. *J.Cetacean Res. Manag.* **11**, 1-8 (2010).

110. J. Redfern *et al.*, Assessing the risk of ships striking large whales in marine spatial planning. *Conserv. Biol.* **27**, 292-302 (2013).

111. L. M. Nichol, B. M. Wright, P. O. Hara, J. K. Ford, Risk of lethal vessel strikes to humpback and fin whales off the west coast of Vancouver Island, Canada. *Endanger. Species Res.* **32**, 373-390 (2017).

112. R. C. Rockwood, J. Calambokidis, J. Jahncke, High mortality of blue, humpback and fin whales from modeling of vessel collisions on the U.S. West Coast suggests population impacts and insufficient protection. *PLOS ONE* **12**, e0183052 (2017).

113. H. L. Kite-Powell, A. Knowlton, M. Brown, Modeling the effect of vessel speed on right whale ship strike risk. *Project report for NOAA/NMFS Project NA04NMF47202394*, (2007).

114. R. C. Rockwood, J. Calambokidis, J. Jahncke, High mortality of blue, humpback and fin whales from modeling of vessel collisions on the US West Coast suggests population impacts and insufficient protection. *PLOS ONE* **12**, e0183052 (2017).

115. A. S. Vanderlaan, C. T. Taggart, Vessel collisions with whales: the probability of lethal injury based on vessel speed. *Mar. Mamm. Sci.* **23**, 144-156 (2007).

116. P. B. Conn, G. K. Silber, Vessel speed restrictions reduce risk of collision-related mortality for North Atlantic right whales. *Ecosphere* **4**, 1-16 (2013).

117. J. M. Brunnschweiler, D. W. Sims, Diel oscillations in whale shark vertical movements associated with meso-and bathypelagic diving *in American Fisheries Society Symposium*. 76, 1- 14 (2011)

118. R. T. Graham *et al.*, Satellite tracking of manta rays highlights challenges to their conservation. *PLOS ONE* **7**, e36834 (2012).

119. R. A. Valverde, K. R. Holzwart, 'Sea turtles of the Gulf of Mexico' in *Habitats and Biota of the Gulf of Mexico: Before the Deepwater Horizon Oil Spill: Volume 2: Fish Resources, Fisheries, Sea Turtles, Avian Resources, Marine Mammals, Diseases and Mortalities,* C. H. Ward, Eds. (Springer New York, New York, NY, 2017), pp. 1189-1351.

120. M. S. Soldevilla *et al.*, Spatial distribution and dive behavior of Gulf of Mexico Bryde's whales: potential risk of vessel strikes and fisheries interactions. *Endanger. Species Res.* **32**, 533-550 (2017).

121. J. V. Redfern *et al.*, Evaluating stakeholder-derived strategies to reduce the risk of ships striking whales. *Divers. Distrib.* **25**, 1575-1585 (2019).

122. A. Capietto *et al.*, Mortality of marine megafauna induced by fisheries: Insights from the whale shark, the world's largest fish. *Biol. Conserv.* **174**, 147-151 (2014).

123. K. Van Waerebeek *et al.*, The Bight of Benin, a North Atlantic breeding ground of a Southern Hemisphere humpback whale population, likely related to Gabon and Angola substocks. *International Whaling Commission, Scientific Committee Document SC/53/IA21, Cambridge, UK*, (2001).

124. A. H. Cordesman, *Iran, oil, and the Strait of Hormuz*. Center for Strategic and International Studies Washington (2007).

125. L. E. Beckley, G. Cliff, M. J. Smale, L. J. Compagno, Recent strandings and sightings of whale sharks in South Africa. *Environ. Biol. Fishes* **50**, 343-348 (1997).

126. P. B. Best, V. M. Peddemors, V. G. Cockcroft, N. Rice, Mortalities of right whales and related anthropogenic factors in South African waters, 1963-1998. *J. Cetacean Res. Manage.* 171-176 (2020).

127. P. A. Wickens, P. F. Sims, Trawling operations and South African (Cape) fur seals, *Arctocephalus pusillus pusillus*. *Mar. Fish. Rev.* **56**, 1-12 (1994).

128. C. A. Rohner *et al.*, No place like home? High residency and predictable seasonal movement of whale sharks off Tanzania. *Front. Mar. Sci.* **7**, 423 (2020).

129. L. Escalle *et al.*, Catch and bycatch captured by tropical tuna purse-seine fishery in whale and whale shark associated sets: comparison with free school and FAD sets. *Biodivers. Conserv.* **28**, 467-499 (2019).

130. L. Escalle *et al.*, Post-capture survival of whale sharks encircled in tuna purse-seine nets: tagging and safe release methods. *Aquat. Conserv.* **26**, 782-789 (2016).

131. T. Logan, L, Jose, 'WA coast caught in what's believed to be the most prolonged marine heatwave in a decade' in *ABC News*. (2021) https://www.abc.net.au/news/2021-02-20/what-is-causing-the-wa-marine-heatwave/13164454 Accessed 25 January 2022

132. B. Dugan, 'Whale shark sighting in Rockingham as swimmers treated to rare encounter' in *PerthNow*. (2021) https://www.perthnow.com.au/news/wildlife/whale-shark-sighting-in-rockingham-as-swimmers-treated-to-rare-encounter-ng-b881776008z Accessed 25 January 2022.

133. S. Rennie *et al.*, Physical properties and processes in the Perth Canyon, Western Australia: Links to water column production and seasonal pygmy blue whale abundance. *J. Mar. Syst.* **77**, 21-44 (2009).

134. M. C. Double *et al.*, Migratory movements of pygmy blue whales (*Balaenoptera musculus brevicauda*) between Australia and Indonesia as revealed by satellite telemetry. *PLOS ONE* **9**, e93578 (2014).

135. L. M. Möller *et al.*, Movements and behaviour of blue whales satellite tagged in an Australian upwelling system. *Sci. Rep.* **10**, 21165 (2020).

136. J. Catlin, R. Jones, Whale shark tourism at Ningaloo Marine Park: A longitudinal study of wildlife tourism. *Tour. Manag.* **31**, 386-394 (2010).

137. A. M. Foley *et al.*, Characterizing watercraft-related mortality of sea turtles in Florida. *J. Wildl. Manag.* **83**, 1057-1072 (2019).

138. R. Maitland, I. Lawler, J. Sheppard, Assessing the risk of boat strike on Dugongs *Dugong dugon* at Burrum Heads, Queensland, Australia. *Pac. Conserv. Biol.* **12**, 321-326 (2006).

139. M. Alava, E.R.Z. Dolumbaló, A.A. Yaptinchay, R.B. Trono, Fishery and trade of whale sharks and manta rays in the Bohol Sea, Philippines. pp. 132-148. *In: S.L. Fowler, T.M. Reed & F.A. Dipper (eds), Elasmobranch Biodiversity, Conservation and Management. Proceedings of the International Seminar and Workshop, Sabah, Malaysia, July 1997.* (2002).

140. L. Penketh *et al.*, Scarring patterns of whale sharks, *Rhincodon typus*, at a provisioning site in the Philippines. *Aquat. Conserv.* **31**, 99-111 (2020).

141. H. M. Guzman, C. G. Gomez, C. A. Guevara, L. Kleivane, Potential vessel collisions with Southern Hemisphere humpback whales wintering off Pacific Panama. *Mar. Mamm. Sci.* **29**, 629-642 (2013).

142. J. P. Ryan, J. R. Green, E. Espinoza, A. R. Hearn, Association of whale sharks (*Rhincodon typus*) with thermo-biological frontal systems of the eastern tropical Pacific. *PLOS ONE* **12**, e0182599 (2017).

143. The Inter-American Tropical Tuna Commission, 'The Inter-American Tropical Tuna Commission (IATTC) 94th meeting', *Resolution C-19-06* (Bilbao, Spain, 2019).

144. D. Rowat *et al.*, New records of neonatal and juvenile whale sharks (*Rhincodon typus*) from the Indian Ocean. *Environ. Biol. Fishes* **82**, 215-219 (2007).

145. J. S. Gunn, J. D. Stevens, T. L. O. Davis, B. M. Norman, Observations on the short-term movements and behaviour of whale sharks (*Rhincodon typus*) at Ningaloo Reef, Western Australia. *Mar. Biol.* **135**, 553-559 (1999).

146. A. M. M. Sequeira, C. Mellin, D. Rowat, M. G. Meekan, C. J. A. Bradshaw, Ocean-scale prediction of whale shark distribution. *Divers. Distrib.* **18**, 504-518 (2012).

147. A. L. Quiros, Tourist compliance to a Code of Conduct and the resulting effects on whale shark (*Rhincodon typus*) behavior in Donsol, Philippines. *Fish. Res.* **84**, 102-108 (2007).

148. D. P. Nowacek, M. P. Johnson, P. L. Tyack, North Atlantic right whales (*Eubalaena glacialis*) ignore ships but respond to alerting stimuli. *Proc. Royal Soc. B* **271**, 227-231 (2004).

149. L. Chapuis *et al.*, The effect of underwater sounds on shark behaviour. *Sci. Rep.* **9**, 6924 (2019).

150. J. A. A. Myrberg, S. J. Ha, S. Walewski, J. C. Banbury, Effectiveness of acoustic signals in attracting epipelagic sharks to an underwater sound source. *Bull. Mar. Sci.* **22**, 926-949 (1972).

151. J. T. Corwin, Functional anatomy of the auditory system in sharks and rays. *J. Exp. Zool.* **252**, 62-74 (1989).

152. A. A. Myrberg, 'The acoustical biology of elasmobranchs' in *The behavior and sensory biology of elasmobranch fishes: an anthology in memory of Donald Richard Nelson*. (Springer, 2001), pp. 31-46.

153. G. Araujo, J. Labaja, S. Snow, C. Huveneers, A. Ponzo, Changes in diving behaviour and habitat use of provisioned whale sharks: implications for management. *Sci. Rep.* **10**, 1-12 (2020).

154. P. J. Haskell *et al.*, Monitoring the effects of tourism on whale shark *Rhincodon typus* behaviour in Mozambique. *Oryx* **49**, 492-499 (2014).

155. R. Dukas, Behavioural and ecological consequences of limited attention. *Philos. Trans. R. Soc. Lond., B, Biol. Sci.* **357**, 1539-1547 (2002).

156. H. Blondin, B. Abrahms, L. B. Crowder, E. L. Hazen, Combining high temporal resolution whale distribution and vessel tracking data improves estimates of ship strike risk. *Biol. Conserv.* **250**, 108757 (2020).

157. T. Shimada, C. Limpus, R. Jones, M. Hamann, Aligning habitat use with management zoning to reduce vessel strike of sea turtles. *Ocean Coast. Manag.* **142**, 163-172 (2017).

158. A. Frantzis, R. Leaper, P. Alexiadou, A. Prospathopoulos, D. Lekkas, Shipping routes through core habitat of endangered sperm whales along the Hellenic Trench, Greece: Can we reduce collision risks? *PLOS ONE* **14**, e0212016 (2019).

159. A. S. Vanderlaan, C. T. Taggart, A. R. Serdynska, R. D. Kenney, M. W. Brown, Reducing the risk of lethal encounters: vessels and right whales in the Bay of Fundy and on the Scotian Shelf. *Endanger. Species Res.* **4**, 283-297 (2008).

160. A. S. Vanderlaan, C. T. Taggart, Efficacy of a voluntary area to be avoided to reduce risk of lethal vessel strikes to endangered whales. *Conserv. Biol.* **23**, 1467-1474 (2009).

161. International Maritime Organization, Routing measures other than traffic separation schemes. *REF T2-OSS/2.7, SN. a/Circ. 263*, (2007).

162. J. Hazel, I. R. Lawler, H. Marsh, S. Robson, Vessel speed increases collision risk for the green turtle *Chelonia mydas*. *Endanger. Species Res.* **3**, 105-113 (2007).

163. M. F. McKenna, S. L. Katz, C. Condit, S. Walbridge, Response of commercial ships to a voluntary speed reduction measure: are voluntary strategies adequate for mitigating ship-strike risk? *Coast. Manag.* **40**, 634-650 (2012).

164. J. Currie, S. Stack, G. Kaufman, Modelling whale-vessel encounters: the role of speed in mitigating collisions with humpback whales (*Megaptera novaeangliae*). *J. Cetac. Res. Manage* **17**, 57-64 (2017).

165. C. Wang, S. B. Lyons, J. Corbett, J. Firestone, J. J. Corbett, 'Using ship speed and mass to describe potntial collision severity with whales: An application of ship traffic, enerfy and environment model (STEEM) in *Compendium of Papers: Transportation Research Board 86th Annual Meeting*. (2007).

166. F. Ritter, N. A. de Soto, V. Martín, 'Towards Ship Strike Mitigation In The Canary Islands' (Report SC, 2019).

6. Supplementary Acknowledgements

Funding for data analysis was provided by the UK Natural Environment Research Council (NERC) through a University of Southampton INSPIRE DTP Studentship to **F.C.W.** Additional funding for data analysis was provided by NERC Discovery Science (NE/R00997/X/1) and the European Research Council (ERC-AdG-2019 883583 OCEAN DEOXYFISH) to **D.W.S.**, Fundação para a Ciência e a Tecnologia (FCT) under PTDC/BIA/28855/2017 and COMPETE POCI-01–0145-FEDER-028855, and MARINFO–NORTE-01–0145-FEDER-000031 (funded by Norte Portugal Regional Operational Program [NORTE2020] under the PORTUGAL 2020 Partnership Agreement, through the European Regional Development Fund–ERDF) to **N.Q.** FCT also supported **N.Q.** (CEECIND/02857/2018) and **M.V.** (PTDC/BIA-COM/28855/2017). **D.W.S.** was supported by a Marine Biological Association Senior Research Fellowship. This research is part of the Global Shark Movement Project (globalsharkmovement.org).

G.A. and **J.L.** thank Mrs Angelique Songco and the Park Rangers for their collaboration and support while in Tubbataha Reefs Natural Park, and the Local Government Units and local communities of Cagayancillo, Talisayan, Malimono, Pintuyan and San Ricardo.

A.B. thanks Great Barrier Reef Marathon Research Fund and Slattery Family Trust for funding and Daniel McCarthy for tagging the first whale shark.

S.B.-L. acknowledges the Natural National Parks of Colombia, Fondo Patrimonial Malpelo, Foundation Prince Alberto II of Monaco, Colombia Bio and Embarcaciones Asturias.

A.D.M.D. acknowledges the support of the Environment and Natural Resources Directorate of the St Helena Government and the staff of Georgia Aquarium in Atlanta.

M.V.E., A.B.S., A.H. and I.S. would like to thank the Indonesian Ministry of Environment and Forestry, the Ministry of Marine Affairs and Fisheries, the Cenderawasih Bay National Park Authority, and the people and governments of West Papua and Nusa Tenggara Barat provinces (especially those from Desa Labuhan Jambu and Desa Kwatisore) for sponsoring and supporting this work. We thank the following donors who financially supported our whale shark tagging: the Sunbridge Foundation, MAC3 Impact Philanthropies, the Wolcott Henry Foundation, the owners and guests of the MV True North, Asia Coating Enterprise, M.E. Mali, D. Roozen, A. and S. Wong, E. Tan, S. Argyropolous, and D. Arnall.

H.G. acknowledges field assistance from Levan Mantell.

F.H.V.H. and B.C.L.M. research was funded by Coordenação de Aperfeiçoamento de Pessoal do Ensino Superior (CAPES- CIMAR II) and by Brazilian Council for Scientific and Technological Development (CNPq; 482557/2011-7).

A.R.H. research was funded by a grant from the Blake, Kymberly and George Rapier Foundation to the Galapagos Whale Shark Project (through Conservation International and the Galapagos Conservancy) and by the Galapagos Conservation Trust. Fieldwork was carried out under permits (PC-37-11 and MAE-PNG/CDS-2012-0020) issued by the Galapagos National Park Directorate.

R.E.H. acknowledges support and assistance of the Georgia Aquarium, Christopher Reynolds Foundation, National Geographic Society, NOAA, Mote Marine Laboratory, the Natural Protected Areas National Commission of Mexico (SEMARNAT/CONANP), and the UNDP/Global Environment Facility.

B.M.N. acknowledges the many supporters, funders, donors and volunteers of ECOCEAN Inc., without whom our long-term tagging programme could not have been conducted. We also thank the Western Australian Department of Biodiversity Conservation and Attractions (formerly Department of Environment and Conservation and Department of Parks and Wildlife) and all involved in the whale shark ecotourism industry at Ningaloo Marine Park for their ongoing support of our work.

C.R. and **S.J.P.** thank the staff of Les Baleines Rand'eau and other tourism operators for their assistance, the Mada Megafauna team for practical and logistical support, and CNRO for their help with research permits in Madagascar. This work was supported by two private trusts, the Shark Foundation, Aqua-Firma, Waterlust, a Rufford Small Grant and the PADI Foundation, and we thank all Marine Megafauna Foundation staff and volunteers for their assistance.

D.R.-M. acknowledges funding for tags provided by Save our Seas Foundation, Project Aware, WWF-Telcel, Royal Geographical Society through (EXERCISE JURASSIC SHARK 2), A1 scuba, downtown aquarium, Azul Marino Restaurant, Palapas Ventana. Whale Shark Mexico field work team.

D.P.R. acknowledges logistics for this project provided by the Qatar Ministry of Municipality and Environment (QMMOE) and, Maersk Oil Research and Technology Centre (MORTC). **S.S.B.** acted as an independent researcher throughout this study with financial support in the form of a salary from the MORTC. The MORTC or North Oil Company did not have any additional role in the study design, data collection and analysis, decision to publish, or preparation of the manuscript and only provided financial support in the form of S.S.B.'s salary and research materials. D.P.R.'s work on this manuscript was supported by two small grants from the Save Our Seas Foundation. Many thanks to the Save Our Seas Foundation, Al Ghurair Foods and the Emirates Diving Association, Emirates Natural History Group and, Le Meridien Al Aqah Beach Resort for providing financial support for individual satellite tags.

A.M.M.S. was funded by a Pew Marine Conservation Fellowship 2020 and an ARC DE170100841.

M.S.S. and **B.W.M.** acknowledge financial support provided by Guy Harvey Ocean Foundation.

M.T. and **M.G.M.** acknowledge the generous support of Apache Energy Ltd (now Santos Ltd). AIMS acknowledges the Yinggarda, Baiyungu and Thalanyji Traditional Owners of Country adjacent to where this whale shark research was undertaken. We recognise these People's ongoing spiritual and physical connection to Country and pay our respects to their Aboriginal Elders past, present and emerging.

7. Supplementary Author Contributions

The Global Shark Movement Project (GSMP) (www.globalsharkmovement.org) is coordinated by D.W.S. D.W.S. conceived the study, and F.C.W., N.E.H., N.Q. and D.W.S designed the study. F.C.W led the data analysis with additional data analysis by N.E.H and J.P.T and compilation by N.E.H., N.Q., M.V. and D.W.S. F.C.W., N.E.H., N.Q. and M.V. contributed software tools. F.C.W. wrote the first draft manuscript with contributions from D.W.S. F.C.W. and D.W.S. led writing of subsequent and final drafts. M.V., I. da C., M.F., L.M.A., E.K.L., M.M.M., L.R.P. and A.M.M.S. contributed to writing and review of final drafts. All authors contributed to and reviewed the final drafts.

Led fieldwork: G.A., J.L., A.B., R.F., M.L.B., J.E.M.C., C.D.B., S.B.L., A.D.M.D., H.G., A.B.S., M.V.E., B.C.L.M., A.R.H., J.R.G., R.E.H., R.D.L.P., B.M.N., C.A.R., S.J.P., S.D., D.R.-M., D.P.R., M.Y.T., S.S.B., D.R.L.R., M.S.S., L.F. and M.G.M.

Undertook tagging: G.A., R.F., J.E.M.C., C.D.B., R.H., S.B.L., D.H.W. A.D.M.D., E.C., H.G., R.D.L.P., A.B.S., A.H., I.S., B.C.L.M., A.R.H., J.R.G., R.E.H., J.P.T., J.G.C., J.J.M., B.M.N., C.A.R., S.J.P., D.R.-M., D.P.R., M.Y.T., S.S.B., D.R.L.R., M.G.M. and M.T.

Participated in fieldwork: K.A., C.L.D., S.R.T., G.B.S., R.H., D.H.W., E.C., R.D.L.P., A.H., I.S, B.C.L.M, A.R.H., E.E., C.P.-P., R.E.H., J.P.T., J.G.C., J.J.M., S.D.R., D.R.-M., D.P.R., M.Y.J., S.S.B., L.F. and M.T.

Compiled raw data: A.B., K.A., J.E.M.C., C.D.B., R.H., D.H.W., H.G., A.B.S., F.H.V.H., B.C.L.M., A.R.H., C.P.-P., R.E.H, J.P.T., R.D.L.P., B.M.N., S.D.R., C.A.R., D.R-.M., D.P.R., M.Y.J., S.S.B., D.R.L.R., A.M.M.S., M.S.S., B.M.W. and M.T.

Analysed raw data: F.C.W., N.Q., J.E.M.C., C.D.B., R.H., H.G., F.H.V.H., B.C.L.M., A.R.H., J.P.T., S.D.R., C.A.R., D.P.R., M.Y.J., S.S.B., A.J.R., D.R.L.R., M.S.S., L.M.Q., G.S. and B.M.W.

Contributed tools: M.S., M.L.B., C.D.B., S.R.T., G.B.S., C.M.D., V.M.E., S.J.P., D.P.R., M.Y.J., S.S.B. and A.J.R.

8. Details of ethical compliance and approvals

All animal handling and tagging procedures were completed by trained personnel under permissions granted by institutional ethical review bodies and complied with all relevant ethical regulations in the jurisdictions in which they were performed. Details from individual research teams are given below with initials of lead investigators in bold.

Research in the Philippines was performed in collaboration with the respective Regional Offices of the Department of Environment and Natural Resources, the Department of Agriculture-Bureau of Fisheries and Aquatic Resources and the Palawan Council for Sustainable Development (Wildlife Gratuitous Permit 2017-13). All research in Tubbataha Reefs Natural Park was done in collaboration with the Tubbataha Management Office (**G.A., J.L.** and **S.J.P.**).

Whale sharks were tagged in Queensland with approval from James Cook University Animal Ethics Committee (ID - A2649) (**A.B.**).

Research was carried out under the general auspices of King Abdullah University of Science and Technology's (KAUST) arrangements for marine research with the Saudi Arabian Coast Guard and the Saudi Arabian Presidency of Meteorology and Environment. These are the relevant Saudi Arabian authorities governing all sea-going research actions in the Saudi marine environment. KAUST has negotiated a general and broad permission for marine research in Saudi Arabian Red Sea waters with these two agencies and thus there is no permit number to provide. The animal use protocol was performed in accordance with Woods Hole Oceanographic Institution's Animal Care and Use Committee (IACUC) protocol #16518 and approved by KAUST's Biosafety and Ethics Committee (**M.L.B., C.D.B.**).

Research off Colombia was carried out according to Migramar animal ethical statements under permits from the Environmental Ministry of Colombia and the National Parks of Colombia (**S.B-L.**).

Research was approved by the Research and Animal Care Committee at Georgia Aquarium and carried out under permit (2019-SRE-01) from the St Helena Government (**A.D.M.D.**).

Tagging procedures were approved by the Cendrawasih Bay National Park Authority and are in accordance with the protocols established by Conservation International Indonesia's animal ethics review committee (**A.B.S., A.H.** and **M.V.E.**).

All procedures involving research animals were approved by the Smithsonian Institution's Institutional Animal Care and Use Committee (IACUC) (**H.G.**).

All tagging procedures were performed under a research license provided by the Brazilian Environmental Agency- Chico Mendes Institute for the Conservation of Biodiversity (ICMBio),

Ministry of the Environment, under permit SISBIO/ Nº 14.124; and under the permit CEUA/Nº 044, by the Committee of Ethics and Use of Animals, of Universidade Federal Rural de Pernambuco-UFRPE (**F.H.V.H**. and **B.C.L.M**.).

All procedures performed in studies involving animals were in accordance with the ethical standards of the University of California Davis, under Institutional Animal Care and Use Committee (IACUC) Protocol #16022, and with permission from the authority of the Galapagos Marine Reserve in the figure of Permit PC-37-11 from the Galapagos National Park Directorate (**A.R.H.**).

All procedures involving research animals were approved by Mote Marine Laboratory's Institutional Animal Care and Use Committee (IACUC) (**R.E.H.**).

All tagging was conducted under animal ethics approvals from Murdoch University (permit numbers: W2058/7; W2402/11; R2926/17) and the University of Queensland (permit number: SBS/085/18/WA/INTERNATIONAL). In addition, permits to conduct fieldwork on wildlife in Western Australian were issued from the Western Australian Department of Environment and Conservation (DEC) (permit numbers: SF007471; SF007949; SF008572), Department of Parks and Wildlife (DPaW) (permit numbers: SF009184; SF009897; SF010414; SF010781; 08-000533-2; 08-002082-2) and Department of Biodiversity Conservation and Attractions (DBCA) (permit numbers: FO25000033-4; FO25000033-9) (**B.M.N.**).

Research was conducted with the approval of and in partnership with the Centre National de Recherches Océano- graphiques (CNRO) in Madagascar (**S.D.** and **S.J.P.**).

In Mozambique, no animal was restrained, caught or removed from its natural habitat for the purpose of this study. Whale shark tagging was compliant with ethics guidelines from the University of Queensland's Animal Ethics Committee and was conducted under their approval certificate GPEM/186/10/MMF/WCS/SF (**C.A.R.** and **S.J.P.**).

Research was carried out under the general auspices of relevant Mexican authorities governing all research actions on wildlife and protected animals and areas in Mexico: CONACYT (Consejo Nacional de Ciencia y Tecnología), DGVS (Dirección General de Vida Silvestre), and SEMARNAT (Secretaría del Medio Ambiente y Recursos Naturales) (**D.R.-M.**).

Permissions for fieldwork and data collection on whale sharks in the Al Shaheen region of Qatar were given by the Qatar Ministry of Environment with whom this work was conducted (**D.P.R.**, **M.Y.J.** and **S.S.B.**).

Seychelles work was approved by the Ministry of Environment and in Djibouti the work was permitted under the Ministry of Tourism through the local non-governmental organization DECAN (**D.R.L.R.**).

All procedures were performed under Mexico Government Permits N° SGPA/DGVS/006539/18, N° SGPA/DGVS/5273/19 and Nova Southeastern University IACUC Permit 2017.11.MS1-A1 (**M.S.S.** and **B.M.W.**).

All procedures were approved by either the University of Western Australia, University of Adelaide, South Australia, or Charles Darwin University Animal Ethics Committees (**M.G.M.** and **M.T.**).